Advanced materials for smart protective coatings: Unleashing the potential of metal/covalent organic frameworks, 2D nanomaterials and carbonaceous structures

Ghaderi, Mohammad; Bi, Huichao; Dam-Johansen, Kim

Published in:
Advances in Colloid and Interface Science

Link to article, DOI:
10.1016/j.cis.2023.103055

Publication date:
2024

Document Version
Publisher's PDF, also known as Version of record

Advances in Colloid and Interface Science 323 (2024) 103055

Contents lists available at ScienceDirect

Advances in Colloid and Interface Science

journal homepage: www.elsevier.com/locate/cis

Historical Perspective

Advanced materials for smart protective coatings: Unleashing the potential of metal/covalent organic frameworks, 2D nanomaterials and carbonaceous structures

Mohammad Ghaderi, Huichao Bi *, Kim Dam-Johansen

CoaST, Department of Chemical and Biochemical Engineering, Technical University of Denmark (DTU), Building 229, 2800 Kgs. Lyngby, Denmark

ARTICLE INFO

Keywords:
Metal-organic framework
Covalent-organic framework
Corrosion protection
Nano carrier
2D materials
Container

ABSTRACT

The detrimental impact of corrosion on metallic materials remains a pressing concern across industries. Recently, intelligent anti-corrosive coatings for safeguarding metal infrastructures have garnered significant interest. These coatings are equipped with micro/nano carriers that store corrosion inhibitors and release them when triggered by external stimuli. These advanced coatings have the capability to elevate the electrochemical impedance values of steel by 2-3 orders of magnitude compared to the blank coating. However, achieving intelligent, durable, and reliable anti-corrosive coatings requires careful consideration in the design of these micro/nano carriers. This review paper primarily focuses on investigating the corrosion inhibition mechanism of various nano/micro carriers/barriers and identifying the challenges associated with using them for achieving desired properties in anti-corrosive coatings. Furthermore, the fundamental aspects required for nano/micro carriers, including compatibility with the coating matrix, high specific surface area, stability in different environments, stimuli-responsive behavior, and facile synthesis were investigated. To achieve this aim, we explored the properties of micro/nanocarriers based on oxide nanoparticles, carbonaceous and two-dimensional (2D) nanomaterials. Finally, we reviewed recent literature on the application of state-of the art nanocarriers based on metal-organic frameworks (MOFs) and covalent-organic frameworks (COFs). We believe that the outcomes of this review paper offer valuable insights for researchers in selecting appropriate materials that can effectively enhance the corrosion resistance of coatings.

1. Introduction

1.1. Organic coatings against corrosion

Corrosion-induced failures of metallic materials are a significant challenge across numerous industries, leading to substantial financial losses, environmental degradation, and potential threats to human safety. It has been estimated that corrosion results in losses of a staggering 2.5 trillion US dollars worldwide annually. This amounts to roughly 3.4 % of the total domestic product, underscoring the far-reaching impact of this issue [1–3]. Developing coatings for metallic substrates is a cost-effective and scalable approach for safeguarding

Abbreviations: 2D nanomaterials, Two-dimensional nanomaterials; MOF, Metal-organic framework; COF, Covalent-organic framework; GO, Graphene oxide; g-C_3N_4, Graphitic Carbon nitride; LDH, layered double hydroxide; h-BN, hexagonal boron nitride; TMDC, transition-metal dichalcogenide; ZrP, zirconium phosphate; CNT, carbon nanotube; CNF, carbon nanofibers; 2-MBI, 2-mercaptobenzimidazole; HMCe, mesoporous CeO_2 carrier; EIS, Electrochemical impedance spectroscopy; GA, Gum Arabic; TGA, thermogravimetric analysis; BET, Brunauer-Emmett-Teller; DDA, Dodecylamine; MSN, Mesoporous silica nanoparticles; CTAB, hexadecyltrimethylammonium bromide; TEOS, tetraethyl orthosilicate; ICP, inductively coupled plasma optical emission spectroscopy; Phen-NH2, 1,10-phenanthroline-5-amine; BTA, Benzotriazole; XRD, X-Ray diffraction analysis; UV–vis, Ultraviolet–visible spectroscopy; MoS_2, molybdenum disulfide; PDA, Polydopamine; APTES, (3-aminopropyl) triethoxysilane; LEIS, localized electrochemical impedance spectroscopy; Poly aniline, PAni; Sulfonated poly aniline, SPAni; MWCNT, multi-walled carbon nanotube; OMWCNT, Oxidezed multi-walled carbon nanotube; ZIF, Zeolite imidazole frameworks; BDC, 1,4-benzenedicarboxylate; SEM, Scanning electron microscopy; FE-SEM, Field-emission scanning electron microscopy; CS, Chitosan; rGO, Reduced graphene oxide; ZnG, zinc gluconate; TO, tung oil; CTF, Covalent triazine-based frameworks; DSC, Differential scanning calorimetry; Tp, 1,3,5-triformylphrogroglucinol; Pa-1, 1,4-phenylenediamine; PPy, Polypyrrole; POSS, Polyhedral oligomeric silsesquioxane; APhen, 1,10-phenanthrolin-5-amine.

* Corresponding author.
E-mail address: hubi@kt.dtu.dk (H. Bi).

https://doi.org/10.1016/j.cis.2023.103055
Received in revised form 20 November 2023;
Available online 29 November 2023

metallic materials. These coatings function as a physical barrier, preventing direct contact between metal substrates and harsh corrosive species, such as dissolved O_2, water, and corrosive species like Cl^- anions [4]. Organic coatings such as epoxy resin, polyurethane, and acrylic resin have been widely embraced due to their exceptional adhesion, electrical insulation, and mechanical properties [5,6]. The success of these coatings depends largely on their ability to resist permeation [7]. Traditional organic coatings that rely on chromium are being phased out due to their hazardous impact on the environment [8,9]. As a result, the pursuit of eco-friendly and efficient pigments has become a focal point in coating science.

1.2. The effect of micro/nano fillers in the coatings

The formation of coating defects, including pinholes, cavities, cracks, mechanical scrapes, and scratches, is inevitable during the preparation, curing and service period of the coating [10,11]. These defects can significantly compromise the efficacy of the protective coating, resulting in increased vulnerability to corrosion-related incidents, with potentially severe consequences for load-bearing structures, and industrial operations [12]. As a result, it is imperative to develop novel coatings with improved and long-lasting anticorrosion properties.

In recent decades, the integration of micro/nanofillers into organic coatings has emerged as a promising technique for mitigating corrosion, owing to their ability to enhance the protective properties of coatings [13]. The use of micro/nanofillers can result in an increase in the diffusion path for corrosive species, thereby delaying the onset of metal corrosion [14]. However, merely introducing micro/nanofillers into coatings does not offer a comprehensive solution for long-term protection against corrosion, due to the fact that the corrosive agents can eventually penetrate the coating and attack the metal substrate underneath [15].

1.3. The effect of corrosion inhibitors

The application of corrosion inhibitors holds significant promise for achieving long-term protection against corrosion when employed optimally. Corrosion typically initiates following the contact of a steel substrate with corrosive species. During the anodic reaction, iron metal undergoes oxidation, leading to the production of Fe^{2+}/Fe^{3+} ions (**Eq. 1 and 2**). The presence of chloride ions in the solution further exacerbates the corrosion process, giving rise to the formation of intermediate compounds such as $FeCl_2$ and $FeCl_3$ (**Eq. 3 and 4**). Subsequent reactions with water result in the production of iron hydroxide and HCl (**Eq. 5 and 6**). Consequently, the localized acidity arising from HCl production at the anodic site intensifies the corrosion reaction. On the other hand, within the cathodic zones, the oxygen reduction reaction leads to the production of hydroxyl ions (**Eq. 7**) and the establishment of a localized alkaline environment at the cathode [16].

$$Fe \rightarrow Fe^{2+} + e^- \quad \text{(Eq. 1)}$$

$$Fe^{2+} \rightarrow Fe^{3+} + e^- \quad \text{(Eq. 2)}$$

$$Fe^{2+} + 2Cl^- \rightarrow FeCl_2 \quad \text{(Eq. 3)}$$

$$Fe^{3+} + 3Cl^- \rightarrow FeCl_3 \quad \text{(Eq. 4)}$$

$$FeCl_2 + 2H_2O \rightarrow Fe(OH)_2 + 2HCl \quad \text{(Eq. 5)}$$

$$FeCl_3 + 3H_2O \rightarrow Fe(OH)_3 + 3HCl \quad \text{(Eq. 6)}$$

$$O_2 + 2H_2O + 4e^- \rightarrow 4OH^- \quad \text{(Eq. 7)}$$

Corrosion inhibitors are substances that can hinder metal corrosion through creating protective film on the metal surface. They may adsorb on the metal surface through either physical adsorption, involving the interaction between the corrosion inhibitor and the oppositely charged metal surface, or chemical adsorption, wherein a chemical bond is formed with the metal. Corrosion inhibitors can be classified into organic and inorganic types. Effective organic corrosion inhibitors typically feature electron-donating heteroatoms (such as N, P, S, O) and/or contain aliphatic and aromatic groups with double and triple bonds [16–18]. By carefully considering the electron configuration of iron [Ar] $4s^2 3d^6$, it becomes evident that the 3d orbital is not fully occupied. Consequently, unshared electron pairs present in heteroatoms or π electrons found in aromatic rings and aliphatic compounds (with double or triple bonds) have the potential to undergo a donor-acceptor reaction with this unoccupied iron orbital [19–23]. This interaction leads to the formation of coordination bonds, resulting in the establishment of a protective layer. In other words, when organic corrosion inhibitors are present, chloride intermediate compounds (**Eq. 3 and 4**) react with corrosion inhibitors, and Inhibitor-Fe^{2+} or Inhibitor-Fe^{3+} complexes are produced (**Eq. 8 and 9**) [16].

$$FeCl_2 + \text{Inhibitor} \rightarrow Fe^{2+} - \text{Inhibitor} + 2Cl^- \quad \text{(Eq. 8)}$$

$$FeCl_3 + \text{Inhibitor} \rightarrow Fe^{3+} - \text{Inhibitor} + 3Cl^- \quad \text{(Eq. 9)}$$

Inorganic corrosion inhibitors can be divided into cathodic and anodic types. Anodic inorganic corrosion inhibitors such as chromate, phosphate, and molybdate with negative charges interact with Fe^{2+} and Fe^{3+} ions, leading to a reduction in the oxidation rate. On the other hand, cathodic inorganic corrosion inhibitors such as Ce^{3+}, Zn^{2+}, and La^{3+} have positive charges and can react with OH^- produced in the cathodic site (**Eq. 7**) and form oxide/hydroxide protective layer [24].

Despite the mentioned merits, it has been reported that the direct addition of corrosion inhibitors to the coatings can pose challenges, including interference with the curing process, uncontrollable consumption, potential inactivation, and the potential risk of compromising the coating's integrity [25]. Therefore, alternative methods for incorporating corrosion inhibitors into coatings should be considered to mitigate these issues.

1.4. Self-healing materials and self-healing coatings

Self-healing materials are substances that possess the ability to repair damage or restore their original functions automatically or by external stimuli [26]. In nature, self-healing mechanisms are prevalent and serve as a source of inspiration for the development of man-made self-healing materials. Biological systems, ranging from plants to animals, exhibit remarkable abilities to regenerate and repair damage. For instance, some animals possess the capacity to regenerate lost body parts. By mimicking these natural processes, scientists are harnessing the principles observed in living organisms to create innovative materials for different applications.

In recent years, considerable research efforts have been dedicated to exploring the concept of “self-healing coatings”. These coatings employ intrinsic or extrinsic self-healing mechanisms to achieve their desired functionality. Intrinsic self-healing coatings rely on the disruption and subsequent reorganization of molecular chains within the material itself. This molecular-level response enables autonomous self-repair, capitalizing on the inherent properties of the material [27]. However, intrinsic self-healing coatings require specialized resin, which may not be cost-effective. In contrast, extrinsic smart coatings incorporate micro/nano carriers loaded with active agents, such as corrosion inhibitors, that can readily release and adsorb onto the metal surface in a chemical or physical manner when the corrosion reaction begins. The released corrosion inhibitors can subsequently create a protective layer on the metal surface through mechanisms described in the previous section and, so-called, heal the damage [28–30].

Utilizing micro/nano carriers offers a promising solution to tackle the problem associated with the direct addition of corrosion inhibitors. By loading corrosion inhibitors into the pores or between the sheets of

these carriers, they can be released on-demand at the sites of corrosion. Fig. 1 schematically summarizes the function of organic coatings containing fillers or corrosion inhibitor loaded carriers to reduce the corrosion rate of steel substrates. According to this figure, a steel surface without any protective coating comes into direct contact with aggressive elements, leading to the production of corrosion products within a few hours. On the contrary, a coated steel surface acts as a physical barrier, separating the metal surface from corrosive ions. However, the presence of coating defects and cracks serves as potential penetration points for corrosive agents. The addition of fillers serves to elongate the diffusion path of corrosive ions, cover voids within the coating, and improve the mechanical properties of the coating. Despite these benefits, all three coating systems lack active inhibition properties, making them vulnerable to failure when mechanical cracks develop in the coating. The last system contains carriers loaded with corrosion inhibitors. This system not only encompasses the positive attributes of the preceding coatings but also, through the release of active corrosion inhibitors, provides ongoing protection to the metal even in the presence of coating cracks.

To design an effective carrier, the following considerations must be taken into account which are summarized in Fig. 2 [31]:

1) Compatibility with the coating matrix: Ensuring that carriers are compatible with the coating matrix is vital to avoid negative outcomes such as poor barrier properties, carrier leaching, and accelerated electrolyte uptake caused by defects, voids, lack of adhesion, or unintended side reactions [32].
2) Compatibility of corrosion inhibitors with the carriers: It is crucial to verify that the functional species can be loaded and stored effortlessly within the carriers and do not adversely interact with them, thereby altering their essential properties [33].
3) Loading capacity: The larger the specific surface area and pore volume, the higher the amount of the corrosion inhibitor that can potentially be loaded into the nanocontainer. However, the diffusion limit into these nanocontainers should be considered [34].
4) Stability in acidic, neutral, and basic environments: The stability of nanocarriers in various environments is a crucial aspect often overlooked by researchers. Localized corrosion reactions lead to a change in pH, rendering the anodic site acidic and the cathodic site alkaline [35]. Consequently, carriers that are not pH-stable are susceptible to structural degradation, resulting in unregulated release of the corrosion inhibitor over time.
5) Stimuli-responsive behavior: The release of healing agents and corrosion inhibitors can occur under various stimuli, including redox [36–38], photothermal [39–41], mechanical damage [42,43], etc. One of the most extensively adopted methods for the controlled release of corrosion inhibitors is the use of carriers that are stimulated by the pH change which, according to the previous information, indicates the beginning of the corrosion reaction. Corrosion inhibitor-loaded carriers are integrated into the coating matrix, leading them to be exposed to corrosive species that diffuse into the coating. However, the actual corrosion process only commences when these corrosive species reach the metal surface beneath the coating. Therefore, it is crucial to design the carriers in such a way that they remain inert upon contact with the corrosive species yet become active or responsive when the corrosion reactions begin. This ensures that the carriers effectively protect the metal substrate

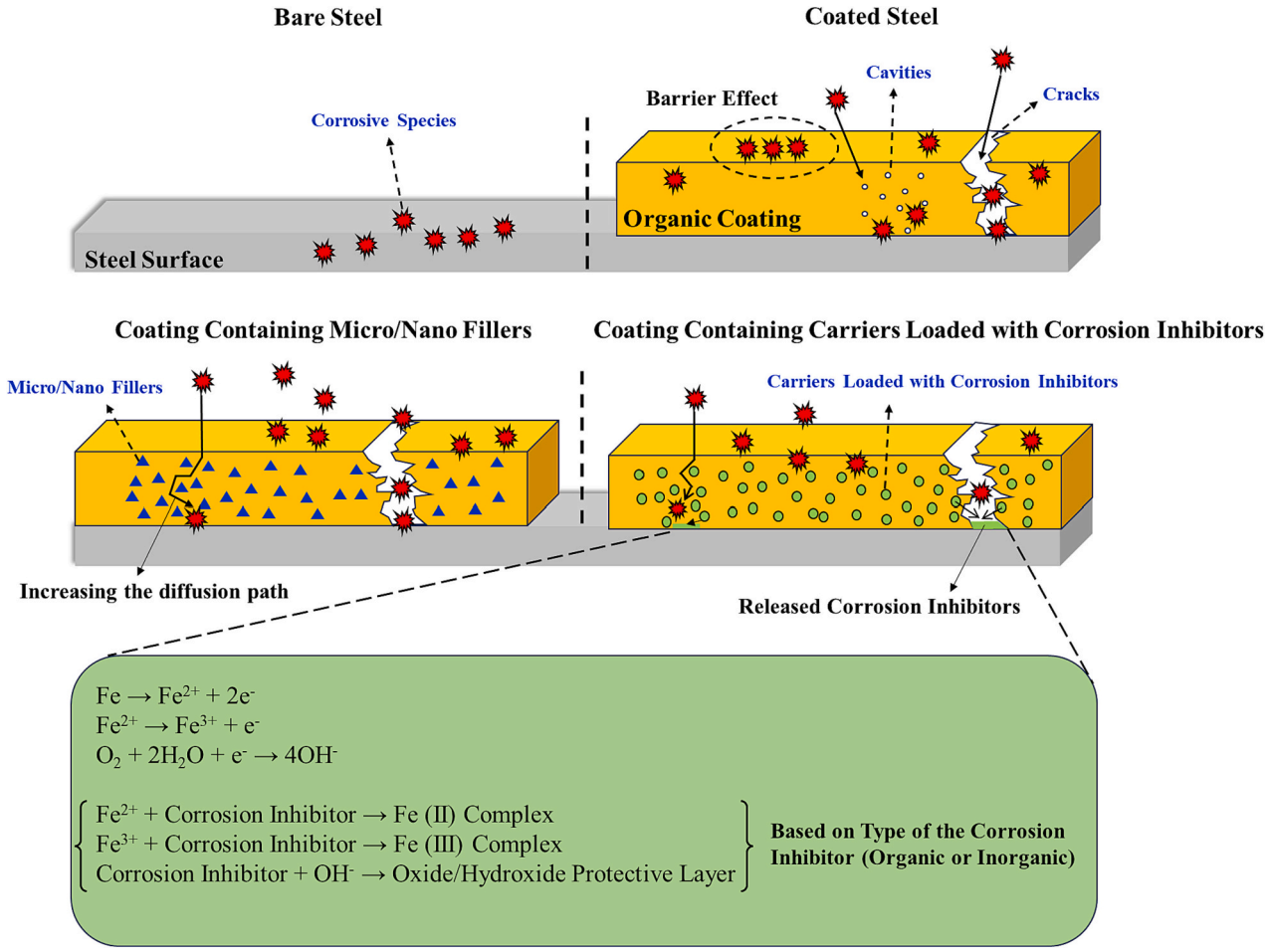

Fig. 1. Schematic illustration of the mechanism of corrosion mitigation of mild steel using organic coatings without and with fillers and carriers loaded with corrosion inhibitor.

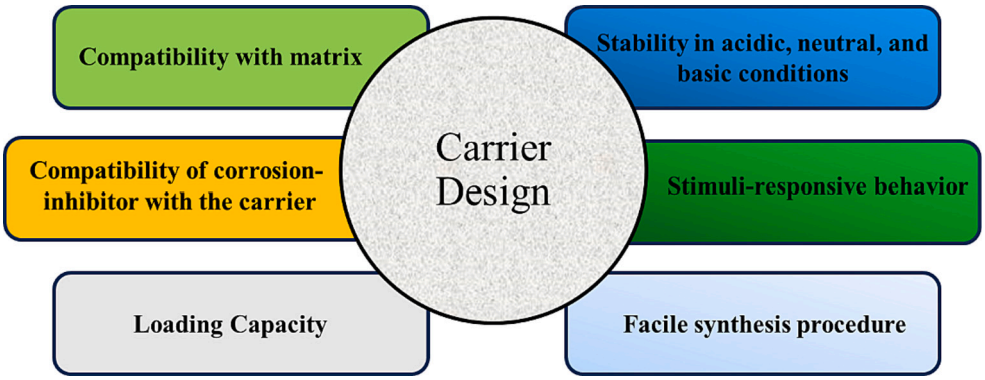

Fig. 2. Criteria for designing an effective carrier.

from corrosion, providing an optimized and reliable corrosion protection system.

6) Facile synthesis: Designing active anti-corrosive coatings is a challenging task that involves the development of micro/nano carriers as the basis for constructing smart coatings. These carriers are loaded with inhibitors and may require additional steps, such as hybridization with other materials or surface modification, to improve their effectiveness and dispersion. From an industrial perspective, the simplicity of synthesis, affordability, and efficacy of pigments are crucial factors that should be considered while designing these materials.

In this review, we aim to provide a thorough examination of the latest advancements of micro/nano carriers in anti-corrosive coatings with self-healing properties and long-term protection. Our objective is to offer a meticulous exploration of these technologies, highlighting their strengths and weaknesses. To begin, we analyze the properties of oxide-based carriers, which serve not only as containers for corrosion inhibitors but also as surface modifiers to enhance the characteristics of other materials. We then delve into the remarkable attributes of two-dimensional (2D) materials, including graphene oxide (GO), graphitic carbon nitride (g-C_3N_4), layered double hydroxides (LDHs), montmorillonite, hexagonal boron nitride (h-BN), transition-metal dichalcogenides (TMDCs), zirconium phosphate (ZrP), and MXene, shedding light on their potential applications in corrosion protection. Furthermore, we investigate the role of carbon materials, such as carbon nanotubes (CNTs) and carbon nanofibers (CNFs), in corrosion prevention. Finally, we examine the latest advancements in nanocarriers, focusing on metal-organic frameworks (MOFs) and covalent-organic frameworks (COFs), renowned for their unique properties and high specific surfaces. Fig. 3 represents various carriers scrutinized in this review. We believe that this review can serve as a valuable resource for researchers, aiding them in the selection of appropriate materials and facilitating the design of pigments with desired properties for corrosion protection of metals. By examining and presenting the latest advancements in the field, we aspire to provide insights that can guide researchers in their pursuit of effective corrosion prevention strategies.

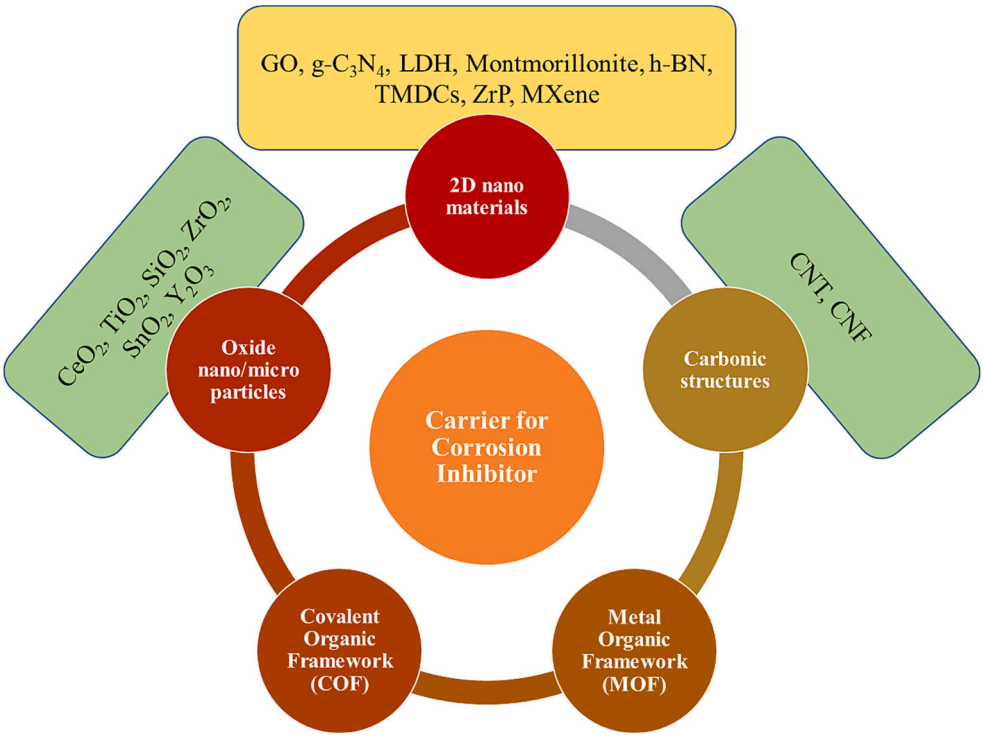

Fig. 3. Different carriers explored in the present review.

2. Carriers based on oxide nano/micro particles

2.1. Cerium oxide

The utilization of oxide nanocarriers within a polymer matrix is a useful approach for corrosion prevention, showcasing good mechanical capabilities and corrosion resistance. One of the inorganic nanocarriers that has gained attention as an additive or carrier for polymeric coatings is cerium oxide (CeO_2). This is due to its remarkable properties, including chemical stability, diverse morphologies, and low toxicity. Despite its good stability, particularly in alkaline environments, ceria is capable of releasing cerium ions in acidic conditions that arise during anodic dissolution of steel. These cerium ions can subsequently interact with hydroxyl anions, yielding protective cerium hydroxides that function as cathodic protection. Moreover, the dispersion of CeO_2 nanoparticles in various coatings has led to heightened corrosion protection by engendering an ultrafine network characterized by reduced porosity. CeO_2 can also act as a carrier for corrosion inhibitors thanks to its chemical (and sometimes porous) nature [44].

Gu et al. [45] synthesized a mesoporous CeO_2 carrier (HMCe) for loading 2-mercaptobenzimidazole (2-MBI), which was subsequently coated with Eudragit EE100, a copolymer comprising amino methacrylates (Fig. 4). EE100 acts as a proton acceptor and polyalkali; under acidic conditions (pH < 5), it acquires a positive charge and loosens its polymer chain, making it a suitable candidate for a pH-sensitive release shell. The loading capacity of 2-MBI was determined to be 6 wt% using UV–vis analysis. Electrochemical impedance spectroscopy (EIS) of coated steel demonstrated that the addition of 1% of 2-MBI@HM-Ce@EE100 to the epoxy coating resulted in a higher impedance value at lowest frequency compared to the blank epoxy coating. This is due to the release of the 2-MBI from the CeO_2 support and the partial dissolution of CeO_2, which results in the release of Ce ions and the formation of a cerium hydroxide-oxide protective film.

In another study, Nawaz et al. [46] employed CeO_2 as a carrier to load Gum Arabic (GA) as an environmentally friendly corrosion inhibitor. The loading of the corrosion inhibitor was estimated to be approximately 30 wt % via thermogravimetric analysis (TGA). Brunauer-Emmett-Teller (BET) analysis revealed that the specific surface area of CeO_2 nanoparticles was 137.96 m^2/g, which decreased to 31.07 m^2/g following GA corrosion inhibitor loading. Notably, the impedance value of the nanocomposite coating containing GA@CeO_2 displayed an increasing trend, reaching a value of 2.16 GΩ.cm^2 after 15 days of immersion in a 3.5 wt% NaCl solution (Fig. 5). This value was approximately four orders of magnitude greater than that of the neat epoxy coating.

2.2. Titanium dioxide

Titanium dioxide is a cost-effective and efficient material that possesses distinctive attributes, including non-toxicity, chemical stability, corrosion resistance, and compatibility with various resins. Ubaid et al. [47] constructed a novel nanopigments based on TiO_2 which was loaded separately with epoxy monomer (as healing agent) and dodecylamine (DDA, as a corrosion inhibitor). These nanopigments were simultaneously added to the epoxy coating. The SEM images of the scratched coatings (Fig. 6) that were immersed in salt solution revealed that the width of scratches in the epoxy coatings lacking nanopigments remained constant over time. Conversely, the coatings containing nanopigments experienced coverage over time, leading to a decrease in scratch diameter. This phenomenon is attributed to the release of epoxy monomers that react with the amino groups of DDA, thereby initiating the curing process of the epoxy resin and facilitating the repair of the coating.

2.3. Mesoporous silica

Mesoporous silica nanoparticles (MSN) are another promising candidate for inorganic nanocarriers in anti-corrosive applications, owing to their high surface area and mesoporous structure, which render them favorable for adsorption and desorption-related processes [48]. However, maximizing the loading of corrosion inhibitors into the MSN nanocarriers requires careful consideration of factors such as inhibitor dimensions, chemistry, and the porosity, which affects the inhibitor's penetration and distribution within the carrier structure [49]. Furthermore, designing and tailoring the chemical interactions between the nanocarrier and inhibitor is crucial to ensure timely and controlled release of the inhibitor [50]. The nanocarriers should also exhibit chemical stability in the intended environment and maintain the loaded inhibitor for a reasonable duration [49]. The remarkable porosity and high specific surface area of MSN make them an ideal host for accommodating high amounts of active anticorrosive agents in polymeric coatings, enabling the surpassing of solubility limitations, and leading to improved efficiency. Furthermore, it is possible to design MSN-based systems that are engineered to release corrosion inhibitors in a stimuli-responsive manner when subjected to specific conditions, such as changes in pH. This feature can be tailored to optimize the effectiveness of the anticorrosive agent and enhance the protective properties of the coating.

Lamprakou et al. [51] explored the corrosion inhibition of calcium phosphate encapsulated in silica nano particles. The silica nanoparticles were synthesized using hexadecyltrimethylammonium bromide (CTAB)

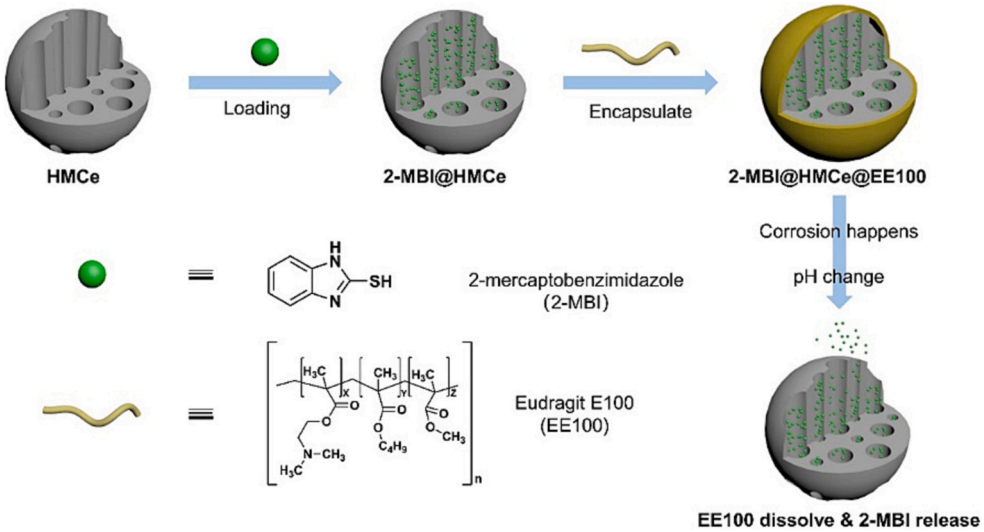

Fig. 4. Schematic of synthesis procedure of 2-MBI@HMCe@EE100 pigment [45].

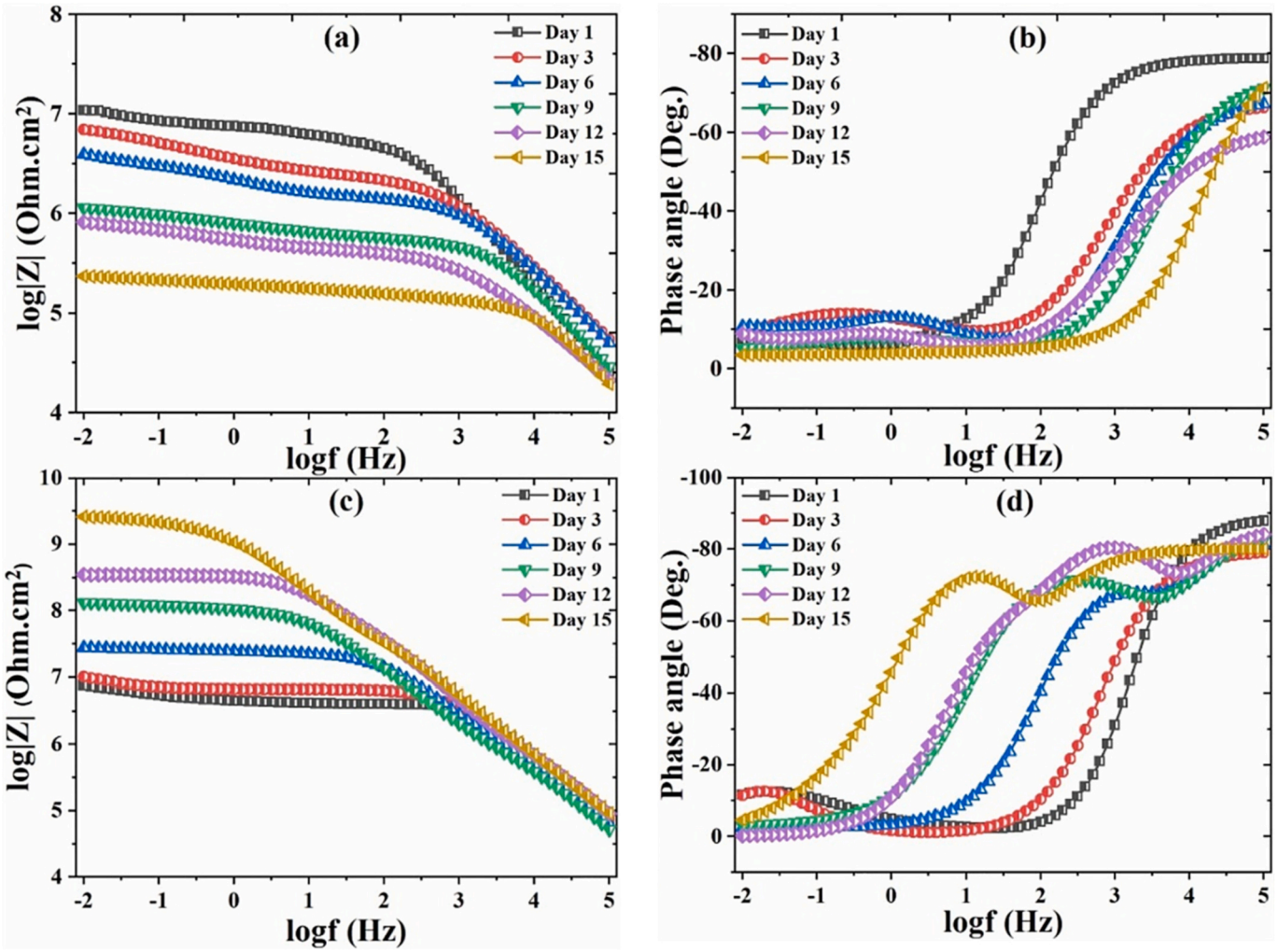

Fig. 5. Bode plots of nanocomposite coatings without (a, b) and with CeO_2@GA (c, d) nanopigments after different immersion time in 3.5 wt% NaCl solution [46].

and tetraethyl orthosilicate (TEOS) followed by calcination in air at 550 °C. The resulting silica exhibited a high specific surface area of 1134.6 m^2/g and an average pore size of 1.4 nm, indicating a prevalence of micropores. Upon loading with calcium phosphate, the specific surface area decreased to 646.6 m^2/g. The release behavior of the corrosion inhibitor and degradation of the silica carrier were studied at pH 7 and 13 using inductively coupled plasma optical emission spectroscopy (ICP-OES). The results showed that the release of calcium ions was greater at pH 13 compared to pH 7, which was attributed to the electrostatic repulsion between silica and calcium phosphate under alkaline conditions (Fig. 7a). It was also observed that the nanoparticles released silicon ions in both neutral and alkaline environments, with a more pronounced release occurring in alkaline conditions (Fig. 7b). This was due to the nucleophilic attack of hydroxyl ions, leading to the release of silicic acid. These findings, consistent with other studies [52], suggest that silica nanoparticles are not stable in neutral and alkaline environments.

Wang et al. [53] have formulated a smart coating with exceptional self-healing properties and a highly responsive corrosion detection system by utilizing a unique type of nanocontainer with dual functionality. As shown in Fig. 8, the nanocontainers were synthesized via a straightforward single-step process that entailed the encapsulation of CTAB and 1,10-phenanthroline-5-amine (Phen-NH_2) within mesoporous silica nanoparticles (MSN-PC). These materials exhibited pH-triggered release characteristics, allowing for the prompt release of CTAB and Phen-NH_2 upon corrosion reaction. When corrosion commenced, CTAB and Phen-NH_2 acted in concert as potent corrosion inhibitors, effectively impeding the corrosion reactions on the steel surface. Additionally, Fe^{2+} ions that emerged due to the corrosion could interact with the Phen-NH_2 released from MSN-PC, generating a striking red coloration that enabled rapid identification of coating damage (Fig. 9). The results of EIS showed that, after 120 h of immersion in 3.5 wt% NaCl, the $|Z|_{0.01\ Hz}$ value of the epoxy coating with 4 % MSN-PC was roughly 20 times higher than that of the blank epoxy coating.

2.4. Other oxide micro/nano carriers

Moreover, other micro/nano carriers including ZrO_2 [54], SnO_2 [55], Y_2O_3 [56], Ni/Al_2O_3 [57] etc. have been employed in literatures. Table 1 presents previous studies that utilized oxide nano/micro containers.

Overall, oxide carriers play a critical role in improving the mechanical properties and corrosion protection of coatings by serving as physical barriers or corrosion inhibitors, particularly in response to specific pH changes. However, utilizing these materials as carriers for corrosion inhibitors presents certain challenges. The first drawback associated with oxide carriers (especially metal oxides) is their limited loading capacity, which is an important consideration in the design and application. When employing oxide carriers to store corrosion inhibitors, there exists a maximum threshold to the amount of inhibitor that can be effectively loaded onto the carrier. This limitation arises due to various factors, including the physical and chemical properties of the

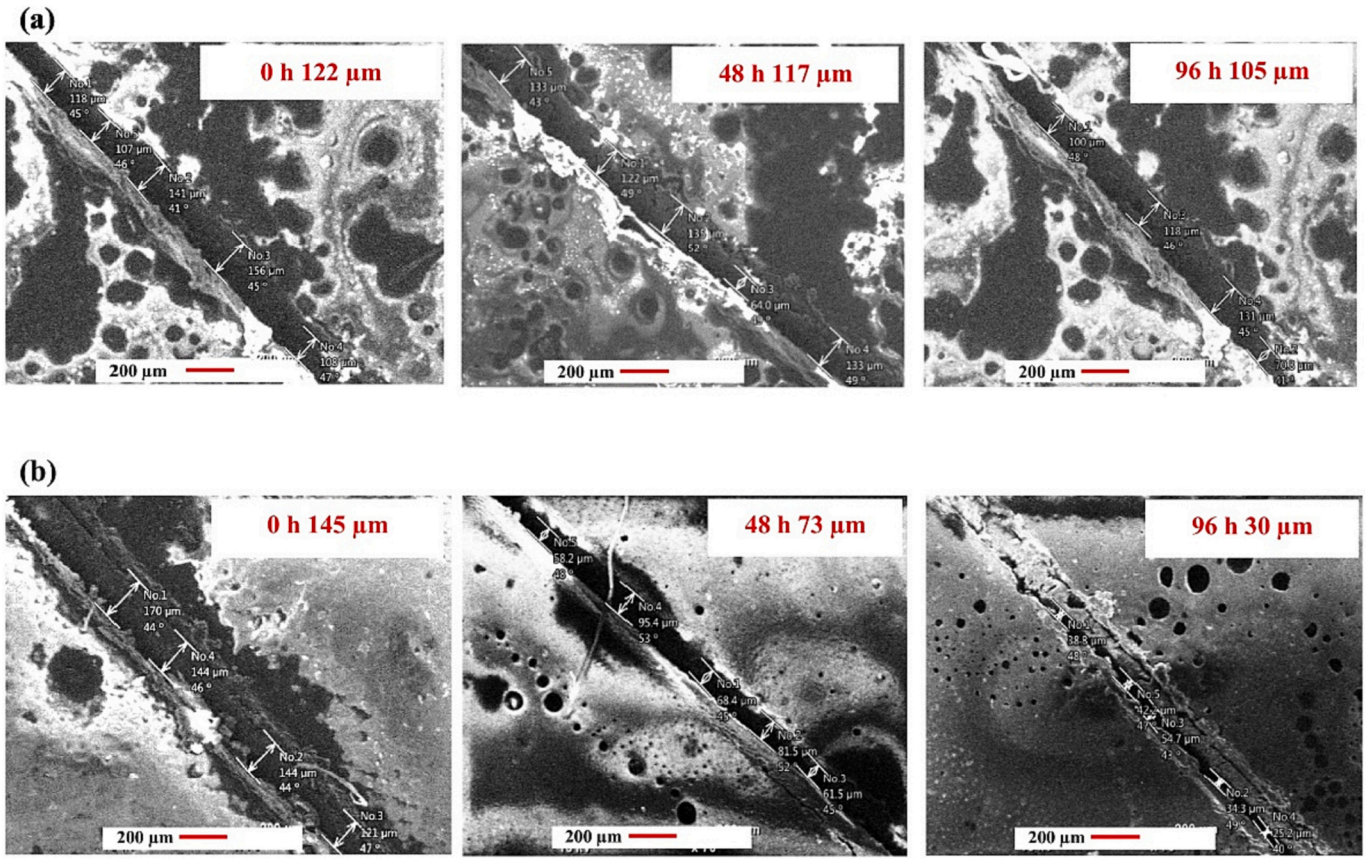

Fig. 6. The SEM images of scratched coating without (a) and with modified TiO_2 (b) nanopigments [47].

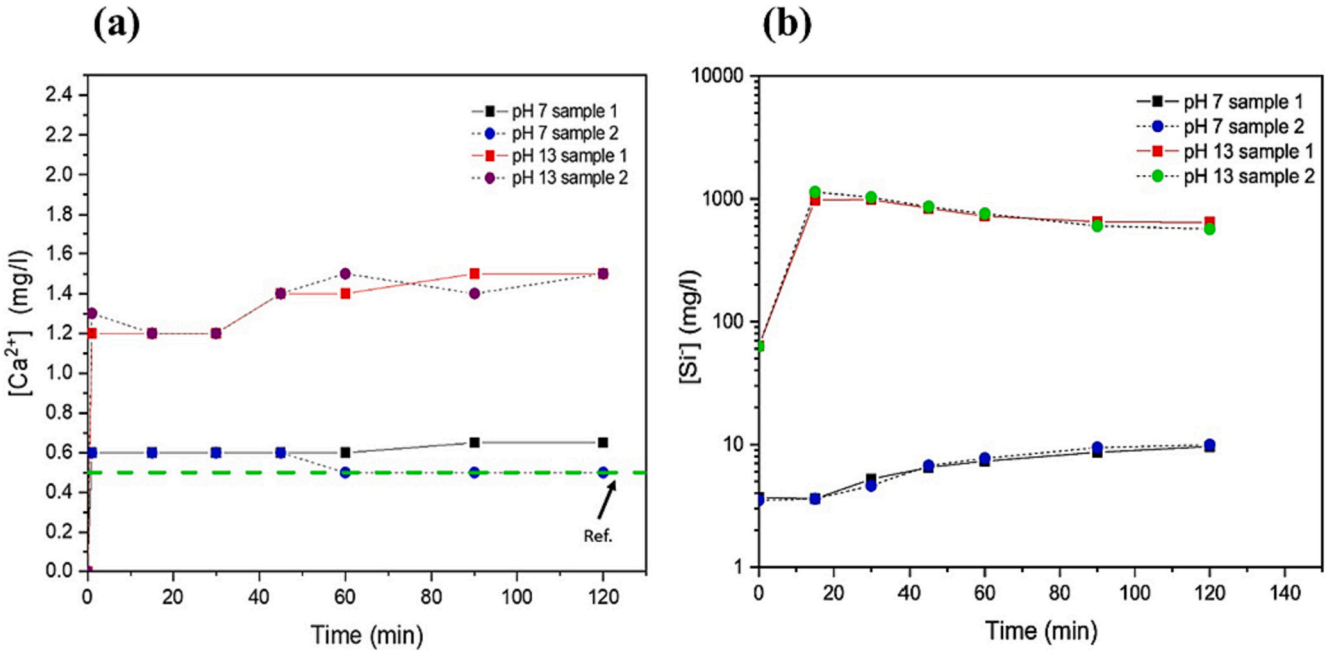

Fig. 7. The release behavior of Ca^{2+} ions (a) and Si ions (b) from SiO_2 carrier at pH 7 and 13 versus time (adapted from reference [51]).

carrier material as well as its structural characteristics. Secondly, as we have discussed, the primary objective of using carriers is to effectively store corrosion inhibitors. Unfortunately, many oxide carriers are vulnerable to acidic (e.g., CeO_2, ZnO, ZrO_2, etc.) or alkaline conditions (e.g., SiO_2), which can result in their decomposition. The decomposition of carriers is undesirable as it leads to the abrupt and uncontrolled release of corrosion inhibitors as well as compromising the coating's integrity.

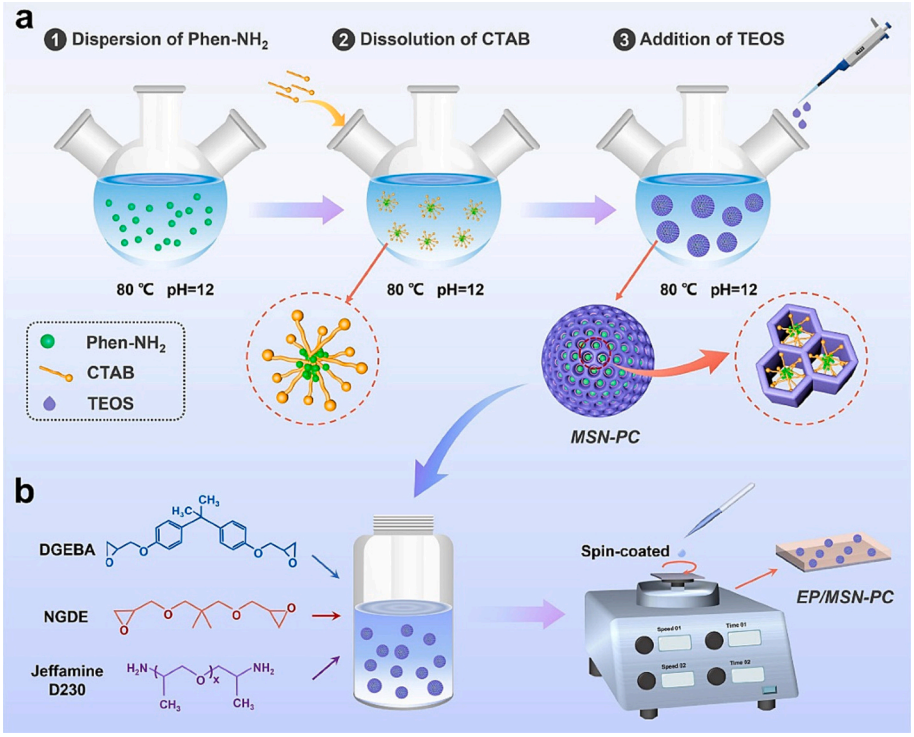

Fig. 8. The synthesis procedure of MSN-PC nanopigments (a) and coating preparation (b) [53].

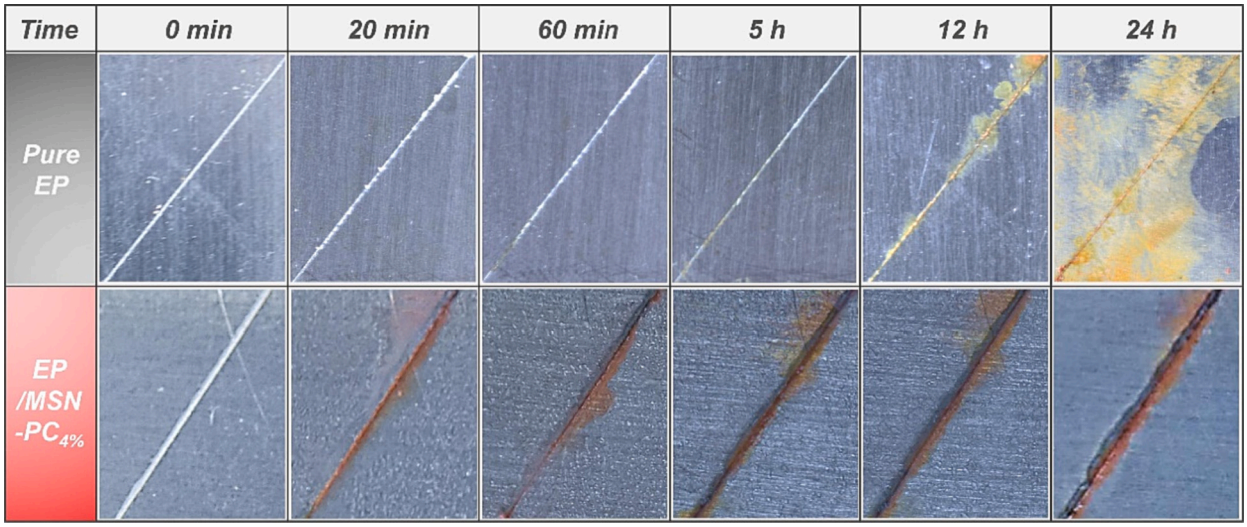

Fig. 9. Images of the scratched coatings during salt spray analysis: neat epoxy (top), and epoxy coating containing 4 % MSN-PC nanopigments [53].

3. Carriers based on 2D nanomaterials

To accomplish the objective of formulating more durable, lightweight, and robust anti-corrosive coatings, researchers have turned to the integration of diverse 2D nanomaterials into polymeric coatings. Since the groundbreaking discovery of graphene in 2004, the unique properties of 2D nanomaterials, such as their high aspect ratio, excellent barrier properties against water and oxygen, impermeability to ions, and chemical stability, have been increasingly acknowledged and utilized [65]. Integrating these 2D materials, which exhibit a "nano-barrier effect" into organic coatings brings significant advantages in constructing a protective composite coating with a "labyrinth effect" (Fig. 10). This effect extends the path of corrosive media penetration, resulting in novel coatings that are lightweight, possess outstanding mechanical properties, and exhibit durable protection against corrosion and weathering [66]. The current selection of 2D nanomaterials employed in anti-corrosive coatings includes graphene, GO, ZrP, molybdenum disulfide (MoS_2), LDHs, h-BN, montmorillonite, the MXene family, and g-C_3N_4, etc. However, widespread application of these lamellar nanomaterials in composite anticorrosive coatings faces challenges related to their large-scale production, stable dispersion, and compatibility with resin interfaces [67].

3.1. Graphene oxide (GO)

The utilization of 2D GO sheets in polymeric systems has garnered significant attention due to their exceptional thermo-chemical properties and unique lamellar structure [69]. Additionally, the

Table 1
Previous studies utilized oxide nano/micro particles as a host for corrosion inhibitors.

Substrate	Type of Container	Corrosion Inhibitor	Modification	Trigger	Comments	Reference
Mild steel	Mesoporous silica	Benzotriazole	Mesoporous silica loaded with benzotriazole was capped with Zn-benzotriazole complex as stopper.	pH	Capping with the Zn-BTA complex controlled the release of BTA from mesoporous silica, in which, at acidic pH, BTA could be rapidly released (> 98% after 5 min at pH 2), whereas at pH 7, it was released gradually (64% after 1 h). On the other hand, the uncapped BTA-loaded mesoporous silica showed fast release even at pH 7 (> 98% after 5 min).	[58]
Mild steel	Mesoporous silica	Sulfamethazine	–	pH	A thorough investigation was conducted to assess the stability of mesoporous silica in different solutions: 0.05 M NaCl (neutral), 1 M HCl (acidic), and 1 M NaOH (alkaline). The structural changes were analyzed using XRD patterns. Prior to immersion, the mesoporous silica exhibited well-defined peaks at (110) and (100), indicating an ordered silica hexagonal structure. Upon immersion, the (110) peak disappeared, indicating a disruption of the structural order. The intensity of the (110) peak varied across the different solutions, with the following trend: mesoporous silica (pre-immersion) > mesoporous silica in 0.05 M NaCl > mesoporous silica in 1 M HCl > mesoporous silica in 1 M NaOH. Notably, the alkaline solution caused the most significant reduction in intensity, suggesting the degradation of Si-O-Si bonds within the mesoporous silica structure.	[59]
Q235 steel	Dendritic mesoporous silica	Cysteine and iron polyacrylate	Two layered epoxy coating: bottom layer consisted of cysteine loaded dendritic mesoporous silica and top layer consisted of iron polyacrylate loaded dendritic mesoporous silica.	–	In this study, dendritic mesoporous silica was utilized as a container due to its high specific surface area and large pore diameter. The carrier demonstrated excellent loading capacity, with 19.75 wt% for cysteine and 30.31 wt% for iron polyacrylate, as indicated by TGA results. When integrated into an epoxy coating, the cysteine@ dendritic mesoporous silica system exhibited corrosion inhibition properties. As corrosion begins, cysteine molecules are released from the dendritic mesoporous silica and adsorb onto the metal surface via S active sites. However, cysteine oxidation can lead to pitting corrosion due to the release of H^+ ions. To overcome this challenge, an epoxy coating was developed containing both cysteine@ dendritic mesoporous silica and iron polyacrylate loaded dendritic mesoporous silica. This combination effectively addresses the issues caused by cysteine oxidation. Iron polyacrylate can be released from the container, adsorbing the H^+ ions released from cysteine through -COO^- bonds and releasing Fe^{3+} ions. Additionally, iron polyacrylate accelerates the oxidation of cysteine, resulting in the formation of cystine, which possesses two S active sites (-S-S-) capable of forming complexes with the steel surface.	[60]
Copper	Mesoporous silica	Benzotriazole	Mesoporous silica loaded with benzotriazole was coated with metal-phenolic network (tannic acid/Fe^{3+} complex).	pH	One notable challenge encountered in pH-controlled release systems is the premature release of the loaded inhibitor during the preparation process. In this study, a tannic acid/Fe^{3+} complex was formed on mesoporous silica containing benzotriazole within just 20 s. The thickness of the complex was controlled by repeating the procedure. At acidic pH levels, the hydroxyl groups of tannic acid are protonated, leading to instability of tannic acid/Fe^{3+}	[61]

(*continued on next page*)

Table 1 (*continued*)

Substrate	Type of Container	Corrosion Inhibitor	Modification	Trigger	Comments	Reference
					complex and the release of benzotriazole corrosion inhibitor.	
Q235 steel	Hollow TiO_2	Benzotriazole	Hollow TiO_2 loaded with benzotriazole was coated by polyethyleneimine and poly(sodium-4-styenesulfonate) using layer-by-layer assembly.	pH	The UV–vis analysis revealed that the polyelectrolyte shell exerted precise control over the release of benzotriazole. Under neutral conditions, a substantial portion (> 90 %) of the benzotriazole corrosion inhibitor molecules remained within the TiO_2 pores after 24 h stirring in deionized water. However, in acidic and, notably, basic conditions, the release rate was accelerated due to the degradation of the polyelectrolyte shell.	[62]
aluminum alloys 2024-T3	Cerium titanium oxide hollow nanosphere	8-hydroxyquinoline and 2-mercaptobenzothiazole	–	–	The loading capacity of cerium titanium oxide hollow nanospheres for 8-hydroxy-quinoline and 2-mercaptobenzothiazole was 4.37 % and 25.36 %, respectively. Furthermore, the corrosion inhibition of nanocontainers loaded with corrosion inhibitor was investigated using EIS analysis. The findings indicated that as the corrosion inhibitor concentration increased, a denser and more effective protective layer was formed.	[63]
–	Hollow mesoporous ZrO_2	2-mercaptobenzothiazole	Hollow mesoporous ZrO_2 (hollow core and mesoporous shell) was prepared using SiO_2 template particle. In this work, only release behavior from container was investigated.	pH	UV–vis analysis revealed that the release of 2-mercaptobenzothiazole from hollow mesoporous silica was more pronounced under acidic (pH 3) and alkaline (pH 10) conditions compared to neutral conditions. This behavior can be attributed to the low solubility of 2-mercaptobenzothiazole at pH 7, as well as the similarity in surface charge between this corrosion inhibitor and hollow mesoporous silica in acidic and alkaline conditions, resulting in repulsion and accelerated release of this compound.	[54]
304 stainless steel	SnO_2	Sodium molybdate	SnO_2-polypyrrole-molybdate-polydopamine was synthesized using layer-by-layer assembly technique.	pH	Polydopamine was employed as a goalkeeper for molybdate corrosion inhibitor. The polarization findings indicated that the epoxy coating incorporating SnO_2/polypyrrole/molybdate/polydopamine exhibited the lowest corrosion current density (1.4×10^{-10} A cm^{-2}), which was five orders of magnitude lower than that of 304 stainless steel (2.99×10^{-5} A cm^{-2}). In addition, the SEM images revealed that the SnO_2/polypyrrole/molybdate/polydopamine pigment exhibited superior dispersion within the epoxy coating in comparison to other coatings.	[64]
steel	Y_2O_3	imidazole	Imidazole corrosion inhibitor was loaded in Y_2O_3.	pH	After loading imidazole in Y_2O_3, the specific surface area reduced from 73.729 m^2/g to 62.671 m^2/g. EIS analysis revealed that the neat epoxy coating exhibited a decreasing trend in total resistance value during time, reaching ~ 7×10^4 Ω cm^2 after 11 days of immersion in a 3.5 wt% NaCl solution. In contrast, the epoxy coating containing Y_2O_3-imidazole demonstrated an increase in total resistance over time, reaching ~ 7×10^8 Ω cm^2 after 11 days. This behavior can be attributed to the release of the imidazole corrosion inhibitor from the Y_2O_3.	[56]

impermeability of GO layers to water solutions positions them as a promising barrier agent for enhancing the protection of polymers against corrosion on metallic substrates [70,71]. However, there are two main drawbacks to employing GO in a polymeric matrix. Firstly, the hydrophilic nature of GO, stemming from the abundance of oxygen-containing functional groups such as hydroxyl and carboxylic, hinders its effective dispersion within the polymeric matrix. Secondly, GO nanosheets lack active inhibition properties, thereby failing to provide comprehensive protection for the metal surface when corrosion species penetrate the coating. To enhance the dispersion of GO, two primary modification approaches have been employed. The first involves covalent modification through reactions with both edge (e.g., epoxide —O— and hydroxyl -OH) and basal (carbonyl C═O and carboxylic -COOH) functional groups. The second method utilizes non-covalent

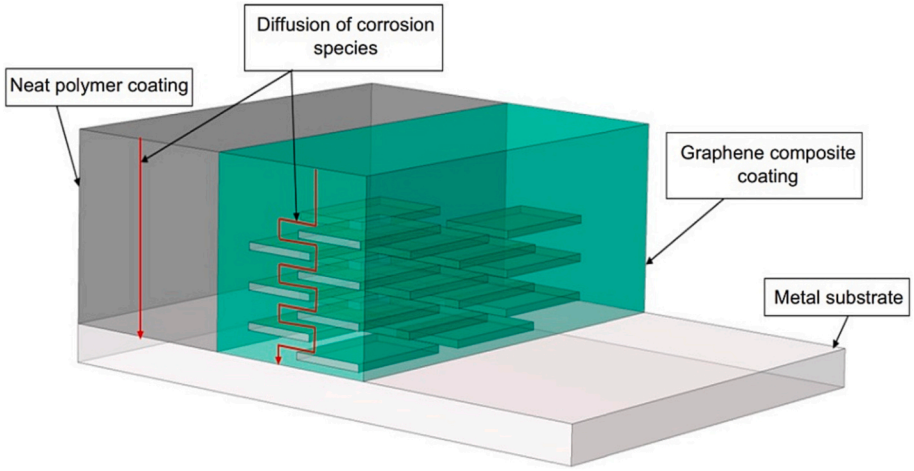

Fig. 10. Schematic of labyrinth effect of graphene composite coating [68].

modification, relying on electrostatic forces, cation-π and π-π interactions, as well as hydrogen and coordination bonding [72].

Considerable efforts have been dedicated to leveraging GO as a stable carrier for corrosion inhibitors [73–78]. In a study conducted by Javidparvar et al. [79], GO was modified with benzimidazole and cerium ions, demonstrating good corrosion protection. The inhibition mechanism involves the interaction between benzimidazole and Fe ions, facilitated by the sharing of non-bonding electrons of N atoms with Fe^{2+} or Ce^{3+} ions. This interaction leads to the formation of benzimidazole-Fe or benzimidazole-Ce precipitates, shielding anodic sites. Furthermore, the released cerium ions contribute to safeguarding cathodic sites by forming oxide/hydroxide layers.

Utilizing reducing agents for the reduction of GO proves to be a promising approach in enhancing corrosion resistance. This method involves partially removing oxygen active sites on GO to make it more hydrophobic and compatible with the polymer matrix, thereby creating a more effective barrier against corrosion. Notably, corrosion inhibitors stand out among various reductants due to their dual functionality- they not only facilitate the reduction of GO but also contribute active inhibition properties [80–84]. For instance, in a study by Habibiyan et al. [85], GO was reduced using polydopamine (PDA). Subsequently, Zn^{2+} cations, serving as an inorganic corrosion inhibitor, were coordinated to the catechol groups of PDA. The efficacy of the resulting GO-PDA-Zn^{2+} complex incorporating epoxy coating in protecting against corrosion was evaluated using salt spray analysis, and the findings indicated that it outperformed the blank epoxy after 400 h of immersion (Fig. 11). The corrosion protection mechanism of the GO-PDA-Zn^{2+} complex involves PDA release triggered by local pH changes during the onset of corrosion. At alkaline pH (caused by cathodic reaction), PDA and GO have the same surface charge, causing PDA to detach from the GO platform. The released PDA then reacts with Fe^{2+} or Fe^{3+} ions to form a protective Fe-PDA layer. Conversely, anodic reactions can create an acidic environment that makes the surface charge of PDA positive, leading to repulsion between PDA and Zn^{2+} ions and causing the release of Zn^{2+} ions. These ions can further protect the metal surface by forming zinc hydroxide/oxide at the cathode. Several studies have shown that P, S and N doping of GO sheets could enhance the adsorption of corrosion inhibitors having positive charges [86]. Different compounds including aminotrimethylene phosphonic acid (P source) [87], *Allium Sativum* extract (N and S source) [88] have been employed, showcasing high corrosion protection. In a study conducted by Keramitinia et al. [89], GO was reduced using urea as an affordable and eco-friendly precursor. The substantial loading capacity of zinc onto N-doped rGO was ascribed to the electron-rich nature of the C═C electron clouds in GO, which exhibit an affinity towards the electronegative nitrogen atoms upon reduction. Also, the introduction of nitrogen functionalities introduces non-

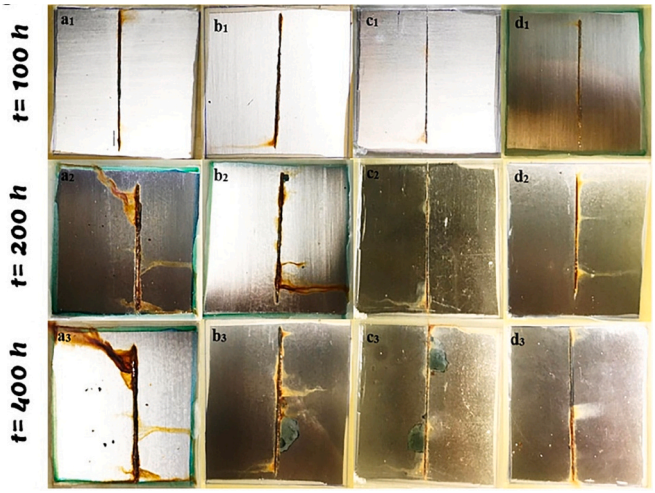

Fig. 11. Images of the scratched coating during 400 h continuous salt spraying: blank/epoxy (a), GO/epoxy (b), GO-PDA/epoxy (c), and GO-PDA-Zn/epoxy (d) [85].

bonding lone electrons, further enhancing the material's propensity to attract zinc ions.

Surface treatment of GO using conducting polymers like polyaniline (PAni) and polypyrrole is another method to boost corrosion protection [90–94]. The underlying mechanism involves the ability of these polymers to capture electrons generated during anodic reactions, leading the transition from their oxidized state to a reduced state. Consequently, iron ions are converted into a passive protective layer of Fe_2O_3 and Fe_3O_4, contributing to corrosion resistance [95–101]. Furthermore, the hydrophilic characteristics of graphene oxide (GO) can be mitigated through the deposition of PAni or polypyrrole, thereby enhancing compatibility with a solvent-based epoxy matrix [102]. Further improvement in surface protection can be achieved by doping inorganic corrosion inhibitors, such as Zn^{2+}, onto the surface of GO-PAni or GO-polypyrrole through π-cation or electrostatic interactions [103,104]. Other methods for enhancing corrosion protection includes hybridizing with other nanomaterials like 2D materials [105], MOFs [106,107] and metal oxide quantum dots [108].

Electrical conductivity of GO can induce galvanic corrosion in anti-corrosive coatings. When corrosive substances penetrate to the interface of the coating and the metal, the conductive GO can participate in electrochemical corrosion with the metal. During this process, GO serves as the cathode, accepting electrons from the metal anode, thereby

promoting the oxidation of the metal [109,110]. Interestingly, the conductivity of graphene can effectively bolster the protective performance of cathodic protection coatings, resulting in superior corrosion resistance. To improve the protection of metal substrates with lower electrochemical activity, active metals like zinc and aluminum are commonly incorporated into cathodic protection coatings. This addition facilitates galvanic corrosion between the high electrochemical activity of the added metal (e.g., zinc) and the metal substrate, thus sacrificing the anode to protect the metal. By adding graphene oxide, which is conductive, the cathodic protection effect can be further enhanced [111].

Huang et al. [112] scrutinized the effect of graphene on the anti-corrosion properties of waterborne zinc rich epoxy coatings. At the beginning of immersion, graphene acts as a physical shield against harsh species. Upon the arrival of the corrosive species at the coating/metal interface, the zinc particles adjacent to the interface will undergo corrosion, ultimately resulting in the formation of corrosion products at the location of the zinc particles. This is where graphene can exhibit its prowess by serving as a bridge, facilitating the connection between isolated zinc particles and the steel matrix, thereby enabling the creation of a galvanic cell. Through this mechanism, the zinc particles located in the interface section are consumed, and subsequently, the electron transfer capability of graphene enables the consumption of the zinc particles located distally within the coating. This ultimately leads to the enhancement of the zinc utilization efficiency and the consequent augmentation of the cathodic protection efficacy of the coating.

3.2. Graphitic carbon nitride (g-C_3N_4)

g-C_3N_4 is a versatile material with exceptional properties and a wide range of potential applications. Its stability and durability make it an ideal choice as a barrier material in composite coatings [113,114]. Additionally, g-C_3N_4 exhibits remarkable adsorption capabilities, specifically for metal cations and organic molecules containing benzene ring structures [115,116]. This unique feature makes it particularly suitable for adsorbing corrosion inhibitors or decorating with other porous materials. One of the significant advantages of g-C_3N_4 is its cost-effective and environmentally friendly synthesis, which sets it apart as a viable alternative to graphene [117]. When incorporated as a nanofiller in epoxy coatings, g-C_3N_4 improves the anti-corrosion performance by filling microcracks and micropores. The presence of -N = bonds in g-C_3N_4 enables interaction with surface hydroxyl groups via hydrogen bonding, thereby enhancing adhesion to the substrate [118]. Moreover, its distinctive properties contribute to enhanced electrochemical stability, and mechanical strength, especially in harsh environments such as acidic or alkaline solutions [119,120]. However, similar to other GO, the tendency of g-C_3N_4 particles to agglomerate poses a challenge by reducing their dispersion and surface area. To improve dispersion, enhance mechanical properties, and maximize surface area, bulk g-C_3N_4 can be transformed into g-C_3N_4 nanosheets using various methods, including ultrasonication and acid treatment [121,122]. Furthermore, different hybridization and surface modifications including hybridization with GO (GO@g-C_3N_4) and grafting with 3-aminopropyl(triethoxysilane) (F-GO@g-C_3N_4) [123], loading nanoparticles such as SiO_2 on g-C_3N_4 [124], modification with polydopamine and KH560 coupling agent [125] and amine functionalization [126] have been used to improve the dispersion of g-C_3N_4 in epoxy coatings.

Interestingly, g-C_3N_4 has gained significant attention as a promising photocatalyst for corrosion protection due to its distinctive properties and photocatalytic capabilities. With its ability to be excited by visible light, g-C_3N_4 efficiently harnesses solar energy to generate photogenerated electrons, which play a crucial role in achieving cathodic polarization without material dissolution or wastage. This environmentally friendly and energy-saving anti-corrosive technology has shown remarkable improvements in the anti-corrosion lifespan of materials. The photocatalytic anti-corrosion mechanism of g-C_3N_4, as depicted in Fig. 12, can be succinctly summarized as follows [127]:

(i) Under light irradiation, g-C_3N_4 facilitates the generation of excited electrons, which preferentially transfer unidirectionally to the steel surface. Notably, these excited electrons possess a more negative reduction potential than the free electrons naturally present on the steel surface. Consequently, during the corrosion process, the excited electrons are selectively consumed, thereby reducing the overall consumption of free electrons on the steel surface. This selective consumption plays a crucial role in achieving the desired anti-corrosion effect.

(ii) Simultaneously, the transfer of excited electrons to the steel surface induces the formation of electron holes (h^+). These positively charged electron holes engage in an essential chemical reaction, oxidizing the water molecules at the surface and promoting the generation of molecular oxygen (O_2). Molecular oxygen can passivate the surface of the steel by forming a protective oxide layer. When oxygen is available, it can react with the steel surface to form a thin, protective oxide layer (such as γ-Fe_2O_3 or Fe_3O_4), which acts as a barrier between the steel and corrosive agents. This oxide layer inhibits further corrosion by preventing direct contact between the steel and corrosive substances, protecting the steel surface.

(iii) The anti-corrosion mechanism is further reinforced by the ability of the excited electrons to exhibit a robust reducing ability. This enables them to effectively interact with and reduce Fe_2O_3, the corrosion product formed during the corrosion process. By reducing Fe_2O_3 back to iron (Fe), the excited electrons actively suppress corrosion and facilitate the transformation of Fe_2O_3 rust into a more stable form of iron that is less susceptible to further corrosion.

(iv) An advantageous characteristic of this mechanism is the continuous generation of excited electrons when exposed to light. As long as light irradiation is present, g-C_3N_4 consistently generates excited electrons, thereby providing uninterrupted and sustained protection against corrosion.

Despite the numerous advantages offered by g-C_3N_4 in corrosion protection, certain challenges still need to be addressed. One of the key challenges is enhancing the oxidation capability of g-C_3N_4. Its relatively low valence band potential limits its oxidation ability, particularly in commonly utilized corrosive electrolyte systems such as 3.5 wt% NaCl. However, several strategies have been proposed to overcome this limitation. These include defect engineering [128], protonation [129], modifying g-C_3N_4 with nanomaterials to reduce the energy barrier of anodic depolarization reactions, compositing g-C_3N_4 with other semiconductors possessing more positive valence band potentials, and utilizing doping techniques to positively shift the valence band potential [130–132]. Lv et al. [133] developed an epoxy coating incorporating g-C_3N_4 and ZnO nanoring to improve its resistance to corrosion. The inclusion of ZnO, which has a bandgap of 3.37 eV, facilitated the formation of a heterojunction structure with g-C_3N_4, which has a narrower bandgap of 2.7 eV. This heterojunction structure effectively enhanced the separation of photogenerated charges and holes, particularly under visible light conditions. Additionally, ZnO exhibited corrosion inhibition by releasing Zn^{2+} ions, further augmenting the anti-corrosion properties of the coating.

In a separate study, Ge et al. [134] developed *Z*-scheme g-C_3N_4/tungsten oxide (WO_3) heterojunctions to address issues related to poor reduction ability and transmission inefficiency. The incorporation of Z-scheme heterojunctions into the epoxy coating enabled controlled and unidirectional electron transfer. Additionally, the accumulation of reduced electrons on the surface of the iron substrates created a robust driving force that effectively impeded corrosion onset. Furthermore, through the introduction of oxygen vacancies, g-C_3N_4/$W_{18}O_{49}$ heterojunction structures were designed. This design was based on the $W_{18}O_{49}$

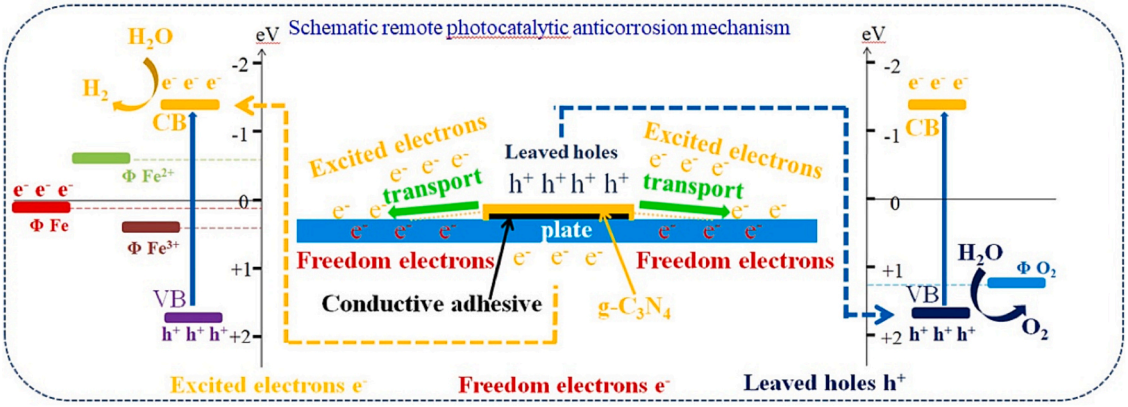

Fig. 12. Anti-corrosion mechanism of coating containing g-C_3N_4 [127].

semiconductor's ability to absorb the entire spectrum of sunlight and enhance electron density. Fig. 13 clearly demonstrated the higher impedance and lower corrosion current density of the coating incorporating g-C_3N_4/$W_{18}O_{49}$. The stable spectral absorption and the generation of hot electrons facilitated the reversal of the anodic corrosion reaction, resulting in an enhanced corrosion inhibition effect.

3.3. Layered double hydroxide (LDH)

LDHs are commonly utilized for corrosion protection of metallic substrates, employing several mechanisms to ensure effective preservation. One crucial role of LDHs is to serve as a physical barrier on the metal surface, preventing the intrusion of aggressive anions and minimizing the exposed surface area available for interaction between the substrate and these detrimental ions [135]. Moreover, LDHs exhibit the ability to exchange intercalated anions (which could be corrosion inhibitor) with the surrounding electrolyte, allowing for the replacement of chloride ions (Cl^-) with intercalated anions [136]. These intercalated anions become trapped within the interlayer galleries of the LDH structure. This entrapment process enhances the corrosion resistance of the substrate. Additionally, the intercalated corrosion inhibitor could react with substrate ions generated during immersion, leading to the formation of chelates. These chelates have the propensity to deposit on the metal surface, blocking the active sites [137]. The interaction between anions and LDHs can impart hydrophobic characteristics to the resulting LDH coating. This hydrophobicity arises from the altered structure and water-repellent properties of the intercalated anions (e.g., 8-hydroxyquinoline), thereby increasing the overall hydrophobicity of the coating [138].

Tabish et al. [139] developed a novel self-healing epoxy coating that incorporates CaFe-tolyl-triazole LDH/g-C_3N_4 nanofiller for enhanced steel protection. To evaluate the self-healing capability, localized electrochemical impedance spectroscopy (LEIS) was employed. Fig. 14 illustrates the performance of various coatings, demonstrating that the epoxy coating exhibited the lowest resistance and experienced severe corrosion in both intact and scratched areas. In contrast, the CaFe-tolyl-triazole LDH/epoxy coating initially exhibited high impedance after 3 h of immersion, which slightly decreased thereafter due to the release of

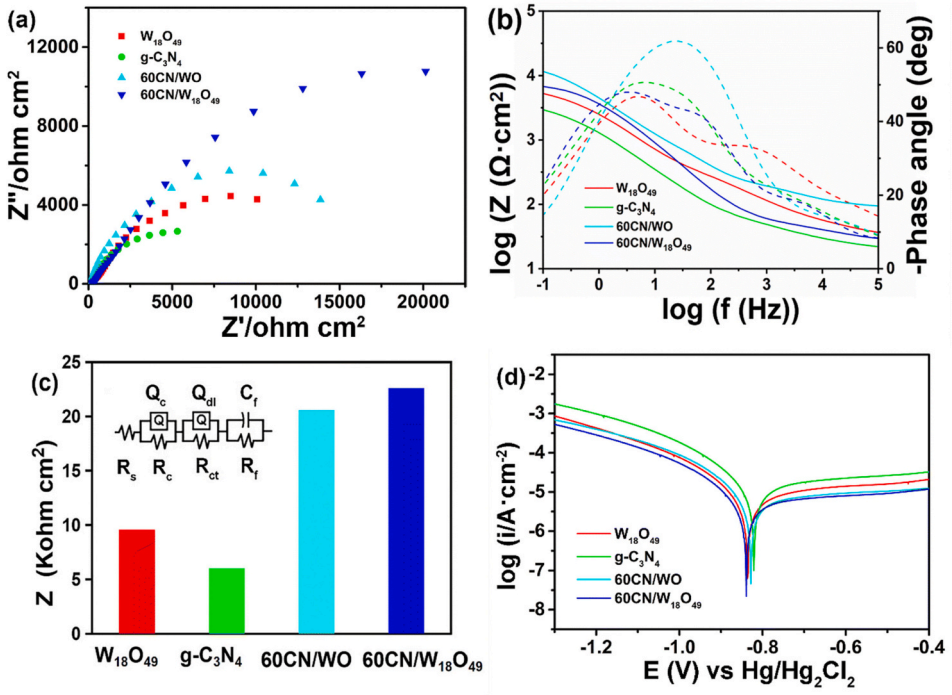

Fig. 13. Nyquist (a) and Bode (b) diagrams of various coating after 72 h immersion in 3.5 wt% NaCl solution. Total impedance (c) and corrosion current density (d) of various coating after 72 h in 3.5 wt% NaCl solution [134].

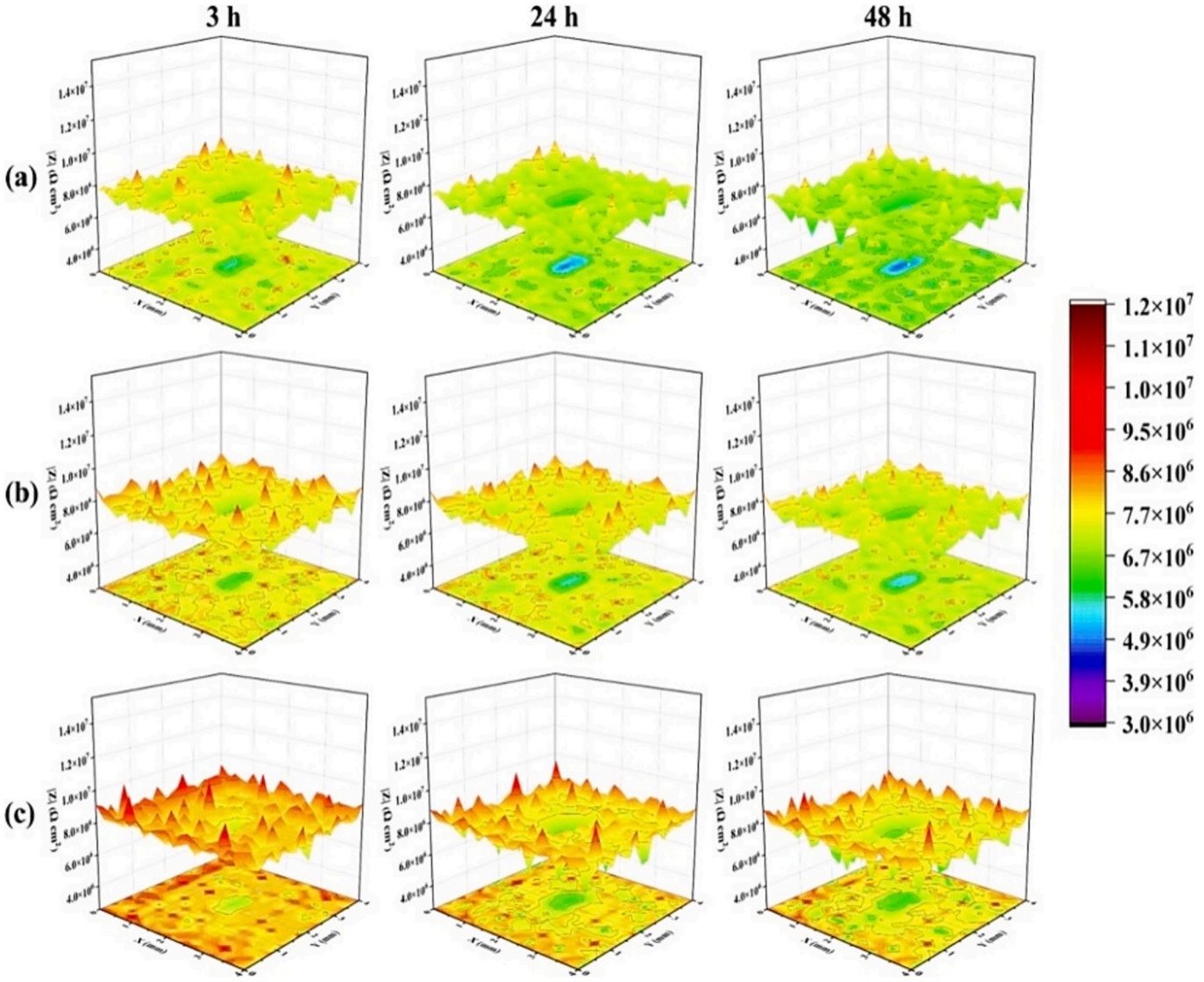

Fig. 14. LEIS analysis of epoxy (a), CaFe-tolyl-triazole LDH/epoxy (b), and CaFe-tolyl-triazole LDH/g-C_3N_4 (c) coatings during different immersion times in 3.5 wt% NaCl solution [139].

the tolyl-triazole corrosion inhibitor. Remarkably, the CaFe-tolyl-triazole LDH/g-C_3N_4 coating demonstrated the highest resistance among all coatings. Initially, the presence of g-C_3N_4 in the coating prevented corrosion by forming complexes with Fe^{2+} ions and generating a passive protective layer. As time progressed, corrosion reactions altered the pH, triggering the release of the inhibitor, which resulted in sustained high corrosion resistance even after 48 h of immersion. Additionally, adhesion strength was evaluated through a pull-off test, revealing that the CaFe-tolyl-triazole LDH/g-C_3N_4/epoxy coating (5.05 MPa) exhibited superior adhesion compared to the CaFe-tolyl-triazole LDH/epoxy (4.26 MPa) and neat epoxy (3.6 MPa) coatings.

Despite the advantages attributed to LDH crystals, their application as nanocarriers in polymeric matrices presents certain weaknesses. Firstly, the limited inter-gallery spaces of LDH impose restrictions on the intercalation of inhibitors, allowing only a constrained amount to be accommodated [140]. Secondly, the loading capacity of corrosion-inhibiting materials into the LDH structure is limited to those with anionic properties, excluding a wide range of options [141]. Thirdly, the poor compatibility between inorganic LDH crystals and organic matrixes results in inadequate dispersion properties. Fourthly, the LDH structure lacks a controlled mechanism for the release of loaded corrosion inhibitors, leading to their premature release when the Cl^- ions permeate the coating. This premature release often occurs prior to the onset of corrosion on the metal substrate. Fifthly, the LDH structure exhibits instability in both acidic and highly alkaline circumstances, thereby rendering it an unsuitable material for achieving an effective barrier effect [142].

3.4. Montmorillonite

Montmorillonite is a mineral composed of layered aluminosilicate sheets, exhibiting cation exchange capability. It carries a negative charge, which can be neutralized by the introduction of positively charged metal ions or corrosion inhibitors. As an example, Xing et al. [143] conducted a study where they incorporated the 8-hydroxyquinoline corrosion inhibitor within the layers of montmorillonite. They discovered that during the corrosion process, the 8-hydroxyquinoline corrosion inhibitor could be released by exchanging with the Na^+ cations that had penetrated the material. This release of the inhibitor helped to mitigate the propagation of corrosion. Sun et al. [144] developed a novel hybrid pigment for the formulation of epoxy coatings that possess exceptional resistance against both corrosion and UV radiation. The researchers achieved this by incorporating cerium ions into montmorillonite and in-situ polymerization of polyfluoroaniline on their

surface. The cerium ions served multiple functions within the coating system: as cathodic corrosion inhibitors, as intercalators to increase the interlayer spacing of montmorillonite, as anti-UV agents, and as oxidants to facilitate the polymerization of polyfluoroaniline. The selection of polyfluoroaniline as the polymer was based on its ability to induce steel surface passivation while also providing UV resistance properties. Nevertheless, montmorillonite, like LDH, has certain limitations. One of the drawbacks is its inability to provide controlled or on-demand release of corrosion inhibitors. Additionally, montmorillonite may not be compatible with certain polymer matrices, posing challenges in the formulation process. Furthermore, the choice of corrosion inhibitors for montmorillonite is limited to those with positive charges, which restricts the range of options available. Notably, montmorillonite is sensitive to moisture and can undergo swelling in the presence of water [145]. This swelling behavior can lead to changes in the physical properties of the coating and potentially affect its ability to provide long-term corrosion resistance.

3.5. Hexagonal boron nitride (h-BN)

h-BN nanosheets (**Fig. 15a**), share similarities with graphene in terms of their mechanical strength, thermal conductivity, and impermeability [146–150]. However, a notable distinction arises from the high electronegativity of nitrogen in BN, resulting in its electrical insulation properties with substantial band gap [151]. This characteristic offers a distinct advantage by minimizing the risk of galvanic corrosion between BN and the metal substrate beneath it [152]. Moreover, BN boasts a manufacturing capacity and emerges as a promising substitute for graphene as an effective filler material in anti-corrosion applications. Nonetheless, the absence of surface functional groups on h-BN nanosheets poses challenges when attempting to disperse them effectively in water and polymer matrices [153,154].

In contrast to graphene or GO, which can be exfoliated into single-layer structures, h-BN nanosheets naturally exist as multilayered structures [158]. Consequently, it is necessary to exfoliate BN nanosheets into fewer-layered states to enhance their effective diameter/thickness ratio. The exfoliation process typically involves noncovalent modification to separate the h-BN layers, followed by covalent modification for subsequent surface modification. Taking advantage of the abundant presence of conjugated electron clouds on the h-BN surface, scientists commonly employ aromatic ring-containing compounds along with the assistance of ultrasound to intercalate and effectively separate the nanosheets [67].

3.6. Transition metal dichalcogenide (TMDC)

TMDCs are a class of materials with a molecular formula expressed as MX_2 where M represents transition metals (such as molybdenum, tungsten, titanium, and tantalum) bonded with chalcogen atoms denoted as X (such as sulfur, selenium, and tellurium) [159,160]. They exhibit a layered crystal structure composed of X-M-X layers, where the M atoms are sandwiched between two planes of X atoms. The bonding between the M and X atoms within the planes is characterized by stronger ionic-covalent interactions, while the interactions between the layers are relatively weaker and governed by van der Waals forces [161]. Due to the weak interlayer van der Waals interactions, mechanical exfoliation and liquid-phase exfoliation techniques allow for the facile obtainment of single-layer MX_2 structures [162].

Emerging research indicates that single-layer MX_2 materials exhibit exceptional properties, making them highly suitable fillers in various applications. These materials possess outstanding mechanical properties and demonstrate excellent thermal conductivity. MoS_2 has gained attention for its potential application in organic anticorrosion coatings. The inherent chemical and thermal stability of MoS_2 contribute to the coating's corrosion resistance. However, one notable challenge

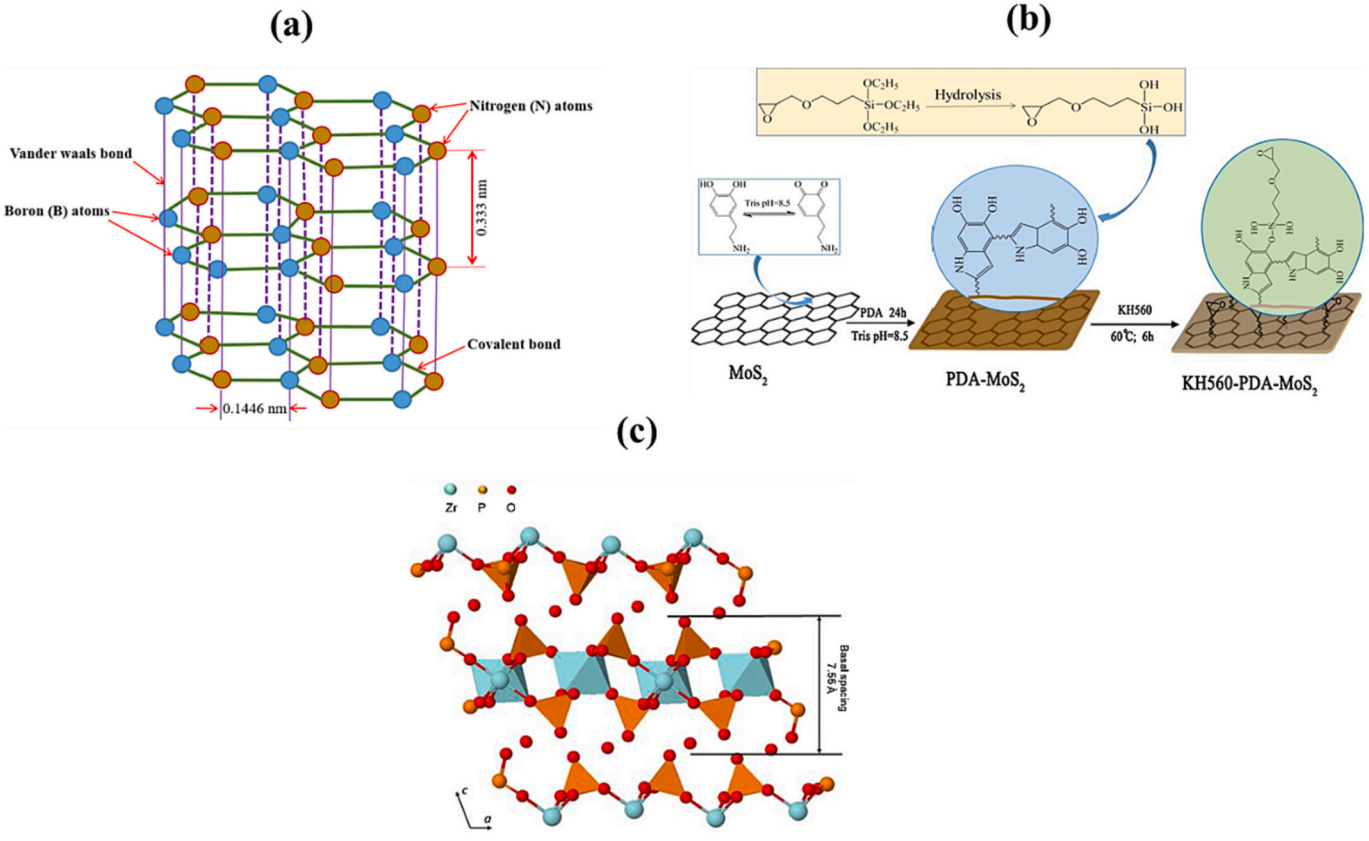

Fig. 15. h-BN crystal structure (a) (adapted from reference [155]). Synthesis procedure of KH560-PDA-MoS_2 (b) (adapted from reference [156]). Crystallographic structure of ZrP (c) (adapted from reference [157]).

encountered with layered MoS_2 nanomaterials is their tendency to agglomerate within polymer composites. To overcome this issue, researchers commonly employ surface organic functionalization techniques, encompassing both noncovalent and covalent modifications, to enhance the dispersibility of MoS_2 nanosheets. In a study by Jing et al. [156], the surface of MoS_2 was modified using polydopamine, followed by functionalization with KH560 silane coupling agent **(Fig. 15b)**. This surface modification strategy resulted in a significant improvement in the dispersion of the MoS_2 nanofiller. As a result, the nanocomposite coating, which contained 0.8 wt% of KH560-PDA-MoS_2, exhibited outstanding corrosion protection performance with high efficacy. In addition to dispersion challenges, research findings suggest that MoS_2 can undergo oxidation when exposed to water vapor, air, and oxygen molecules, which limits the practical application of MoS_2 in marine coatings. This phenomenon is thermodynamically favorable due to the stronger Mo—O bonds in comparison to Mo—S bonds [163,164]. Furthermore, MoS_2 is susceptible to UV irradiation [165].

3.7. Zirconium phosphate (ZrP)

α-ZrP is a versatile inorganic compound that exhibits exceptional thermal stability, high ionic conductivity, and strong cation exchange properties [166]. In the crystal structure of α-ZrP, each layer is composed of zirconium atoms situated on the same plane. Within the layer, each zirconium atom forms bonds with four oxygen atoms derived from the phosphate groups. The phosphate groups themselves consist of four oxygen atoms, with three of them connected to the zirconium atom, contributing to the construction of the layer. The fourth oxygen atom in each phosphate group extends towards the interlayer space and forms a bond with a hydrogen atom, resulting in the formation of a hydroxyl group (**Fig. 15c**). The interlayer distance in α-ZrP is 7.56 Å, consists of one mole of water intercalated within this interlayer region [157]. The layers are held together by relatively weak van der Waals forces, allowing for easy exfoliation into single atomic layers. These nanosheets possess precise size and thickness control, offering an advantage in anti-corrosion applications. Researches have demonstrated that ZrP/polymer composites exhibit good barrier properties, making them well-suited as nanofillers to enhance the corrosion resistance of polymer coatings [167]. The cation exchange ability of α-ZrP can be beneficial to intercalate cations with corrosion inhibition ability (e.g., Ca^{2+}) [168]. However, the narrow interlayer space restricts the access of cations to exchangeable protons of α-ZrP [157]. Moreover, the acidic nature of the hydroxyl groups in α-ZrP can have a negative impact on anti-corrosive coatings [166].

Zhao et al. [169] employed Tris(hydroxymethyl)-aminomethane to prepare exfoliated α-ZrP, which was subsequently modified with eco-friendly phytic acid molecules. They proposed a mechanism to describe the observed enhancement in anti-corrosion performance of waterborne epoxy coating, wherein they highlighted that the exfoliation of ZrP facilitates improved dispersion, leading to enhanced barrier properties of the coating. Furthermore, they proposed that phytic acid molecules have the ability to form complexes with iron ions, thereby reducing the anodic reaction (Fig. 16).

3.8. MXene

MXenes are new classes of 2D materials with a unique structure that has garnered attention in recent years. They are composed of nitrides, carbides, and carbonitrides of transition metals, with the formula $M_{n+1}X_n$ (n = 1–3), where M represents an early transition metal like titanium, tantalum, or niobium, and X refers to carbon or nitrogen [170,171]. MXene nanosheets exhibit a high aspect ratio, abundant surface chemistry, remarkable thermal and electrical conductivity, and hold immense promise in the fabrication of polymeric nanocomposites for electromagnetic interference (EMI) shielding applications [172,173]. Furthermore, the layered structure of MXene nanosheets enables them to enhance the corrosion resistance of composite coatings by fortifying their barrier properties against corrosive media [174]. Additionally, the surface groups of MXene can adsorb corrosive ions [175].

In spite of the numerous advantages offered by MXenes in enhancing corrosion protection, it is crucial to address and control certain notable drawbacks associated with their utilization. Firstly, similar to other 2D nanomaterials, MXenes exhibit a propensity to agglomerate, leading to reduced dispersibility and compatibility within polymeric matrices [176]. This inherent agglomeration tendency poses a significant

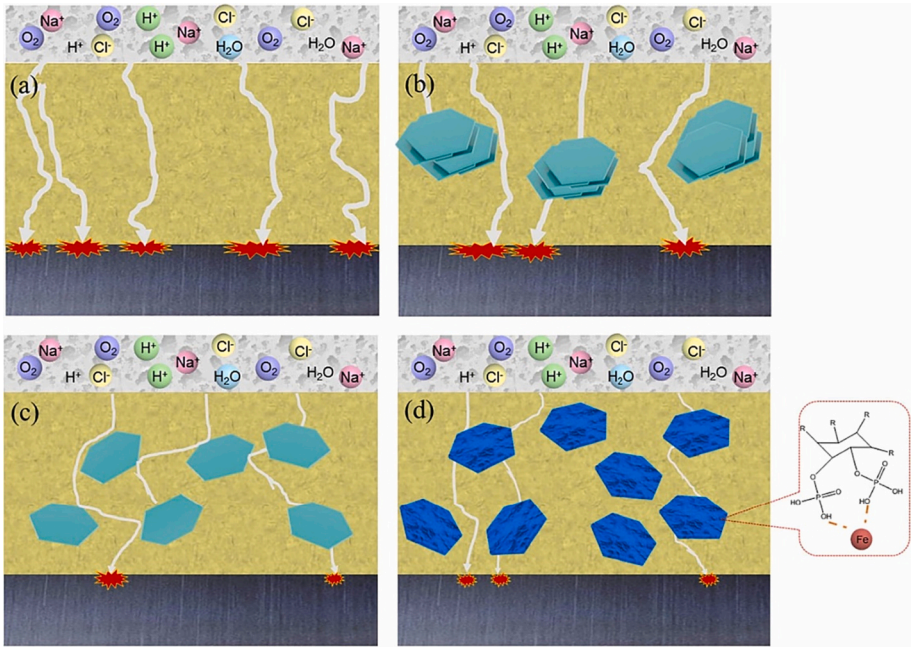

Fig. 16. The anticorrosion mechanism of pure waterborne epoxy coating (a), α-ZrP/epoxy (b), exfoliated α-ZrP/epoxy (c), and exfoliated α-ZrP-phytic acid/epoxy (d) coatings [169].

Table 2
Recent advances in the application of 2D nanomaterials in epoxy anti-corrosive coating for protecting steel substrate.

Type of 2D Material	Corrosion Inhibitor	Comments	Reference
GO	Sodium molybdate	GO was decorated by polypyrrole and doped with sodium molybdate. GO/polypyrrole act as nanocarrier. Furthermore, polypyrrole can enhance the possibility of formation of passive Fe_2O_3 and Fe_3O_4 layers on the steel.	[189]
GO	L-citrulline	L-citrulline was loaded into Beta-cyclodextrin and after that they decorated on GO modified with 3-amino-propyl(triethoxysilane) (APTES). APTES can improve GO dispersion in epoxy matrix.	[190]
GO	cerium acetylacetonate	cerium acetylacetonate was loaded into Beta-cyclodextrin and after that they decorated on GO modified with APTES.	[191]
GO	8-hydroxyquinoline	In this work, 8-hydroxyquinoline corrosion inhibitor was loaded in polystyrene/GO container via Pickering emulsion polymerization.	[192]
MXene	Tannic acid	Tannic acid corrosion inhibitor was loaded in MXene-SiO_2 carrier.	[193]
MXene and LDH	MoO_4^-	ZnAl LDH and MoO_4^- were loaded on MXene surface. LDH is acid responsive and can release Zn^{2+} an intercalated MoO_4^-. Furthermore, both MXene and LDH can provide physical barrier effect.	[194]
MXene	Sulfonated PAni (SPAni)	The first step involved modifying MXene with imidazolium salt, which imparted oxidation resistance properties to it [195]. Next, the modified MXene surface was loaded with SPAni. SPAni exhibits not only the anti-corrosive properties of PAni through electroactivity, passivation, and inhibition, but also offers improved solubility in organic solvents.	[185]
MXene and ZrP	Polydopamine	MXene and exfoliated ZrP heterojunctions were constructed and then dopamine was self-polymerized on the surface of them. Polydopamine can enhance the oxidation resistance of materials as well as act as corrosion inhibitor by forming Fe-catechol complex on the metal surface.	[196]
g-C_3N_4	Benzotriazole, polydopamine and PAni	g-C_3N_4 was utilized as a physical barrier and adsorbent of corrosion inhibition due to its capacity to adsorb metal cations and small organic molecules containing benzene rings. To enhance its performance, a hollow PAni structure was synthesized on g-C3N4, followed by loading benzotriazole into g-C_3N_4@PAni. Lastly, the surface of g-C_3N_4@PAni@BTA was coated with polydopamine, resulting in improved inhibitor retention and better dispersion in waterborne coatings.	[115]
g-C_3N_4	–	The limited photocatalytic activity of g-C_3N_4 stems from its semi crystalline nature, which results in inefficient charge carrier transport and quick recombination of electron-hole pairs generated by light. In this work, a hydrophobic epoxy coating containing crystalline g-C_3N_4 (by subjecting melamine to a furnace with a temperature of 550 °C without heating ramp for 4 h) was designed. This coating showed high coating resistance (2.98×10^8) which was higher that semi-crystalline g-C_3N_4 containing coating (1.43×10^7) and blank epoxy (1.51×10^3)	[197]
GO and montmorillonite	–	In this research, the utilization of APTES was employed for the purpose of intercalating montmorillonite and couple it with GO. The results showed that the epoxy coating containing this filler had higher corrosion resistance, higher water contact angle and lower surface roughness and defect.	[145]

challenge in achieving coatings with exceptional anti-corrosion performance. To enhance the dispersion of MXene, various surface modifications have been carried out. The researchers utilized APTES to modify the MXene surface. This modification not only enhanced corrosion protection but also increased adhesion strength. The improved dispersion was attributed to the interaction between amino groups of APTES and the epoxy matrix [177,178]. Zhao et al. [179] employed 1-(3-Aminopropyl)-3-methylimidazolium bromide ionic liquids as both corrosion inhibitors and dispersing agents for MXene nanosheets. The EIS findings revealed impedance values 1-2 orders of magnitude higher than those observed for neat epoxy. Hybridization with other nanomaterials is another method to improve the dispersion. For example, Cai et al. [180] conducted a study wherein they hybridized MXene with MgAl-LDH nanosheets. The stability assessment revealed that, in an epoxy slurry, both MgAl-LDH and MXene underwent precipitation after 30 days. However, MXene@MgAl-LDH hybrids exhibited remarkable stability, remaining stable even after 160 days.

It has been reported that MXenes are susceptible to rapid oxidation and subsequent decomposition when exposed to aqueous environments, with significant degradation occurring within a relatively short timeframe of one week [181,182]. To mitigate rapid oxidation, Ning et al. [183] employed a non-covalent modification approach, utilizing 1-allyl-3-methylimidazolium bromide ionic liquids to treat MXene. After this modification, it was noted that the modified MXene retained its crystalline structure for a duration of 30 days. This preservation was ascribed to the capability of 1-allyl-3-methylimidazolium bromide ionic liquids to effectively quench the OH radical, identified as the primary contributor to MXene oxidation in aqueous solution. The EIS findings also revealed a two-order-of-magnitude enhancement in $|Z|_{0.01\ Hz}$ when incorporating only 1 wt% of MXene modified with ionic liquid, compared to pristine epoxy. Ding et al. [184] employed carbon dots, synthesized from aminosalicylic acid, to modify MXene, establishing covalent Ti-O-C bonds that effectively deterred MXene oxidation. The superior anti-corrosion performance of the epoxy coating incorporating this filler was ascribed to the corrosion inhibition provided by carbon dots, complemented by the physical barrier created by the stable carbon dot/MXene nanosheets.

MXenes possess metallic-like conductivity, which can potentially initiate galvanic corrosion when in contact with defects in underlying metal substrates [185,186]. Consequently, it is imperative to address these concerns and explore advanced strategies for modifying MXenes to attain improved outcomes in the field of corrosion protection. A potential solution involves surface coverage of MXene nanosheets with polymeric materials, such as PAni, to modulate conductivity and avoid direct contact between MXene and the metal surface [187]. On the other hand, the conductive properties exhibited by MXene nanosheets prove advantageous in the context of zinc-rich epoxy coatings. Shen et al. [188] successfully synthesized GO/MXene heterojunctions specifically designed for incorporation into zinc-rich epoxy coatings. The notable conductivity of GO/MXene (1380 ± 10 S/cm), serves to augment the interconnection among isolated zinc particles, thereby amplifying cathodic protection. Furthermore, the inclusion of GO/MXene nanosheets contributes to the enhancement of the coating's barrier properties.

Table 2 provides the recent advances in the application of 2D nanomaterials in epoxy anti-corrosive coating for protecting steel substrate. The advantages and drawbacks of these materials will be discussed in **section 7**.

4. Carbon-based nano carriers

4.1. Carbon nanotube (CNT)

CNTs are cylindrical carbon structures renowned for their

exceptional properties in electrical and thermal conductivity, mechanical strength, and chemical stability [198,199]. Among them, multi-walled CNTs (MWCNTs) have garnered attention due to their superior Young's modulus compared to graphene. With a typical modulus of approximately 1.8 ± 0.9 TPa [200], MWCNTs have the potential to greatly enhance the mechanical properties of polymer nanocomposites, fortifying their structural integrity and strength [201,202]. However, the large surface to volume ratio and hydrophobic nature of MWCNTs, characterized by a lack of polar sites on their surface, presents notable challenges when incorporating them directly into coatings [203,204]. These challenges primarily arise from difficulties in achieving proper dispersion and mitigating the agglomeration of MWCNTs within the coating matrix, hindering the attainment of a uniform distribution throughout the coating material. In order to tackle the challenge, Ghahremani et al. [205] implemented a series of modifications to enhance the surface properties of MWCNT. They achieved this by subjecting the MWCNT to acid treatment, utilizing a mixture of nitric acid (HNO_3) and sulfuric acid (H_2SO_4). Subsequently, they synthesized polydopamine and chitosan (OMWCNT-PDA-CH) layers onto the treated MWCNT surface, employing π-π stacking and hydrogen bonding. The final step involved anchoring Zn^{2+} ions onto this modified platform. Notably, Fig. 17 demonstrated that even after a prolonged immersion period of 9 weeks in salt solution, the OMWCNT-PDA-CH-Zn coating maintained an impedance level exceeding 10^{10} Ω cm^2 at the lowest frequency (0.01 Hz). This remarkable outcome suggests that the coating exhibits exceptional barrier properties, affirming its high-performance capabilities in preventing metal corrosion.

4.2. Carbon nanofiber (CNF)

CNF is another carbonaceous material known for its excellent mechanical, electrical, and barrier properties, making it a valuable component in anti-corrosive coatings [206]. Ge et al. [207] conducted a study wherein carbon nanofibers were integrated into zinc-rich coatings to establish a conductive pathway, enabling the formation of a galvanic cell between a copper substrate and zinc dust. In a separate investigation by Ghaderi et al. [35], the surface of CNF was modified with polydopamine, followed by the loading of La^{3+} ions. This surface modification improved dispersion and endowed the coating with self-healing capabilities. At basic pH, polydopamine detached from the carbon nanofiber platform, forming PDA-Fe complexes, while at acidic pH, La^{3+} ions were released from polydopamine and precipitated in the cathodic region. These actions effectively prevent steel corrosion.

5. Metal organic framework (MOF)

As a new class of nanocontainers, MOFs have emerged as a highly promising class of materials with diverse applications, thanks to their unique properties. MOFs are crystalline porous materials comprising of metal ions or clusters and organic ligands, which can be synthesized with precise control over their structure and composition [208]. The tunable morphology, ultra-high porosity, and well-exposed functional sites make MOFs highly attractive for various applications, from gas adsorption to catalysis and energy storage [209,210]. In the field of corrosion protection, MOFs have shown great potential due to their high specific surface area, abundance of functional groups, and supramolecular characters. While MOFs have traditionally been employed as corrosion inhibitors for metal protection, recent research has explored their use in constructing corrosion-resistant coatings. Unlike traditional nanomaterials, MOFs offer a versatile platform for developing adaptive materials with multiple modes of corrosion protection, enabling the protection of metallic substrates from diverse corrosive agents [211]. In the next section, we will introduce the most frequently used MOFs in the field of anti-corrosive coatings.

5.1. Properties of frequently used MOFs in anti-corrosive coatings

5.1.1. Zeolite imidazole frameworks (ZIFs)

ZIFs are a type of MOFs with a zeolite-like skeleton structure that can be produced through the reaction of zinc or cobalt as metal sources and imidazole or its derivatives as organic ligands in a solvent [212]. ZIFs inherit the structural benefits of MOFs while overcoming their weak chemical and thermal stability to a certain degree. ZIF-8 is a well-known example of ZIFs that was first synthesized by the Chen group [213] and later studied by the Yaghi research group [214]. The chemical formula of ZIF-8 is $Zn(Hmim)_2$, which consists of 2-methylimidazole and zinc ions [215]. Compared to other MOF materials, ZIF-8 is easy to synthesize and has superior chemical and hydrothermal stability, thanks to its robust bonds. Furthermore, ZIF-8 with high specific surface area (typically 1500-2500 m^2/g [216]) can also be tailored to have different structures and pore sizes, which is advantageous for modification. The growth of mesoporous and multistage porous ZIF-8 not only enhances its application versatility but also surpasses the limitations of traditional microporous ZIF-8[217]. Notably, in acidic environment, the coordination between Zn^{2+} cations and $Imidazole^-$ anions undergoes dissociation, leading to the decomposition of ZIF-8 [218].

ZIF-67 belongs to the ZIFs family of MOFs and is composed of Co^{2+} ions coordinated with 2-methylimidazole ligands [219]. The structure of ZIF-67 features pores with an aperture size of approximately 3.4 Å and cavities with a size of around 11.6 Å [220]. These pores and cavities contribute to ZIF-67's significant surface area and excellent adsorption capacity, making it highly desirable for various applications. Moreover, both the Co^{2+} ions and 2-methylimidazole ligands present in ZIF-67 have demonstrated effective corrosion inhibition properties. This suggests that incorporating ZIF-67 into an epoxy matrix could boost the corrosion mitigation characteristics of coatings. However, one of the challenges faced is the water solubility and hydrophilicity of ZIF-67, which can limit its performance in aquatic environments [221].

5.1.2. UiO-66 (Universitetet i Oslo MOF)

UiO-66 was first synthesized at the University of Oslo in Norway. The researchers at the Department of Chemistry, led by Professor Karl Petter Lillerud, developed, and characterized this MOF material in 2008. Since then, UiO-66 has become one of the most extensively studied and widely utilized MOFs in various fields of research and applications. UiO-66 belongs to the Zirconium-based MOFs family and is composed of zirconium oxide nodes coordinated by organic ligands, typically 1,4-benzenedicarboxylate (BDC). It possesses a three-dimensional porous structure with a high surface area and uniform pore size distribution [222]. The high porosity enables UiO-66 to adsorb and store corrosion inhibitors, making it valuable for nanocontainer in anti-corrosive coatings. UiO-66 typically demonstrates good stability when exposed to neutral conditions. Nevertheless, in acidic and basic environments, UiO-66 may exhibit vulnerability, as the metal-organic bonds can undergo degradation. Consequently, this degradation process can result in the deterioration of the structure of the MOF [223,224].

5.2. Application of MOFs in anti-corrosive coatings

5.2.1. Decorating passive nanofillers with MOF as dispersing agent

MOFs have emerged as a particularly promising class of nanofillers due to their remarkable compatibility with a wide range of organic coatings [225–227]. MOFs possess organic linkers imbued with functional groups that enable the establishment of both covalent and non-covalent interactions. These interactions encompass π-π interactions, hydrogen bonding, hydrophobic interactions, and coordination bonds, effectively interacting with the functional groups present in the coating matrix [228]. The compatibility of MOFs empowers them to achieve a homogeneous dispersion within the coating, mitigating the risks of agglomeration and facilitating the formation of a well-integrated composite structure.

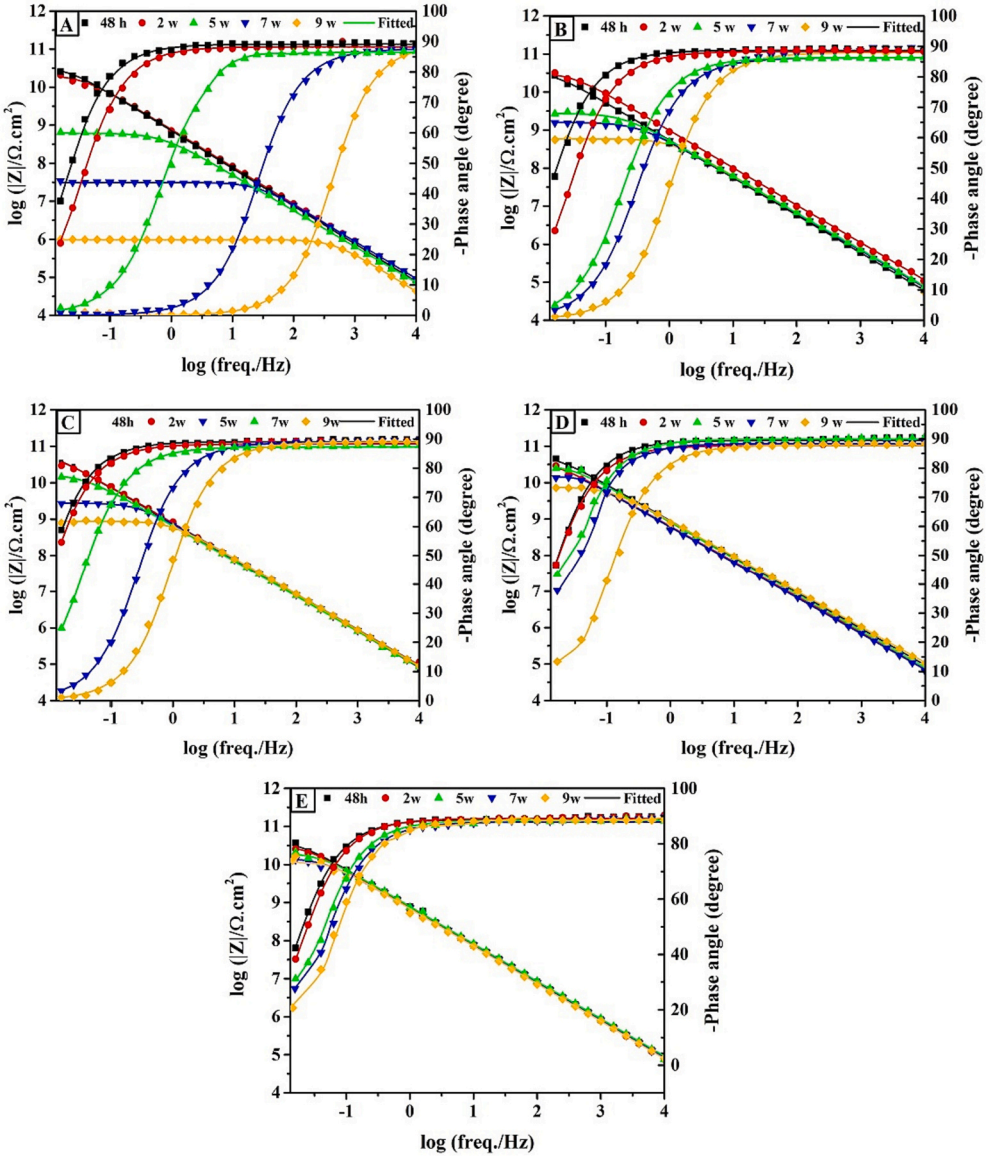

Fig. 17. Bode diagrams of different coatings during exposure in salt solution: Blank/epoxy (A), OMWCNT/epoxy (B), OMWCNT-PDA/epoxy (C). OMWCNT-PDA-CH (D), and OMWCNT-PDA-CH-Zn (E) [205].

MOFs offer a valuable solution as surface modification materials for passive nanofillers. Capitalizing on their extensive functional groups, MOFs possess the ability to tailor the surface characteristics of nanofillers, thereby enhancing their compatibility with coating matrices. For example, as discussed earlier, graphene and its derivatives have remarkable impermeability to corrosion media. However, one of the challenges they face in organic coatings is their tendency to form aggregates owing to the van der Waals forces between graphene layers [229]. Additionally, in certain cases, when graphene is in contact with metal substrates, it may create galvanic pairs, which can accelerate the corrosion process [230]. MOFs present an effective approach to address the challenge of GO (and other nanofillers) dispersion. Through the application of MOFs as surface modifiers, the dispersion of GO can be improved [231]. Moreover, the incorporation of MOFs creates a protective layer, effectively isolating graphene from direct contact with metal substrates. This insulation property serves to prevent the onset of galvanic corrosion, ensuring enhanced corrosion resistance in the system [232].

5.2.2. *Decorating passive nanofillers with MOF as corrosion inhibitor*

It has been shown that MOFs can undergo decomposition in response to external stimuli encountered in the environment. Generally, MOFs are susceptible to change in pH (they are not stable in acidic and basic conditions) which is common during anodic and cathodic reactions [218]. This arises from the dynamic equilibrium between diverse organic ligands and metal ions, which inherently drives the MOF towards a more thermodynamically stable state. Furthermore, it is noteworthy that numerous MOFs consist of metal ions and ligands that possess inherent corrosion inhibiting properties. As a result, the collapse of MOFs can potentially contribute to corrosion mitigation.

A research endeavor carried out by Keshmiri et al. [233] involved the fabrication of an environmentally sustainable coating system utilizing a cerium-based MOF (Ce-MOF) decorated on GO. The synthesis of Ce-MOF nanoparticles was accomplished through the utilization of Ce $(NO_3)_3.6H_2O$ as center metal ions and 1,3,5-benzene tricarboxylic acid as the organic linker, leading to the formation of a densely packed and structured morphology. Ce-MOF was decorated on the GO surface and Ce-MOF@GO pigment was dispersed in epoxy coating. The findings revealed that the introduction of Ce-MOF onto GO led to enhanced

dispersion of GO within solvent borne epoxy coatings. Moreover, the Ce-MOF demonstrated inherent corrosion inhibition properties whereby, under acidic conditions, the release of Ce^{3+} ions from the MOF facilitated their adsorption onto the metal surface, forming a protective layer of cerium oxide/hydroxide and safeguarding the substrate from corrosion (Fig. 18a).

Majidi et al. [234] designed a composite coating based on CNTs. Due to their high surface energy and inherent electronic configuration, CNTs have a tendency to form large aggregates. This characteristic renders CNTs incompatible with polymers, resulting in inadequate barrier performance. To overcome this challenge, a technique was utilized to modify CNTs by treating them with a combination of H_2SO_4 and HNO_3 acids. Following this, a layer of ZIF-8 was decorated onto the surface of the oxidized CNTs, serving as both a corrosion inhibitor and a dispersing agent. As depicted in Fig. 18b, the salt spray analysis of nanocomposite containing 0.15 wt% oxidized CNT/ZIF-8 showed remarkable corrosion resistance after 37 days exposure.

Dehghani et al. [235], synthesized GO using Hammer method. Nonetheless, recent investigations have demonstrated inadequate anti-corrosion effects of GO in solvent-based epoxy systems. This can be attributed to the high concentration of hydroxyl (OH) and carboxyl (COOH) groups in GO nanolayers. The presence of these polar functional groups leads to poor dispersion of the GO layers within the epoxy matrix. Moreover, the natural hydrophilicity of GO contributes to an elevated water uptake of epoxy coatings. For addressing this challenge, GO was reduced via chitosan biomolecules and decorated by ZIF-9 (a MOF that consists of Co^{2+} ions and benzimidazole). The findings showed considerable improvement in self-healing and barrier properties and adhesion to the substrate, higher contact angle, and lower water uptake for epoxy coating with reduced GO/chitosan (CS)/ZIF-9 pigment (Fig. 19).

5.2.3. Active MOF-based nanocarrier

Based on the previous section, MOFs exhibit exceptional compatibility with organic coating matrices owing to diverse interactions with the organic linkers of MOF and the coating. Furthermore, the high specific surface area and copious porosity inherent in MOFs offers a versatile platform for encapsulating a wide range of healing agents and corrosion inhibitors. Besides, MOFs have the capability of undergoing controlled decomposition when exposed to external stimuli present in the environment. Consequently, this intrinsic property facilitates the controlled and regulated release of the loaded cargoes. Given the aforementioned attributes of MOFs, it is a rational and compelling approach to design active nanofillers based on MOFs that not only demonstrate compatibility with the coating matrix but also exhibit adjustable release properties when subjected to external stimuli, while maintaining a notable loading capacity.

Active nanofillers based on MOFs can be categorized into two primary groups: MOFs nanocontainers and hybrid fillers that utilize MOFs as gatekeepers that are responsive to external stimuli. In the case of MOFs nanocontainers, the healing agents or corrosion inhibitors are encapsulated within the pores and cavities of MOFs. By adopting this configuration, MOFs are able to fulfill dual roles as carriers and regulators, granting control over the release of the loaded substances. On the other hand, hybrid nanofillers employ other porous materials as hosts for the healing agents/corrosion inhibitors, while MOFs act as surface nanovalves on the nanocomposites. These nanovalves provide the means to regulate and modulate the release process as desired.

The conventional methodology for fabricating MOF containers typically involves a two-step process, starting with the synthesis of MOFs followed by the adsorption of corrosion inhibitors under vacuum with continuous stirring. Nevertheless, a prevalent challenge encountered in this strategy is that the corrosion inhibitor molecules are often smaller than the pores of the chosen MOFs. Consequently, the inadvertent leakage of corrosion inhibitors during both the washing procedure and the operational lifespan becomes an inevitable concern. Furthermore, in order to enhance the intermolecular interactions and achieve maximum loading capacity, it is crucial to ensure congruent polarity between the corrosion inhibitors and MOFs. This entails selecting corrosion inhibitors with polarity that aligns with the core characteristics of the MOFs, thereby optimizing their affinity and binding efficiency. By carefully considering the polarity match, the effectiveness of corrosion protection applications can be significantly enhanced [228].

In a study by Mohammadkhah et al. [236], a new functional pigment utilizing MoS_2/ZIF-8 was reported. Subsequently, a hybrid organic-inorganic corrosion inhibitor based on glutamate-Zn^{2+} was incorporated into ZIF-8 (as shown in Fig. 20a). The resulting nanocomposite, comprised of MoS_2/ZIF-8/glutamate-Zn^{2+}, demonstrated remarkable corrosion resistance. This superior performance was attributed to the barrier properties of MoS_2 and the controlled release of corrosion inhibitors from the ZIF-8 nanocontainer.

In a study conducted by Sanaei et al. [140], LDH was utilized for its ion exchange properties, which enable the storage of anionic corrosion inhibitors within its galleries. However, to address the limitations mentioned earlier, such as restricted intergallery space, limited options for corrosion inhibitors, poor compatibility with polymer matrices, unregulated release of inhibitors, and instability in acidic and basic environments, a hybrid material was formed by incorporating rGO (graphene oxide reduced with L-cysteine) with LDH. This hybridization was motivated by the low water permeability of GO. Subsequently, a core-shell structure of ZIF-67/ZIF-8 was synthesized on the surface of the rGO/LDH composite, offering a high specific surface area and controlled release capabilities. Finally, the formed structure was filled with sodium glutamate, which served as the corrosion inhibitor. The rGO/LDH/ZIF-67/ZIF-8 core/shell structures loaded with sodium glutamate demonstrated the highest level of inhibition and exhibited exceptional durability in their anti-corrosion function. Intriguingly, the introduction of ZIF-8 shells around the ZIF-67 particles optimized particle stability and allowed for controlled release of the inhibitor, thereby controlling the rate of MOF particle destruction. The remarkable barrier properties achieved in the fabricated coating can be attributed to two key factors: the enhanced hydrophobicity of GO layers resulting from reduction by L-cysteine, and the improved dispersion of LDHs within the epoxy matrix. Furthermore, the LDHs effectively adsorbed Cl^- ions and released sodium glutamate molecules, while the pH sensitivity of the ZIF-67/ZIF-8 core/shell structures, along with the controlled release of inorganic (e.g., Zn^{2+} of ZIF-8 and Co^{2+} of ZIF-67) ions and organic (e.g., sodium glutamate and 2-methylimidazole) molecules, contributed to active corrosion mitigation in saline media (Fig. 20b).

Dehghani et al. [237] designed a nanopigment based on APTES-MWCNT- ZIF67-MoO_4^{2-}. In this work, ZIF-67 was loaded on acid modified MWCNT and then loaded with MoO_4^{2-} corrosion inhibitor. To improve dispersion within the silane matrix, the prepared filler was coated with APTES. The total resistance of the silane coating, which contained APTES-MWCNT-ZIF67-MoO_4^{2-}, exhibited a significant increase from 7059 Ω cm^2 (after 1 h of immersion) to 13,565 Ω cm^2 (after 24 h). This substantial increase implies the self-healing capability of the coating. The inhibition mechanism relies on the interaction between released 2-methylimidazole and MoO_4^{2-} corrosion inhibitors with iron ions, resulting in the formation of a protective layer. However, it has been reported in the literature that 2-methylimidazole alone is not capable of providing adequate inhibition. Nevertheless, the existence of MoO_4^{2-} compensates for this limitation by facilitating the formation of $FeMoO_4$ and $Fe2(MoO_4)_3$ through the following reactions:

$$Fe^{2+} + {MoO_4}^{2-} \rightarrow FeMoO_4$$

$$Fe^{3+} + {MoO_4}^{2-} \rightarrow Fe_2(MoO_4)_3$$

Moreover, Co^{2+} has the ability to form protective layers such as $Co(OH)_2$ and CoO on the metal surface, offering additional protection (Fig. 20c).

The in-situ preparation strategy is a highly effective method for

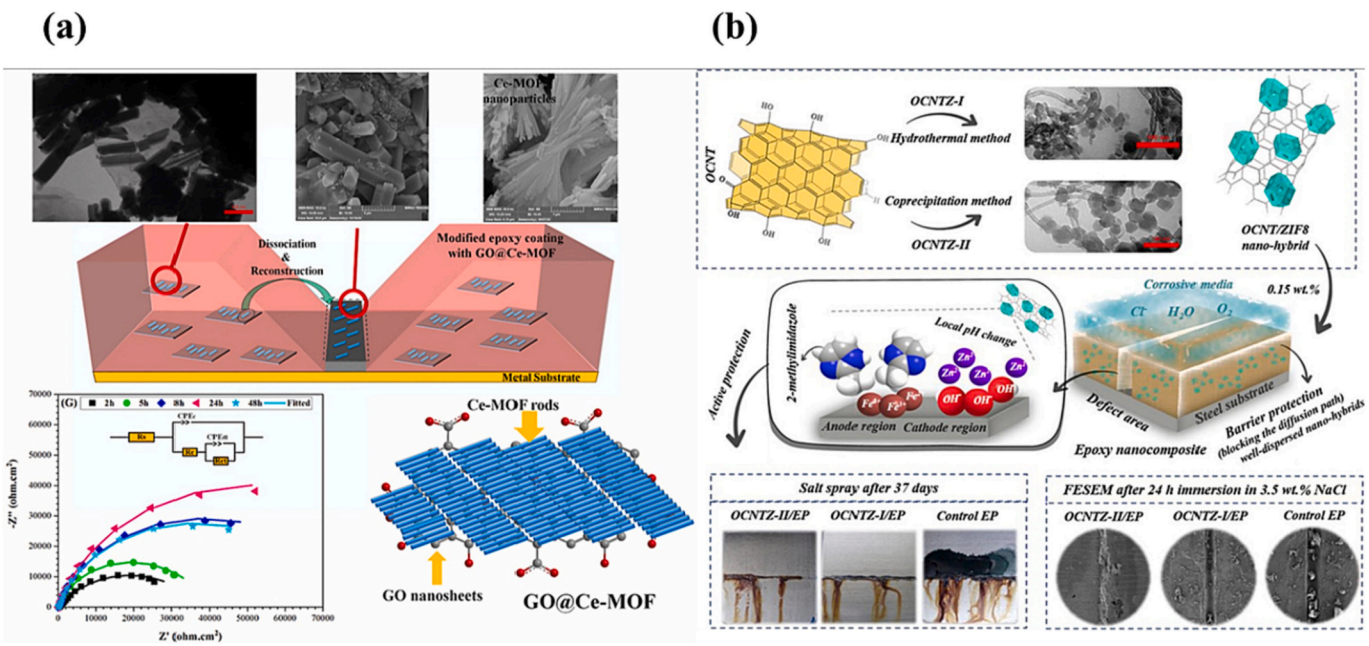

Fig. 18. Decorating passive nanofillers with MOFs: Inhibition mechanism of Ce-MOF@GO pigments in saline media (a) (adapted from reference [233]). Synthesis procedure, anti-corrosion mechanism, salt spray and FE-SEM images of nanocomposite coating with and without oxidized CNT/ZIF-8 pigments (b) (adapted from reference [234]).

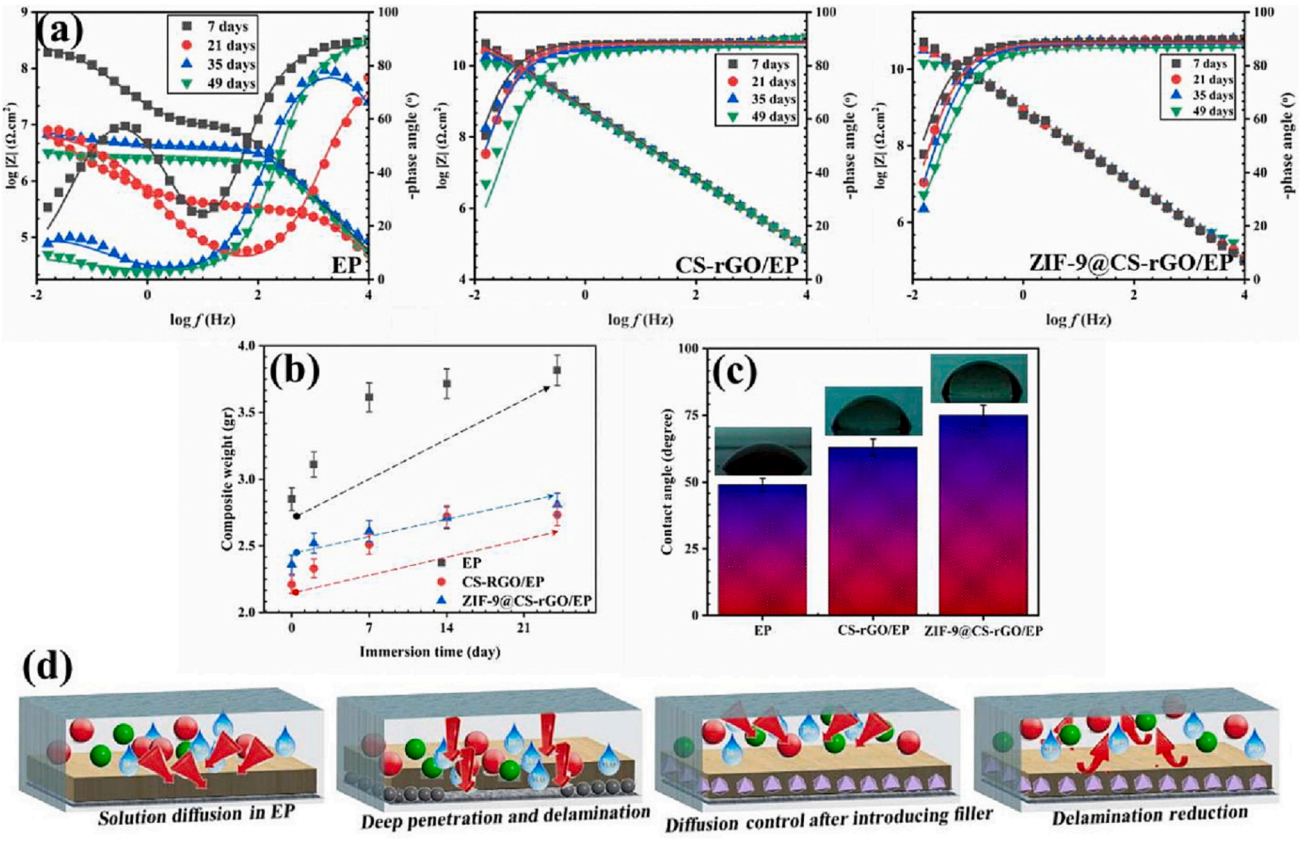

Fig. 19. Nyquist and Bode plots of intact coatings after 49 days immersion in saline solution (a), water uptake of different coating during 24 days of exposure in saline solution (b), contact angle of the coating before exposure(c) and protection mechanism of reduced GO/CS/ZIF-9 pigment (d) [235].

integrating corrosion inhibitors into MOFs, offering two distinct avenues. Firstly, during the formation process of MOFs, corrosion inhibitors can be directly encapsulated within the nanochannels. Secondly, healing agents/corrosion inhibitors can be synthesized within the cavities of MOFs, starting from small molecules, and gradually building up to larger components. The ligand exchange technique serves as a convenient and

efficient approach for in-situ synthesis of MOFs containers. In this method, corrosion inhibitors containing elements such as N, O, and S function as modulating ligands, competing with the organic ligands of the desired MOFs. Initially, these corrosion inhibitors form coordination bonds with the central ions of the MOFs. Subsequently, the corrosion inhibitors are substituted by the organic ligands, resulting in the formation of MOF containers where the corrosion inhibitors are retained within the pores or situated onto the surface of the MOFs [241]. For example, in a study conducted by Yang et al. [242], they successfully synthesized BTA@ZIF-8 using a one-pot method. The synthesis process involved the preparation of two solutions. Solution A comprised 2-methylimidazole dissolved in methanol, while solution B consisted of BTA,

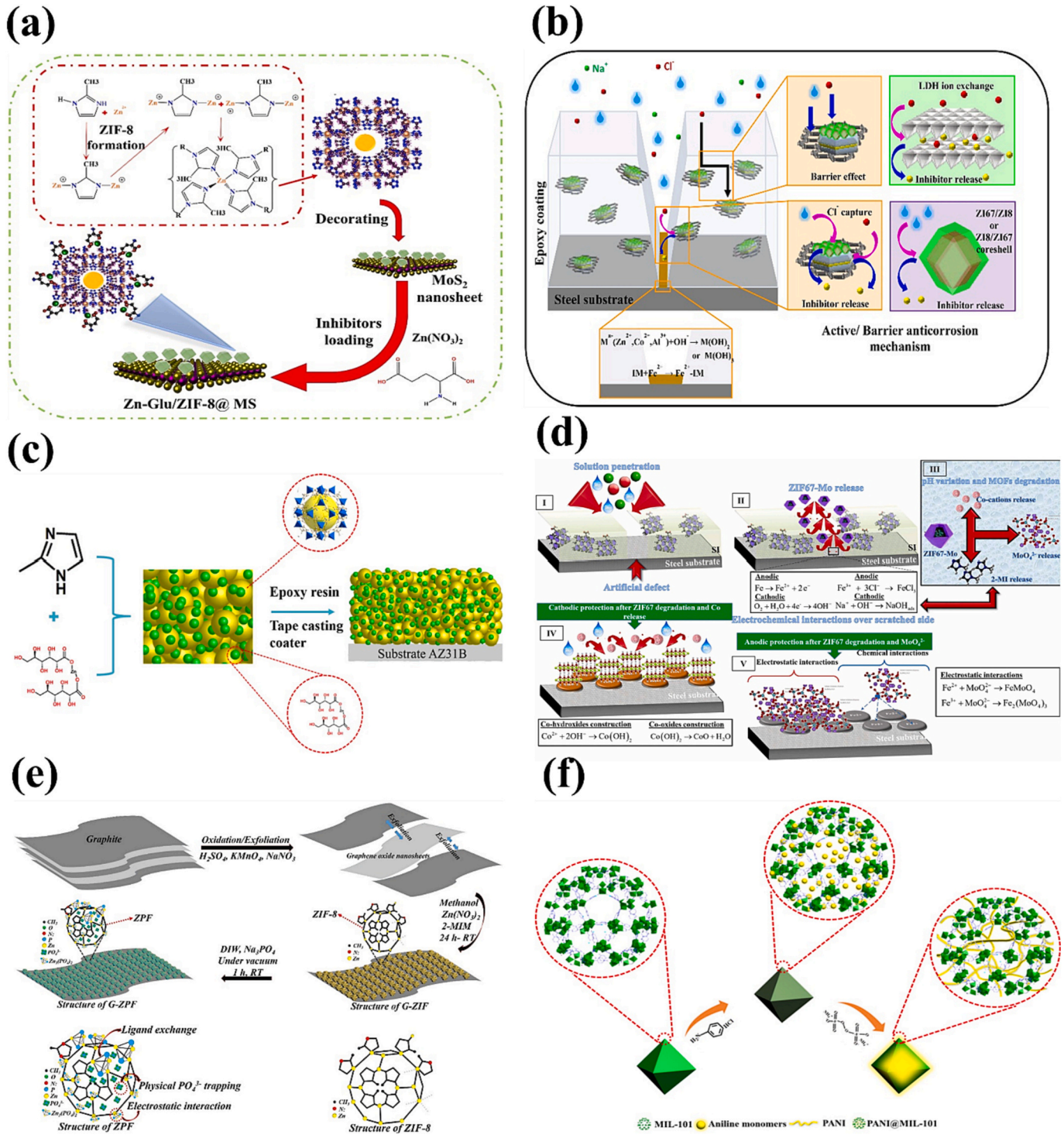

Fig. 20. Synthesis procedure MoS_2/ZIF-8/glutamate-Zn^{2+} pigments (a) (adapted from reference [236]). Inhibition mechanism of sodium glutamate loaded into rGO/LDH/ZIF-67/ZIF-8 core-shell structure (b) (adapted from reference [140]). The inhibition mechanism of silane coating incorporating APTES-MWCNT- ZIF67-MoO_4^{2-} (c) (adapted from reference [237]). The schematic of synthesis process of ZnG@ZIF-8 (d) (adapted from reference [238]). Synthesis procedure and different mechanism of formation of zinc phosphate based double ligand MOF (e) (adapted from reference [239]). Fabrication process of PAni@MIL-101 (f) (adapted from reference [240]).

and zinc nitrate hexahydrate dissolved in methanol. The synthesis process involved pouring solution A into solution B and stirring the mixture for a duration of 3 h. Subsequently, the resulting product, BTA@ZIF-8, was subjected to washing and drying under vacuum to obtain the final material. It is important to note that in this study, the encapsulation of BTA took place in-situ and in a single step during the synthesis of ZIF-8.

Another technique involves the direct incorporation of corrosion inhibitors in a composite mixture comprising metal ions and organic ligands, thereby enabling the production of MOF-based nanocontainers. During the nucleation phase of MOFs, a significant quantity of corrosion inhibitors becomes in-situ intercalated within the core and channels of the MOFs, eliminating the need for additional encapsulation steps. The distinction between this technique and previous methods lies in the fact that in this approach, the metal salt consists of a metal cation that actively participates in the nucleation process of MOFs, in conjunction with an anion that inherently possesses corrosion inhibition ability. As the metal cation forms coordination bonds with the organic ligands to produce MOFs, the anionic corrosion inhibitors become entrapped within the MOFs structure. Ren et al. [238] utilized eco-friendly zinc gluconate (ZnG) as a source of zinc cation, which is crucial for constructing ZIF-8. Additionally, gluconate anions in zinc gluconate possess corrosion inhibition properties. They added the solution containing zinc gluconate in methanol to the solution of 2-methylimidazole in methanol, leading to the formation of ZnG@ZIF-8 pigments. These nanopigments were then incorporated into an epoxy coating to provide protection for AZ31B Mg alloy (Fig. 20d).

The double ligand strategy is another interesting approach for the formation of MOFs. This method involves the simultaneous use of two different ligands during the synthesis of a MOF, resulting in a material with enhanced properties and tailored functionalities. This strategy is specially employed for MOFs that incorporate ligands containing nitrogen and polycarboxylic groups [243]. The primary objective of the double ligand strategy is to combine the coordination chemistry of two distinct ligands to control and fine-tune the structural characteristics of the MOF. Typically, one ligand serves as the primary linker, coordinating with the metal ions to form the framework's backbone. This primary linker determines the connectivity and geometry of the resulting MOF structure. On the other hand, the second ligand, known as the modulator or auxiliary ligand, plays a crucial role in modifying the MOF properties. It can influence various aspects, such as the pore size, surface area, thermal stability, and chemical reactivity of the material. By carefully selecting and incorporating the auxiliary ligand, researchers can customize the MOF's functionality to suit specific applications. The double ligand strategy provides an avenue for introducing diverse functionalities and chemical environments within the MOF framework. This flexibility allows for the creation of MOFs with tailored properties, making them suitable for a wide range of applications. For instance, by using an auxiliary ligand with specific functional groups, the MOF can exhibit selective adsorption properties, catalytic activity, or guest molecule recognition capabilities. Additionally, the double ligand strategy enables the incorporation of multiple metal ions or metal clusters within the MOF framework, enhancing its structural complexity and diversity.

Ramezanzadeh et al. [239] employed a double ligand strategy to construct an advanced zinc phosphate-based MOF with high thermal resistivity on GO. The synthesis procedure, illustrated in Fig. 20e, involved the formation of ZIF-8 on GO, followed by the addition of PO_4^{3-} as a second ligand. They suggested that the phosphate ion could be incorporated into the structure via ligand exchange with 2-methylimidazole, physical entrapment within the ZIF-8 framework, and electrostatic attraction between Zn^{2+} cations and PO_4^{3-} anions. The results showed higher mechanical and anti-corrosion (synergetic effects of GO barrier and released Zn^{2+}, PO_4^{3-}, and 2-methylimidazole corrosion inhibitor) properties as well as lower adhesion loss and cathodic disbonding for epoxy coating containing zinc phosphate-based MOF/GO.

The pores of MOFs offer a favorable medium for the incorporation of small molecular components or monomers. This enables the in-situ polymerization of the loaded monomers within the pores, resulting in the formation of a composite. Notably, conductive polymers hold significant promise in the realm of anti-corrosion applications due to their excellent substrate adhesion, electrochemical activity, and non-toxic nature [244–246]. PAni is a highly promising conductive polymer extensively utilized in anti-corrosive coatings. This is primarily due to its straightforward synthesis method, electrical conductivity, and environmental-friendly properties [247,248]. The protective properties of PAni against metal corrosion stem from its ability to undergo reversible reactions between various oxidation states [249]. This phenomenon facilitates the formation of a passive Fe_2O_3 layer, thereby

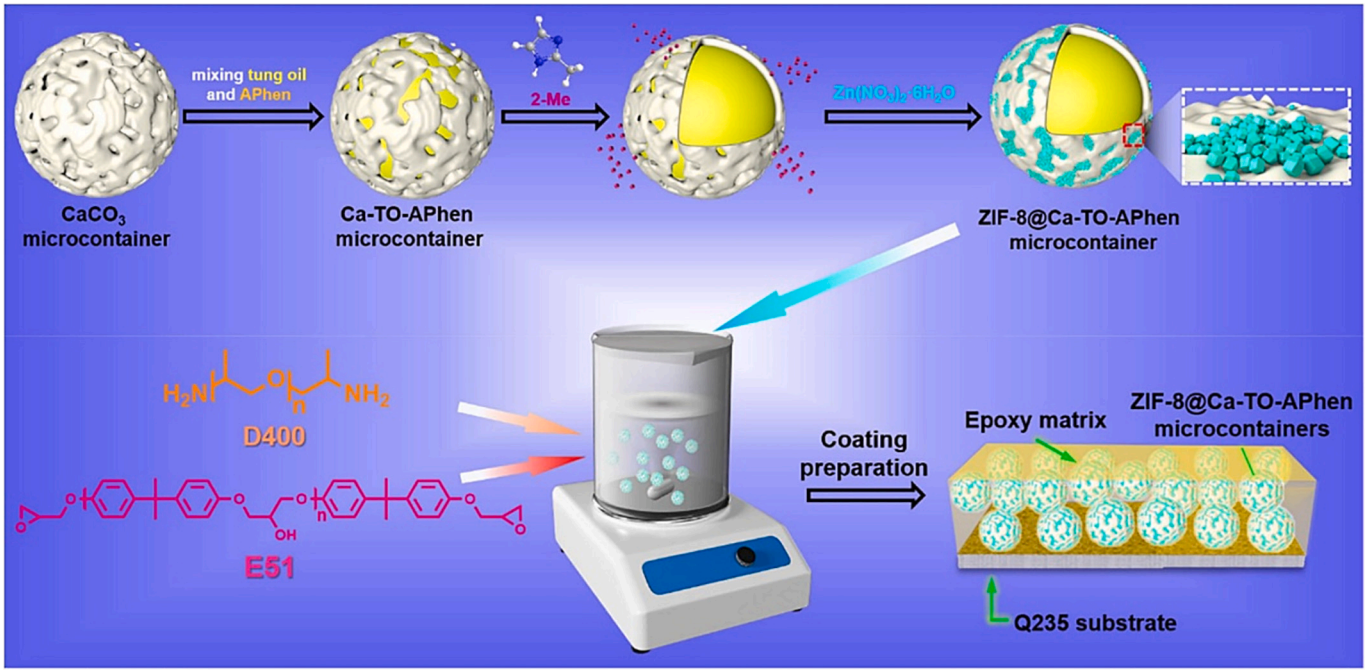

Fig. 21. Schematic of synthesis process of ZIF-8@Ca-TO-APhen [252].

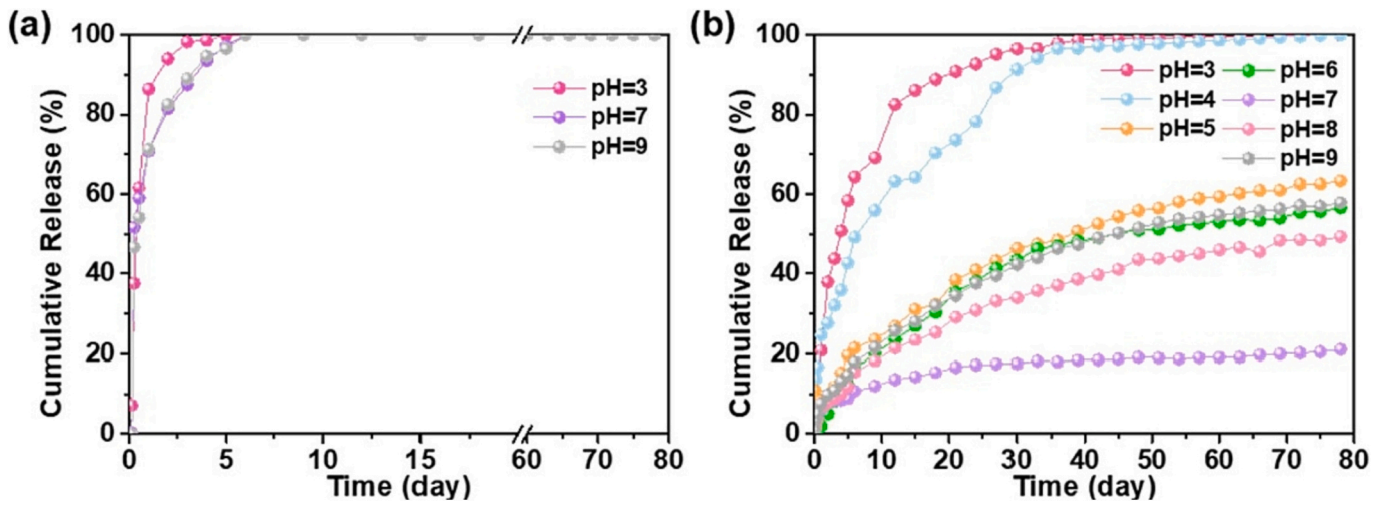

Fig. 22. Release behavior of APhen from Ca-TO-APhen (a) and ZIF-8@Ca-TO-APhen (b) (adapted from reference [252]).

reducing metal corrosion [250]. However, the limited dispersion of PAni in water and other organic solvents restricts its usage as a filler in coatings. Ren et al. [240], utilized MIL-101 metal organic framework as a host for loading PAni as shown in Fig. 20f. The in-situ polymerization of aniline within the pores of MIL-101 offers several advantages for the corrosion protection of the PAni@MIL-101 nanocomposite. This approach not only enhances the corrosion protection capabilities of the composite but also resolves the challenges associated with the direct incorporation of PAni.

Moreover, MOFs have emerged as versatile decorations with stimuli-responsive characteristics, serving as gatekeepers on the surfaces of diverse porous materials that accommodate healing agents or corrosion inhibitors. This innovative configuration enables precise modulation of the release kinetics of these agents. Acidic or alkaline conditions are commonly employed as stimuli to trigger the controlled degradation of the MOFs gatekeepers. Notably, during the corrosion processes, the formation of micro-anodic and micro-cathodic regions occurs at localized defect sites. These micro-anodic areas are typically associated with an acidic environment due to the hydrolysis of metal cations, while the micro-cathodic regions exhibit alkaline conditions resulting from the oxygen reduction reaction. Moreover, the acidic or alkaline conditions exert an influential effect on the coordination bonds within the MOFs. In acidic environments, the Lewis acid nature of H^+ ions compete with the metal ions of the MOFs, forming complexes with the Lewis base organic linkers and inducing their protonation. Furthermore, under alkaline conditions, certain metal ions within the MOFs can be transformed into $M(OH)_n$ species through interactions with OH^- ions [251].

Tong et al. [252], reported a self-sensing and self-healing coating incorporating $CaCO_3$ (Ca) filled with tung oil (TO, as healing agent), and 1,10-phenanthrolin-5-amine (APhen, as corrosion inhibitor and sensing indicator) capped by ZIF-8 (Fig. 21). Fig. 22 shows the release behavior APhen from Ca-TO-APhen and ZIF-8@Ca-TO-APhen from pH 3 to 9. The figure clearly shows that in the absence of the ZIF-8 gatekeeper, all of the APhen molecules were released from the container within 5 days. The release rate was highest in acidic pH conditions, which can be attributed to the dissolution of the Ca container in acidic media. The incorporation of ZIF-8 as a capping material allows for controlled release of APhen. The release rate of APhen was faster in acidic conditions compared to alkaline conditions because both ZIF-8 and the calcium container dissolved in acidic media, whereas in alkaline conditions, the calcium container retained its structure. Consequently, the presence of ZIF-8 as a gatekeeper enables achieving controlled pH-triggered release over extended periods of immersion.

In summary, MOFs-based nanofillers can work in three ways to improve the performance of the coatings: 1) by obstructing the pathways through which the corrosive media can penetrate the coating (physical barrier), 2) by enabling the release of loaded corrosion inhibitors upon the activation of external stimuli (e.g., change in pH) and, 3) via good dispersion in solvent-based epoxy coating due to abundant functional groups which could effectively react with epoxy matrix, facilitating their dispersion [228]. Nevertheless, there are significant challenges associated with their implementation that must be addressed. As previously discussed, the most fascinating applications of MOFs lies in their ability to serve as nanocontainers for corrosion inhibitors due to their ultra-high specific surface area. The foremost concern with MOFs is their instability in acidic and basic environments [253,254]. Additionally, MOFs tend to undergo self-decomposition over time in water [253]. Some researchers have postulated that the collapse of the MOF structure could potentially protect metals from corrosion, given that numerous MOFs consist of metal ions and ligands that inherently exhibit corrosion inhibition properties [255]. However, such a claim is at odds with the fundamental purpose of utilizing MOFs as nanocontainers, since degraded nanocontainers are incapable of storing corrosion inhibition agents efficaciously. Consequently, while the use of MOFs as nanocontainers for corrosion inhibitors holds great promise, it necessitates an ample understanding of the potential drawbacks that come with their application.

6. Covalent organic framework (COF)

Since their discovery in 2005 by Yaghi et al. [256], COFs have garnered significant attention. These porous polymers, composed of light elements like carbon, hydrogen, oxygen, nitrogen, and boron, are interconnected through reversible covalent bonds. This leads to the formation of 2D or 3D structures with extensive π-conjugated interfaces and reticulated arrangements [257]. COFs showcase exceptional properties, such as high adsorption capacity, low density (down to 0.17 g cm^{-3}) adjustable porosity, high specific surface area (up to 5083 m^2/g), permanent porosity, recyclability, and well-ordered structures [258–260]. In summary, the differences between MOFs and COFs can be summarized as follows:

1- Bonding: MOFs consist of metal ions/clusters connected to organic ligands through coordination bonds, while COFs are constructed from organic ligand with light elements connected through strong covalent bonds [261].
2- Stability: COFs exhibit excellent chemical (in water and acidic and basic conditions) and thermal stability due to their covalent bonds, while MOFs can be less stable due to the potential degradation of metal-organic coordination bonds [259,261–264].

3- Tunability: COFs offer the advantage of tunable structures, allowing precise control over their chemical composition and connectivity, while MOFs also exhibit tunability to some extent but with limited structural flexibility [265].
4- Synthesis and affordability: Generally, COFs have more complex synthesis procedures and can require expensive raw materials, making their production more challenging and costly compared to MOFs. Additionally, COFs typically exhibit lower crystallinity due to the reversible nature of their covalent bonds [266].

COFs encompass various types based on their structural features and constructing units. The primary classifications include imine-, triazine-, boron-, and imide-based COFs. Boron-containing COFs are further categorized into two groups: those formed through the co-condensation of multiple units and those developed through the self-condensation of single units. These COFs often exhibit low densities, exceptional BET specific surface areas, and impressive thermal stability up to temperatures ranging from 450 to 600 °C. However, despite their good stability in organic solvents, many boron-based COFs are prone to degradation in the presence of water or humid environments [267]. Covalent triazine-based frameworks (CTFs), commonly referred to as triazine-based COFs, are synthesized via cyclotrimerization reactions involving nitrile precursors. CTFs generally possess relatively lower crystallinity compared to boron-containing COFs but showcase remarkable chemical and thermal stability. The abundant nitrogen atoms in CTFs make them highly promising candidates for serving as carriers for catalysts [265,267].

Imine-based COFs are divided into two classes on the basis of the covalent formation modes of -C=N- bonds. One type is known as hydrazone-linked COFs, which are developed via the co-condensation reaction between aldehydes and hydrazides. The other type falls under the “Schiff base” classification, assembled via the co-condensation of aldehydes and amines. Imine-based COFs exhibit comparable crystallinity to boron-based COFs but demonstrate outstanding structural regularity compared to CTFs. They also exhibit outstanding water resistance and maintain their stability in a wide range of organic solvents. The presence of nitrogen atoms within imine-based COFs allows for potential chelation with various metal ions, making them potentially valuable as materials for metal ion sensing [267]. Imide-based COFs, characterized by the presence of imide linkages, are highly noteworthy for their exceptional thermal stability and expansive surface areas. These COFs have drawn significant interest for their potential applications in drug delivery, owing to their porous structures capable of accommodating guest molecules [265].

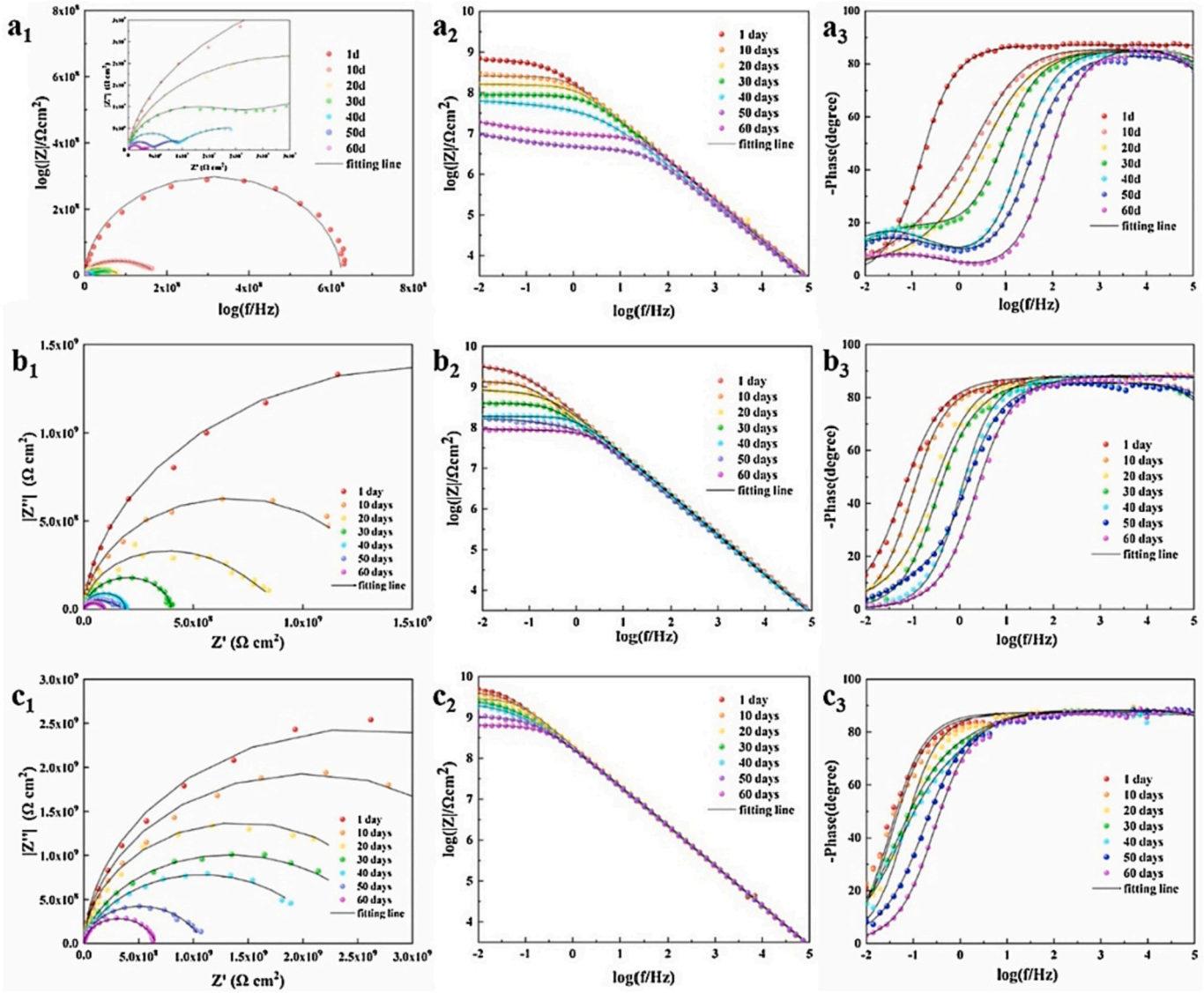

Fig. 23. Nyquist, Bode and phase angle plots of blank (a_1, b_1, c_1), TpPa-1/epoxy (a_2, b_2, c_2), and BTA-TpPa-1 (c_1, c_2, c_3) after exposure in saline solution [270].

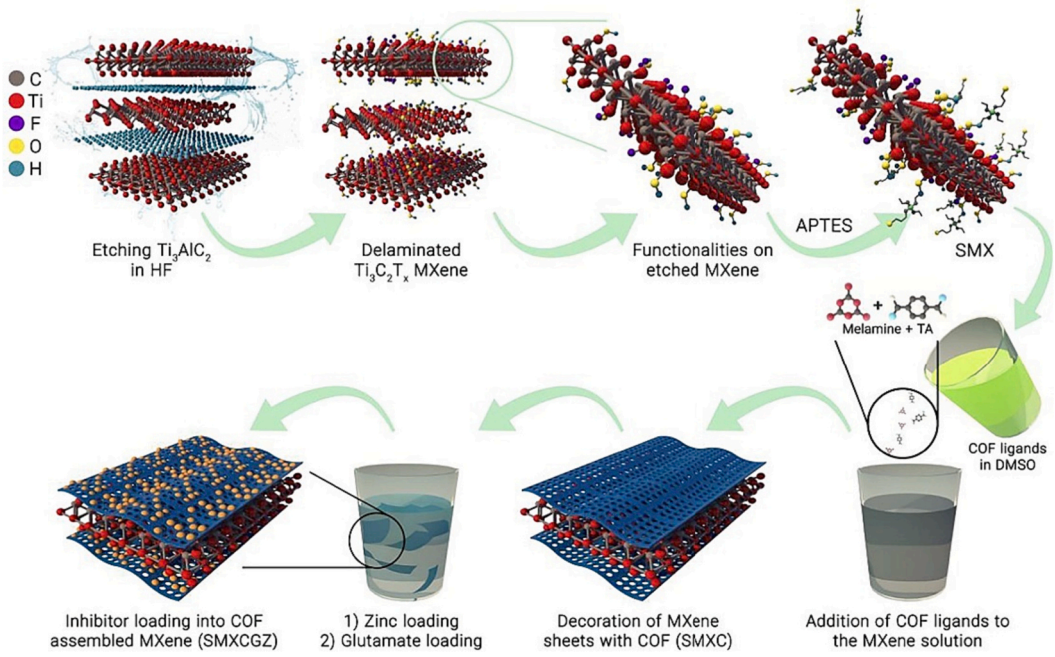

Fig. 24. Synthesis of MXene/imine-based COF loaded with zinc and glutamate [275].

The application of COF in anti-corrosive coatings is new, but it has been attracting increasing attention from researchers in recent times. As an emerging field of study, researchers are now focusing on exploring the potential of COF as a valuable component in anti-corrosive coatings. This growing interest reflects the recognition of COF's unique properties and its potential to enhance the corrosion resistance of various substrates [268]. Several publications by Chen [269–272] have concentrated on the application of 2D TpPa-1 COF, which comprises 1,3,5-triformylphrogroglucinol (Tp) and 1,4-phenylenediamine (Pa-1). This 2D COF demonstrated remarkable properties by harnessing the advantageous features of both 2D materials (labyrinth effect), and porous materials (high specific surface area). This 2D-COF, unlike other traditional 2D materials, exhibits self-dispersibility within an epoxy matrix due to its weaker interlayer interactions. Furthermore, the crosslinking between the amino groups in the COF monomers and the epoxy resin not only improves compatibility but also enhances the physical and mechanical properties of the resulting coating [271].

In one research study, the surface of TpPa-1, characterized by a specific surface area of approximately 154 m^2/g and a pore size of 1.5-2 nm, was utilized for the loading of BTA to construct a self-healing epoxy anti-corrosive coating. Through Zeta potential analysis, it was observed that TpPa-1 and BTA possessed opposite surface charges within the pH range of 4 to 7. Thus, to optimize the adsorption of BTA, the pH was adjusted to 5. The amount of loaded BTA was estimated to be 9 and 11 % based on TGA and DSC analysis, respectively. The EIS analysis showed that coating with 0.5 wt% BTA-TpPa-1 had higher impedance at the lowest frequency (0.01 Hz) compared to TpPa-1 containing and blank epoxy coating, demonstrating good self-healing ability of BTA-TpPa-1 incorporating coating (Fig. 23) [270].

The imine-based COF formed by combining terephthalaldehyde (TA) and melamine is another COF that has garnered significant attention in the field of anti-corrosive coatings. This COF exhibits compatibility with epoxy matrices, low density, relatively high specific surface area, and better chemical stability compared to MOF in harsh conditions [273,274]. These characteristics make it well-suited for applications such as containers for loading corrosion inhibitor and surface modifier for better dispersion of other fillers in the coating [273,275]. In a study conducted by Najmi et al. [275], in order to prevent oxidation and restacking as well as increase specific surface area of MXene, highly porous imine-based COF was decorated on APTES modified MXene and subsequently loaded with zinc and glutamate inorganic-organic corrosion inhibitor (Fig. 24). The incorporation of this nanopigment into epoxy coating resulted in higher corrosion resistance and lower adhesion loss and cathodic disbonding.

Table 3 summarizes the application of different MOFs and COFs in epoxy anti-corrosive coatings for protecting steel substrate.

7. Summary of the advantages and drawbacks of carriers

Table 4 provides a comprehensive summary of the notable advantages and drawbacks associated with various carriers/barriers utilized in the context of anti-corrosive coatings. This table serves as a valuable reference, offering a holistic perspective on the unique characteristics and considerations associated with each material, thereby facilitating informed decision-making in the selection of suitable carriers/barriers for corrosion protection applications.

8. Challenges faced by smart coatings for corrosion protection

Smart coatings have emerged as a transformative technology, promising enhanced surface functionality and durability. However, the journey towards their widespread adoption encounters several challenges. First, the feasibility and cost of large-scale production for the carrier are crucial considerations, especially given that some carriers can be complex and expensive to synthesize. Secondly, the procedure for loading corrosion inhibitors typically involves the adsorption of the inhibitor into/onto the carrier under vacuum, which necessitates energy consumption. Clearly, the adsorption time depends significantly on the type of carrier and corrosion inhibitors, and increasing the time or concentration of corrosion inhibitor does not always result in higher loading. Therefore, optimization is crucial to effectively utilize energy and raw materials. On the other side of the story, a third point is that usually in research investigations, the effect of smart pigments for the protection of metal is investigated using EIS and salt spray tests without attempting to explore other properties of the coating. Practical applications reveal that coating failure is not exclusively related to corrosion. The high crosslinking density adversely affects the coating's flexibility, rendering it more susceptible to brittleness, thereby increasing the

Table 3
Different MOFs and COFs and their roles in epoxy anti-corrosive coatings for protecting steel.

Pigment	Roles of MOF/COF	Corrosion Inhibitor	Comments	Trigger	Reference
ZIF-9@PAni-rGO	Corrosion Inhibitor	ZIF-9 (Co^{2+} ions and benzimidazole)	As previously discussed, GO and PAni act as physical barrier and self-redox catalyst, respectively. The total resistance of epoxy coating containing ZIF-9@PAni-rGO increased by 16 times compared to blank in the best situation. Furthermore, adhesion loss was reduced from 57 % (neat epoxy) to 46 % (ZIF-9@PAni-rGO/epoxy)	pH	[276]
Benzimidazole@bio-MOF-1	Container	Benzimidazole and adenine	Bio-MOF-1 was synthesized by reacting zinc acetate dihydrate, 4,4′-biphenyl dicarboxylic acid, and adenine and then benzimidazole was encapsulated in its structure.	–	[277]
La-MOF	Barrier and corrosion inhibitor	La-MOF (La^{3+} ions and terephthalic acid ligand)	Even after 12 weeks of immersion, the epoxy coating incorporating 0.15 wt% La-MOF demonstrated an impressive impedance value exceeding $10^{10.7}$ at the lowest frequency of 0.01 Hz. Furthermore, the adhesion loss was notably reduced from 31.2% for the neat epoxy to 16.6% for the epoxy coating based on La-MOF.	pH	[278]
2-mercaptobenzothiazole loaded ZIF-67 decorated on Sepiolite	Container and corrosion inhibitor	Co^{2+} and 2-mercaptobenzothiazole	Sepiolite is a natural clay mineral that is primarily composed of magnesium, silicon, hydrogen, and oxygen. In this research sepiolite was used as physical barrier.	pH	[279]
NH_2-Ce-MOF/GO	Dispersing agent	–	Improved dispersion was obtained by applying NH2-Ce-MOF (the synthesis involving of diamino terephthalic acid, cerium trichloride heptahydrate, and triethylamine, onto GO leading to enhanced corrosion resistance.	–	[280]
MIL-88A/GO	Corrosion Inhibitor and dispersing agent	MIL-88A (Fe^{3+} cations and fumarate anions)	MIL-88A synthesized through reaction of iron (III) chloride hexahydrate and fumaric acid.	pH	[281]
BTA/PPy/MIL-88(Fe)	Container and corrosion inhibitor	MIL-88A (Fe^{3+} cations and terephthalate) and BTA	synthesis of MIL-88A involved reacting iron (III) chloride hexahydrate with terephthalic acid. PPy was used to prevent direct contact between the corrosion inhibitor and the epoxy matrix. Additionally, the existence of PPy facilitated the growth of the passive layer.	pH	[282]
Oxidized MWCNT/ZIF-8	Corrosion inhibitor and dispersing agent	ZIF-8 (Zn^{2+} and 2-methylimidazole)	–	pH	[283]
Zn^{2+} and glutamate loaded ZIF-8 decoratedMoS_2	Corrosion inhibitor and dispersing agent and container	Zn^{2+} and 2-methylimidazole and glutamate	–	pH	[284]
APTES modified MoS_2/imine-based COF loaded with europium cation	Container and dispersing agent	Europium cations	MoS_2 was employed as a physical barrier. To address the dispersion problem, an imine-based COF was decorated on the surface of APTES modified MoS_2. Subsequently, europium corrosion inhibitors were adsorbed in the COF nanocontainer. The choice of imine-based COF was based on the presence of nitrogen atoms in its structure, which enhance the adsorption/desorption capability of corrosion inhibitors.	pH	[273]
Oxidized CNT/ with imine-based COF loaded with zinc cations	Container and dispersing agent	Zn^{2+} cations	–	pH	[274]
BTA@mesoporous silica covered with chitosan loaded on 2D TpPa COF	Barrier and dispersing agent	BTA	In this research, researchers utilized mesoporous silica as a container for BTA corrosion inhibitor. To better control the release of the corrosion inhibitor, the surface of BTA@mesoporous silica was coated with chitosan valve. Additionally, 2D TpPa COF was employed to enhance the physical barrier of the coating and improve the dispersion of silica.	pH	[269]
Polyhedral oligomeric silsesquioxane (POSS) grafted on 2D TpPa-1 COF	Barrier	–	POSS was covalently grafted on 2D TpPa-1 COF. The coating showed hydrophobicity and good corrosion and wear resistance.	–	[272]

likelihood of friction-induced failure and crack propagation. Thus, the influence of pigments on coating flexibility and mechanical properties emerges as a pivotal consideration. Fourthly, it has been proved that self-healing coatings possess the capacity to protect damaged surfaces. However, the effects of damage geometry and size are often overlooked, despite being crucial factors that could enhance the comprehensive understanding of the coating's protective abilities. Fifthly, as discussed earlier, the stability of carriers is essential. The dissolution of carriers not only results in irregular inhibitor release but also leaves pores and damages within the coating, providing an accessible pathway for the accumulation/penetration of corrosive species. Although stable carriers lack these drawbacks, they become passive after releasing corrosion inhibitors. Consequently, the self-healing ability cannot remain for numerous cycles, underscoring the significance of demonstrating the smart coating's lifetime to estimate the replacement time. Sixthly, exploring the behavior of coatings in marine environments encompasses a range of distinctive features that set it apart from laboratory-scale conditions. These include constant exposure to corrosive saltwater, the impact of waves and currents, potential biofouling by marine organisms, and the mechanical stresses imposed by maritime activities. Understanding how a coating interacts with and withstands these marine-specific challenges is crucial for ensuring its long-term efficacy and durability. Finally, the cost of the coating is a crucial factor that must be carefully considered when planning for commercialization.

9. Conclusions and outlook

This paper offers current insights into the development of anti-

Table 4
Advantages and drawbacks of different carriers in anti-corrosive coatings.

Nanocarrier	Advantages	Drawbacks	References
Metal/Transition Metal Oxides and Lanthanide Oxides	Act as physical barrier, some of them are easy to synthesize while others are difficult.	Low specific surface area, most of them are dissolved in acidic media so suffer from decomposition of their structure, limited loading capacity.	[31,285–287]
Mesoporous silica	High specific surface area, easy synthesis	Susceptible to alkaline condition, microscopic size: Typically, a greater quantity of nanofiller (3-10%) with dimensions in the microscopic range is required compared to that of nanosized fillers (0,5–2%) to achieve good anti-corrosion performance.	[288,289]
GO nanosheets	Good physical barrier, exceptional thermo-mechanical properties, excellent impermeability to corrosive species, stable in different circumstances, electrical conductivity of GO could be beneficial in cathodic protective coatings (e.g, zinc rich coatings)	Tend to agglomeration, difficult dispersion in epoxy matrix, forming galvanic cell with metal substrate, difficult synthesis procedure, low specific surface area.	[69,71,107,110,111,290,291]
g-C_3N_4	Good physical barrier, affordable, easy synthesis procedure, stable in different media, good mechanical properties, environmentally friendly, enhancing adhesion to the substrate, photocatalytic capability.	Tend to agglomeration, difficult dispersion procedure, low specific surface area, recombination of photo-induced electron-hole pairs.	[113,117–119,127,292]
LDH	Physical barrier, affordable, anion exchange behavior	Unstable in highly alkaline and moderate acidic conditions, difficult dispersion in solvent-borne epoxy coating, limited inter-gallery spaces, limited choose of corrosion inhibitor (just anionic corrosion inhibitor), lacks on-demand release behavior.	[135,136,140–142,293]
Montmorillonite	Low cost, environmentally benign, cation exchange ability, physical barrier	Tend to agglomerate, limited choice of corrosion inhibitor (just cationic corrosion inhibitor), lacks on-demand release behavior, sensitive to moisture and water.	[143,145,294]
h-BN	Good mechanical and barrier properties, good impermeability, electrical insulator, preventing galvanic corrosion.	Absence of functional group, dispersion challenge, multi-layered structure should be exfoliated.	[67,146–154,167]
TMDCs / MoS_2	Physical barrier, defect-free monolayer MoS_2 is corrosion resistance.	high sensitivity to UV, humidity, oxidation, and heating, unstable under air over six months, tend to be stacking, bulk and few layer MoS_2 has relatively high electrical conductivity which leads to micro-galvanic cell formation.	[159–163,165]
α-ZrP nanosheet	Physical barrier, easy synthesis procedure, easy exfoliation specially with amine containing materials, cation exchange ability.	Tend to agglomeration, narrow interlayer space restricts the access of cations and corrosion inhibitors, low specific surface area, the acidic nature of the hydroxyl groups which may be disadvantages in coatings.	[157,166,167,295]
MXene nanosheet	Physical barrier	Susceptible to oxygen and water, leading to decomposition of its structure, very difficult dispersion process, difficult synthesis, expensive precursors, low specific surface area, metallic-like conductivity which could lead to galvanic corrosion.	[174,176,182,186,296]
CNTs	Physical barrier, stability in different circumstances, high mechanical and thermal properties, conductivity of CNT can be beneficial for cathodic protection coating like GO.	High-cost synthesis, dispersion challenge, low specific surface area, conductivity could lead to galvanic corrosion.	[198–200,203,204,297]
CNFs	Physical barrier, stability in acidic, basic, and neutral conditions, high mechanical (lower compared to CNT) and thermal properties, conductivity of CNT can be beneficial for cathodic protection coating like GO.	High-cost synthesis, dispersion challenge, low specific surface area, conductivity could lead to galvanic corrosion.	[35,164,206,207]
MOFs	Ultra-high specific surface area, most of them are compatible with epoxy matrix, control over the structure, tunable morphology, abundance of functional groups, crystalline structure generally metal ions and ligand molecules of MOFs have corrosion inhibition ability.	Instability in acidic, basic conditions which limits their suitability for being nanocontainer, tend to self-decomposition in water during the passage of time, their porous structure may reduce the barrier properties of coating due to the diffusion of corrosive species.	[216,225–227,253,255]
COFs	Ultra-high specific surface area, low density, adjustable porosity, permanent porosity, well-ordered structure, many of them are stable in acidic, basic, and neutral conditions and organic solvents, many of them, unlike other 2D materials can disperse easily in epoxy, enhances the mechanical properties	The synthesis is more complex than MOF, generally the precursors are expensive. The porous structure may open a path for diffusion of corrosive species, lower crystallinity than MOFs.	[258–263,265,266,275]

corrosive coatings using micro/nano carriers. It specifically highlights the recent trend of utilizing various carriers based on oxide nanoparticles, carbonaceous structures, 2D materials, MOFs, and COFs and their surface modifications. The primary focus of the paper lies in exploring the mechanism behind corrosion inhibition action of different materials and identifying the associated challenges which provide valuable guidance for researchers in selecting the appropriate materials to achieve their desired properties in anti-corrosive coatings. The basis of this study was created on the fundamental required aspects of nano/micro carriers including compatibility with the coating matrix, high pore volume and specific surface area, stability in acidic, natural, and alkaline environments, stimuli-responsive behavior, and facile synthesis. The dispersion and compatibility issue can be addressed by employing various techniques, with surface modification being the most effective approach. One of the major challenges associated with these carriers is their instability in acidic or basic conditions, which is

undesirable for nanocarriers. This can result in irregular or rapid release of corrosion inhibitors. Furthermore, a significant drawback of many nanocarriers is their limited specific surface area, which can be overcome through strategic hybridization with other high-surface-area materials like MOFs, COFs, SiO_2, etc.

To advance future research in this domain, it is recommended to consider the following suggestions:

1- Carbonaceous structures, including CNT, CNF, GO, and g-C_3N_4, demonstrate robust stability in various environments, including acidic, basic, and neutral conditions. However, it should be noted that the synthesis procedures of CNT, CNF, and GO are often high cost. On the other hand, g-C_3N_4 exhibits favorable attributes such as being environmentally friendly and cost-effective, making it a promising candidate for utilization as a stable carrier/barrier in anti-corrosive coatings. Despite these advantages, the exploration g-C_3N_4 in this specific application remains relatively limited. Consequently, further in-depth research and investigation are necessary to fully uncover its potential and effectively harness it for enhancing anti-corrosive coatings.

2- The carbonization of high carbon-containing natural compounds offers a sustainable and cost-effective method to construct various carbonaceous structures. This eco-friendly approach can be further enhanced through post-processing techniques, such as activation methods, to create chemically stable carbon materials with exceptional specific surface areas.

3- Despite the promising properties of COF such as high specific surface area, chemical stability and compatibility with polymer matrix, the investigation of its effectiveness in anti-corrosive coatings is in the early stages. Therefore, much more attention should be given to COF and its hybrid with other materials.

4- Based on the literature outcomes, 2D materials, especially graphene-based materials like modified GO and rGO, exhibit potential for high performance industrial applications. Although the production cost of graphene is still high, a discernible downward trend is observed. Moreover, graphene-based coatings typically demonstrate excellent corrosion protection, incorporating only 0.1-1 wt% of graphene-based materials. This small quantity may help counterbalance the high cost. The growing number of patent applications and the establishment of companies specializing in graphene-based coatings highlight the significant interest and potential of these innovative coatings in various industrial applications.

CRediT authorship contribution statement

Mohammad Ghaderi: Conceptualization, Data curation, Investigation, Methodology, Visualization, Writing – original draft. **Huichao Bi:** Conceptualization, Methodology, Project administration, Resources, Supervision, Visualization, Writing – review & editing. **Kim Dam-Johansen:** Conceptualization, Resources, Visualization, Supervision, Writing – review & editing.

Declaration of Competing Interest

The authors declare that they have no known competing financial interests or personal relationships that could have appeared to influence the work reported in this paper.

Data availability

No data was used for the research described in the article.

Acknowledgement

Financial support from the Hempel Foundation to CoaST (The Hempel Foundation Coatings Science & Technology Centre) is gratefully acknowledged.

References

[1] Cheng L, Liu C, Zhao H, Wang L. Hierarchically self-reporting and self-healing photothermal responsive coatings towards smart corrosion protection. Chem Eng J 2023;467:143463. https://doi.org/10.1016/j.cej.2023.143463.
[2] Mehta RK, Yadav M. Corrosion inhibition properties of expired Broclear medicine and its carbon dot as eco-friendly inhibitors for mild steel in 15% HCl. Mater Sci Eng B 2023;295:116566. https://doi.org/10.1016/j.mseb.2023.116566.
[3] Ganjoo R, Sharma S, Sharma PK, Dagdag O, Berisha A, Ebenso EE, et al. Coco monoethanolamide surfactant as a sustainable corrosion inhibitor for mild steel: theoretical and experimental investigations. Molecules. 2023;28. https://doi.org/10.3390/molecules28041581.
[4] Haddadi SA, Alibakhshi E, Labani Motlagh A, Ahmad Ramazani SA, Ghaderi M, Ramezanzadeh B, et al. Synthesis of methyltriethoxysilane-modified calcium zinc phosphate nanopigments toward epoxy nanocomposite coatings: exploring rheological, mechanical, and anti-corrosion properties. Prog Org Coat 2022;171:107055. https://doi.org/10.1016/j.porgcoat.2022.107055.
[5] Wang L, Li SN, Fu JJ. Self-healing anti-corrosion coatings based on micron-nano containers with different structural morphologies. Prog Org Coat 2023;175:107381. https://doi.org/10.1016/J.PORGCOAT.2022.107381.
[6] Ambrosi A, Pumera M. The structural stability of graphene anticorrosion coating materials is compromised at low potentials. Chem A Eur J 2015;21:7896–901. https://doi.org/10.1002/CHEM.201406238.
[7] Lin H, Wang Y. An organic phosphonic acid doped polyaniline/zirconia/epoxy composite coating for metal protection in the marine environment. Prog Org Coat 2023;182:107671. https://doi.org/10.1016/j.porgcoat.2023.107671.
[8] Alibakhshi E, Haddadi SA, Motlagh AL, Ghaderi M, Ramezanzadeh B, Mahdavian M, et al. Epoxy nanocomposite coating based on calcium zinc phosphate with dual active/barrier corrosion mitigation properties. Prog Org Coat 2022;163:106677. https://doi.org/10.1016/j.porgcoat.2021.106677.
[9] Ghaderi M, Ahmad Ramazani SA, Kordzadeh A, Mahdavian M, Alibakhshi E, Ghaderi A. Corrosion inhibition of a novel antihistamine-based compound for mild steel in hydrochloric acid solution: experimental and computational studies. Sci Rep 2022;12:13450. https://doi.org/10.1038/s41598-022-17589-y.
[10] Peñas-Caballero M, Martín-Cordón J, Barranco V, Galván JC, Hernández Santana M, Lopez-Manchado MA, et al. Corrosion control by autonomous self-healing epoxy coatings based on superabsorbent healing agents. Prog Org Coat 2023;182:107600. https://doi.org/10.1016/j.porgcoat.2023.107600.
[11] Tabish M, Zhao J, Wang J, Anjum MJ, Qiang Y, Yang Q, et al. Improving the corrosion protection ability of epoxy coating using CaAl LDH intercalated with 2-mercaptobenzothiazole as a pigment on steel substrate. Prog Org Coat 2022;165:106765. https://doi.org/10.1016/j.porgcoat.2022.106765.
[12] Liu T, Zhang D, Ma L, Huang Y, Hao X, Terryn H, et al. Smart protective coatings with self-sensing and active corrosion protection dual functionality from pH-sensitive calcium carbonate microcontainers. Corros Sci 2022;200:110254. https://doi.org/10.1016/J.CORSCI.2022.110254.
[13] Wu Y, Jiang F, Qiang Y, Zhao W. Synthesizing a novel fluorinated reduced graphene oxide-CeO2 hybrid nanofiller to achieve highly corrosion protection for waterborne epoxy coatings. Carbon N Y 2021;176:39–51. https://doi.org/10.1016/j.carbon.2021.01.135.
[14] Liu T, Zhang D, Zhang R, Wang J, Ma L, Keil P, et al. Self-healing and corrosion-sensing coatings based on pH-sensitive MOF-capped microcontainers for intelligent corrosion control. Chem Eng J 2023;454:140335. https://doi.org/10.1016/J.CEJ.2022.140335.
[15] Haddadi SA, Hu S, Ghaderi S, Ghanbari A, Ahmadipour M, Pung S-Y, et al. Amino-functionalized MXene nanosheets doped with Ce(III) as potent nanocontainers toward self-healing epoxy nanocomposite coating for corrosion protection of mild steel. ACS Appl Mater Interfaces 2021;13:42074–93. https://doi.org/10.1021/acsami.1c13055.
[16] Verma C, Ebenso EE, Quraishi MA. Corrosion inhibitors for ferrous and non-ferrous metals and alloys in ionic sodium chloride solutions: a review. J Mol Liq 2017;248:927–42. https://doi.org/10.1016/j.molliq.2017.10.094.
[17] Umoren SA, Solomon MM. Synergistic corrosion inhibition effect of metal cations and mixtures of organic compounds: a review. J Environ Chem Eng 2017;5. https://doi.org/10.1016/j.jece.2016.12.001.
[18] Alimohammadi M, Ghaderi M, Ahmad Ramazani SA, Mahdavian M. Falcaria vulgaris leaves extract as an eco-friendly corrosion inhibitor for mild steel in hydrochloric acid media. Sci Rep 2023;13. https://doi.org/10.1038/s41598-023-30571-6.
[19] El-Haddad MN. Hydroxyethylcellulose used as an eco-friendly inhibitor for 1018 c-steel corrosion in 3.5% NaCl solution. Carbohydr Polym 2014;112:595–602. https://doi.org/10.1016/j.carbpol.2014.06.032.
[20] Zeino A, Abdulazeez I, Khaled M, Jawich MW, Obot IB. Mechanistic study of polyaspartic acid (PASP) as eco-friendly corrosion inhibitor on mild steel in 3% NaCl aerated solution. J Mol Liq 2018;250:50–62. https://doi.org/10.1016/j.molliq.2017.11.160.
[21] Zeng Y, Kang L, Wu Y, Wan S, Liao B, Li N, et al. Melamine modified carbon dots as high effective corrosion inhibitor for Q235 carbon steel in neutral 3.5 wt% NaCl solution. J Mol Liq 2022;349. https://doi.org/10.1016/j.molliq.2021.118108.
[22] Lu H, Ji X, Ci X, Zhu H, Wang Q, Zong Y, et al. Investigation of triazole derivatives as corrosion inhibitors on Q235 steel in NaCl solution: experimental and theoretical studies. Colloids Surf A Physicochem Eng Asp 2023;674. https://doi.org/10.1016/j.colsurfa.2023.131892.

[23] Saker S, Aliouane N, Hammache H, Chafaa S, Bouet G. Tetraphosphonic acid as eco-friendly corrosion inhibitor on carbon steel in 3 % NaCl aqueous solution. Ionics (Kiel) 2015;21:2079–90. https://doi.org/10.1007/s11581-015-1377-3.
[24] Al-Amiery AA, Yousif E, Isahak WNRW, Al-Azzawi WK. A review of inorganic corrosion inhibitors: types, mechanisms, and applications. Tribol Industry 2023; 45:313–39. https://doi.org/10.24874/ti.1456.03.23.06.
[25] Cui G, Bi Z, Wang S, Liu J, Xing X, Li Z, et al. A comprehensive review on smart anti-corrosive coatings. Prog Org Coat 2020;148:105821. https://doi.org/10.1016/J.PORGCOAT.2020.105821.
[26] Hager MD, Greil P, Leyens C, Van Der Zwaag S, Schubert US. Self-Healing Mater 2010. https://doi.org/10.1002/adma201003036.
[27] Li Y, Zhang D, Li J, Lu J, Zhang X, Gao L. Application of hierarchical bonds for construction an anti-corrosion coating with superior intrinsic self-healing function. Colloids Surf A Physicochem Eng Asp 2022;639:128388. https://doi.org/10.1016/j.colsurfa.2022.128388.
[28] Kumar EK, Patel SS, Kumar V, Panda SK, Mahmoud SR, Balubaid M. State of art review on applications and mechanism of self-healing materials and structure. Arch Comput Methods Eng 2023;30:1041–55. https://doi.org/10.1007/s11831-022-09827-3.
[29] Huang Y, Zhao C, Li Y, Wang C, Shen T, Cheng D, et al. Development of self-healing sol-gel anticorrosion coating with pH-responsive 1H-benzotriazole-inbuilt zeolitic imidazolate framework decorated with silica shell. Surf Coat Technol 2023;466:129622. https://doi.org/10.1016/j.surfcoat.2023.129622.
[30] Chen Z, Scharnagl N, Zheludkevich ML, Ying H, Yang W. Micro/nanocontainer-based intelligent coatings: synthesis, performance and applications – a review. Chem Eng J 2023;451:138582. https://doi.org/10.1016/J.CEJ.2022.138582.
[31] Tian Z, Li S, Chen Y, Li L, An Z, Zhang Y, et al. Self-healing coating with a controllable release of corrosion inhibitors by using multifunctional zinc oxide quantum dots as valves. ACS Appl Mater Interfaces 2022;14:47188–97. https://doi.org/10.1021/acsami.2c16151.
[32] Zehra S, Mobin M, Aslam R, Parveen M, Aslam A. Chapter 23 - Nanocontainer-loaded smart functional anticorrosion coatings. In: Verma C, Srivastava V, Quadri TW, Mustansar Hussain C, Ebenso EE, editors. Smart anticorrosive materials. Elsevier; 2023. p. 481–97. https://doi.org/10.1016/B978-0-323-95158-6.00003-5.
[33] Habib S, Shakoor RA, Kahraman R. A focused review on smart carriers tailored for corrosion protection: developments, applications, and challenges. Prog Org Coat 2021;154:106218. https://doi.org/10.1016/j.porgcoat.2021.106218.
[34] Zhang Z, Chen Y, Wang P, Wang Z, Zuo C, Chen W, et al. Facile fabrication of N-doped hierarchical porous carbons derived from soft-templated ZIF-8 for enhanced adsorptive removal of tetracycline hydrochloride from water. J Hazard Mater 2022;423. https://doi.org/10.1016/j.jhazmat.2021.127103.
[35] Ghaderi M, Saadatabadi AR, Mahdavian M, Haddadi SA. pH-sensitive polydopamine–La (III) complex decorated on carbon nanofiber toward on-demand release functioning of epoxy anti-corrosion coating. Langmuir. 2022;38: 11707–23. https://doi.org/10.1021/acs.langmuir.2c01801.
[36] Taheri N, Sarabi AA, Roshan S. Investigation of intelligent protection and corrosion detection of epoxy-coated St-12 by redox-responsive microcapsules containing dual-functional 8-hydroxyquinoline. Prog Org Coat 2022;172:107073. https://doi.org/10.1016/j.porgcoat.2022.107073.
[37] Siva T, Kandhasamy K, Vaduganathan K, Sathiyanarayanan S, Ramadoss A. Electrosynthesis of silica reservoir incorporated dual stimuli responsive conducting polymer-based self-healing coatings. Ind Eng Chem Res 2023;62: 3942–51. https://doi.org/10.1021/acs.iecr.2c03445.
[38] Huang Y, Liu T, Ma L, Wang J, Zhang D, Li X. Saline-responsive triple-action self-healing coating for intelligent corrosion control. Mater Des 2022;214:110381. https://doi.org/10.1016/j.matdes.2022.110381.
[39] Huang Y, Wang P, Tan W, Hao W, Ma L, Wang J, et al. Photothermal and pH dual-responsive self-healing coating for smart corrosion protection. J Mater Sci Technol 2022;107:34–42. https://doi.org/10.1016/j.jmst.2021.08.044.
[40] Liu C, Cheng L, Hou P, Qian B. Photothermal-responsive wormlike polydopamine-wrapped ethylene-vinyl acetate copolymer toward triple-action self-healing anticorrosion coating. ACS Appl Polym Mater 2022;4:6067–79. https://doi.org/10.1021/acsapm.2c00875.
[41] Li X, Gong B, Zhang J, Di Y, Ding Y, Chen Z, et al. A photothermal and pH-responsive intelligent PSBG nanofiller for enhancing the barrier and self-healing performance of the SMP coatings. Colloids Surf A Physicochem Eng Asp 2023; 674:131899. https://doi.org/10.1016/j.colsurfa.2023.131899.
[42] Auepattana-Aumrung K, Crespy D. Self-healing and anticorrosion coatings based on responsive polymers with metal coordination bonds. Chem Eng J 2023;452: 139055. https://doi.org/10.1016/j.cej.2022.139055.
[43] Haddadi SA, Ahmad Ramazani SA, Mahdavian M, Taheri P, Mol JMC, Gonzalez-Garcia Y. Self-healing epoxy nanocomposite coatings based on dual-encapsulation of nano-carbon hollow spheres with film-forming resin and curing agent. Compos Part B Eng 2019;175:107087. https://doi.org/10.1016/j.compositesb.2019.107087.
[44] Nawaz M, Shakoor RA, Kahraman R, Montemor MF. Cerium oxide loaded with gum Arabic as environmentally friendly anti-corrosion additive for protection of coated steel. Mater Des 2021;198:109361. https://doi.org/10.1016/J.MATDES.2020.109361.
[45] Gu S, Shi H, Zhang C, Wang W, Liu F, Han EH. Mesoporous CeO2 containers in water-borne epoxy coatings for dual active corrosion protection of mild steel. Prog Org Coat 2021;158:106376. https://doi.org/10.1016/J.PORGCOAT.2021.106376.
[46] Nawaz M, Shakoor RA, Kahraman R, Montemor MF. Cerium oxide loaded with Gum Arabic as environmentally friendly anti-corrosion additive for protection of coated steel. Mater Des 2021;198:109361. https://doi.org/10.1016/J.MATDES.2020.109361.
[47] Ubaid F, Radwan AB, Naeem N, Shakoor RA, Ahmad Z, Montemor MF, et al. Multifunctional self-healing polymeric nanocomposite coatings for corrosion inhibition of steel. Surf Coat Technol 2019;372:121–33. https://doi.org/10.1016/J.SURFCOAT.2019.05.017.
[48] Da'na E. Adsorption of heavy metals on functionalized-mesoporous silica: a review. Microporous Mesoporous Mater 2017;247:145–57. https://doi.org/10.1016/j.micromeso.2017.03.050.
[49] Olivieri F, Castaldo R, Cocca M, Gentile G, Lavorgna M. Mesoporous silica nanoparticles as carriers of active agents for smart anticorrosive organic coatings: a critical review. Nanoscale. 2021;13:9091–111. https://doi.org/10.1039/d1nr01899j.
[50] Gao Y, Chen Y, Ji X, He X, Yin Q, Zhang Z, et al. Controlled intracellular release of doxorubicin in multidrug-resistant cancer cells by tuning the shell-pore sizes of mesoporous silica nanoparticles. ACS Nano 2011;5:9788–98. https://doi.org/10.1021/nn2033105.
[51] Lamprakou Z, Bi H, Weinell CE, Tortajada S, Dam-Johansen K. Smart epoxy coating with mesoporous silica nanoparticles loaded with calcium phosphate for corrosion protection. Prog Org Coat 2022;165:106740. https://doi.org/10.1016/J.PORGCOAT.2022.106740.
[52] Yin Y, Zhao H, Prabhakar M, Rohwerder M. Organic composite coatings containing mesoporous silica particles: degradation of the SiO2 leading to self-healing of the delaminated interface. Corros Sci 2022;200:110252. https://doi.org/10.1016/J.CORSCI.2022.110252.
[53] Wang J, Ma L, Guo X, Wu S, Liu T, Yang J, et al. Two birds with one stone: nanocontainers with synergetic inhibition and corrosion sensing abilities towards intelligent self-healing and self-reporting coating. Chem Eng J 2022;433:134515. https://doi.org/10.1016/J.CEJ.2022.134515.
[54] Chenan A, Ramya S, George RP, Kamachi Mudali U. Hollow mesoporous zirconia nanocontainers for storing and controlled releasing of corrosion inhibitors. Ceram Int 2014;40:10457–63. https://doi.org/10.1016/J.CERAMINT.2014.03.016.
[55] Chen Z, Yang W, Chen Y, Yin X, Liu Y. Smart coatings embedded with polydopamine-decorated layer-by-layer assembled SnO2 nanocontainers for the corrosion protection of 304 stainless steels. J Colloid Interface Sci 2020;579: 741–53. https://doi.org/10.1016/J.JCIS.2020.06.118.
[56] Nawaz M, Naeem N, Kahraman R, Montemor MF, Haider W, Shakoor RA. Effectiveness of epoxy coating modified with yttrium oxide loaded with imidazole on the corrosion protection of steel. Nanomaterials. 2021;11. https://doi.org/10.3390/nano11092291.
[57] Movahedzadeh Z, Ghaderi M, SaadatAbadi AR. Ni/Al2O3 waste catalyst loaded with pomegranate peel extract and Ce3+ ions as a sustainable active/barrier pigment for epoxy anti-corrosion coating. J Industr Eng Chem 2023. https://doi.org/10.1016/j.jiec.2023.08.043.
[58] Zhu Q, Xu X, Huang Y, Liu S, Zuo A, Tang Y. pH-responsive mesoporous silica nanocontainers based on Zn-BTA complexes as stoppers for controllable release of corrosion inhibitors and application in epoxy coatings. Prog Org Coat 2023;181: 107581. https://doi.org/10.1016/J.PORGCOAT.2023.107581.
[59] Yeganeh M, Rabizadeh T, Rabiezadeh MS, Kahvazizadeh M, Ramezanalizadeh H. Corrosion and the antibacterial response of epoxy coating/drug-loaded mesoporous silica. Polymer Bull 2022. https://doi.org/10.1007/s00289-022-04261-8.
[60] Yan D, Liu X, Chen Z, Wang Y, Zhang M, Zhang T, et al. A double-layered self-healing coating system based on the synergistic strategy of cysteine and iron polyacrylate for corrosion protection. Chem Eng J 2023;451:138995. https://doi.org/10.1016/J.CEJ.2022.138995.
[61] Guo C, Cao J, Chen Z. Core-shell mesoporous silica–metal–phenolic network microcapsule for the controlled release of corrosion inhibitor. Appl Surf Sci 2022; 605:154747. https://doi.org/10.1016/J.APSUSC.2022.154747.
[62] Liu X, Zheng M, Hongtao T, Kaiwei L, Baorong H. Water-based epoxy coatings with pH-sensitive TiO2 containers for active corrosion protection of carbon steel. Corrosion Eng Sci Technol 2020;55:645–54. https://doi.org/10.1080/1478422X.2020.1772527.
[63] Mekeridis ED, Kartsonakis IA, Pappas GS, Kordas GC. Release studies of corrosion inhibitors from cerium titanium oxide nanocontainers. J Nanopart Res 2011;13: 541–54. https://doi.org/10.1007/s11051-010-0044-x.
[64] Chen Z, Yang W, Chen Y, Yin X, Liu Y. Smart coatings embedded with polydopamine-decorated layer-by-layer assembled SnO2 nanocontainers for the corrosion protection of 304 stainless steels. J Colloid Interface Sci 2020;579: 741–53. https://doi.org/10.1016/J.JCIS.2020.06.118.
[65] Zhang Y, Sun J, Xiao X, Wang N, Meng G, Gu L. Graphene-like two-dimensional nanosheets-based anticorrosive coatings: a review. J Mater Sci Technol 2022;129: 139–62. https://doi.org/10.1016/j.jmst.2022.04.032.
[66] Yao H, Li L, Li W, Qi D, Fu W, Wang N. Application of nanomaterials in waterborne coatings: a review. Resourc Chem Mater 2022;1:184–200. https://doi.org/10.1016/j.recm.2022.06.004.
[67] Huang H, Sheng X, Tian Y, Zhang L, Chen Y, Zhang X. Two-dimensional nanomaterials for anticorrosive polymeric coatings: a review. Ind Eng Chem Res 2020;59:15424–46. https://doi.org/10.1021/acs.iecr.0c02876.
[68] Sharma A, Sharma S. Graphene-based polymer coatings for preventing marine corrosion: a review. J Coat Technol Res 2023. https://doi.org/10.1007/s11998-022-00730-x.
[69] Li F, Ma Y, Chen L, Li H, Zhou H, Chen J. In-situ polymerization of polyurethane/aniline oligomer functionalized graphene oxide composite coatings with enhanced mechanical, tribological and corrosion protection properties. Chem Eng J 2021;425:130006. https://doi.org/10.1016/j.cej.2021.130006.

[70] Sun W, Tang E, Zhao L, Yuan M, Liu S, Xing X, et al. The waterborne epoxy composite coatings with modified graphene oxide nanosheet supported zinc ion and its self-healing anticorrosion properties. Prog Org Coat 2023;182:107609. https://doi.org/10.1016/j.porgcoat.2023.107609.
[71] Li H, Zhang Q-H, Meng X-Z, Liu P, Wu L-K, Cao F-H. A novel cerium organic network modified graphene oxide prepared multifunctional waterborne epoxy-based coating with excellent mechanical and passive/active anti-corrosion properties. Chem Eng J 2023;465:142997. https://doi.org/10.1016/j.cej.2023.142997.
[72] Kasaeian M, Ghasemi E, Ramezanzadeh B, Mahdavian M, Bahlakeh G. Construction of a highly effective self-repair corrosion-resistant epoxy composite through impregnation of 1H-Benzimidazole corrosion inhibitor modified graphene oxide nanosheets (GO-BIM). Corros Sci 2018;145:119–34. https://doi.org/10.1016/j.corsci.2018.09.023.
[73] Asaldoust S, Hosseini MS, Ramezanzadeh B, Bahlakeh G. Construction of a unique anti-corrosion nanocomposite based on graphene oxide@Zn3PO4/epoxy; experimental characterization and detailed-theoretical quantum mechanics (QM) investigations. Construct Build Mater 2020;256. https://doi.org/10.1016/j.conbuildmat.2020.119439.
[74] Kaghazchi L, Naderi R, Ramezanzadeh B. Improvement of the dual barrier/active corrosion inhibition function of the epoxy composite filled with zinc doped-phytic acid-modified graphene oxide nanosheets. Prog Org Coat 2022;168. https://doi.org/10.1016/j.porgcoat.2022.106884.
[75] Javidparvar AA, Naderi R, Ramezanzadeh B. Epoxy-polyamide nanocomposite coating with graphene oxide as cerium nanocontainer generating effective dual active/barrier corrosion protection. Compos Part B Eng 2019;172:363–75. https://doi.org/10.1016/j.compositesb.2019.05.055.
[76] Javidparvar AA, Naderi R, Ramezanzadeh B. Manipulating graphene oxide nanocontainer with benzimidazole and cerium ions: application in epoxy-based nanocomposite for active corrosion protection. Corros Sci 2020;165. https://doi.org/10.1016/j.corsci.2019.108379.
[77] Asaldoust S, Ramezanzadeh B. Synthesis and characterization of a high-quality nanocontainer based on benzimidazole-zinc phosphate (ZP-BIM) tailored graphene oxides; a facile approach to fabricating a smart self-healing anti-corrosion system. J Colloid Interface Sci 2020;564:230–44. https://doi.org/10.1016/j.jcis.2019.12.122.
[78] Khalili Dermani A, Kowsari E, Ramezanzadeh B, Amini R. Utilizing imidazole based ionic liquid as an environmentally friendly process for enhancement of the epoxy coating/graphene oxide composite corrosion resistance. J Industr Eng Chem 2019;79:353–63. https://doi.org/10.1016/j.jiec.2019.07.010.
[79] Javidparvar AA, Naderi R, Ramezanzadeh B. Designing a potent anti-corrosion system based on graphene oxide nanosheets non-covalently modified with cerium/benzimidazole for selective delivery of corrosion inhibitors on steel in NaCl media. J Mol Liq 2019;284:415–30. https://doi.org/10.1016/j.molliq.2019.04.028.
[80] Javidparvar AA, Naderi R, Ramezanzadeh B. L-cysteine reduced/functionalized graphene oxide application as a smart/control release nanocarrier of sustainable cerium ions for epoxy coating anti-corrosion properties improvement. J Hazard Mater 2020;389. https://doi.org/10.1016/j.jhazmat.2020.122135.
[81] Khosravi H, Naderi R, Ramezanzadeh B. Designing an epoxy composite coating having dual-barrier-active self-healing anti-corrosion functions using a multi-functional GO/PDA/MO nano-hybrid. Mater Today Chem 2023;27. https://doi.org/10.1016/j.mtchem.2022.101282.
[82] Motamedi M, Ramezanzadeh M, Ramezanzadeh B, Saadatmandi S. Enhancement of the active/passive anti-corrosion properties of epoxy coating via inclusion of histamine/zinc modified/reduced graphene oxide nanosheets. Appl Surf Sci 2019;488:77–91. https://doi.org/10.1016/j.apsusc.2019.05.180.
[83] Mahmudzadeh M, Yari H, Ramezanzadeh B, Mahdavian M. Urtica dioica extract as a facile green reductant of graphene oxide for UV resistant and corrosion protective polyurethane coating fabrication. J Industr Eng Chem 2019;78:125–36. https://doi.org/10.1016/j.jiec.2019.06.026.
[84] Akbarzadeh S, Ramezanzadeh M, Ramezanzadeh B, Bahlakeh G. A green assisted route for the fabrication of a high-efficiency self-healing anti-corrosion coating through graphene oxide nanoplatform reduction by Tamarindus indiaca extract. J Hazard Mater 2020;390:122147. https://doi.org/10.1016/j.jhazmat.2020.122147.
[85] Habibiyan A, Ramezanzadeh B, Mahdavian M, Bahlakeh G, Kasaeian M. Rational assembly of mussel-inspired polydopamine (PDA)-Zn (II) complex nanospheres on graphene oxide framework tailored for robust self-healing anti-corrosion coatings application. Chem Eng J 2020;391:123630. https://doi.org/10.1016/J.CEJ.2019.123630.
[86] Marhamati F, Ghaderi M, Haddadi SA, Arjmand M, Olivier M-G, Mahdavian M. Nitrogen-doped carbon hollow sphere capsules for a novel hybrid inhibitor based on lanthanum cations and 8-hydroxyquinoline: synthesis, characterization, and self-healing properties in epoxy coating. Colloids Surf A Physicochem Eng Asp 2023;675:132065. https://doi.org/10.1016/j.colsurfa.2023.132065.
[87] Keshmiri N, Najmi P, Ramezanzadeh B, Ramezanzadeh M, Bahlakeh G. Nano-scale P, Zn-codoped reduced-graphene oxide incorporated epoxy composite; synthesis, electronic-level DFT-D modeling, and anti-corrosion properties. Prog Org Coat 2021;159. https://doi.org/10.1016/j.porgcoat.2021.106416.
[88] Nejad SAT, Alibakhshi E, Ramezanzadeh B, Haddadi SA, Arjmand M, Mahdavian M. A novel nitrogen- and sulfur-grafted reduced graphene oxide doped with zinc cations for corrosion mitigation of mild steel. Prog Org Coat 2022;167. https://doi.org/10.1016/j.porgcoat.2022.106828.
[89] Keramatinia M, Ramezanzadeh B, Mahdavian M, Bahlakeh G. Chemically controlled nitrogen-doped reduced-graphene/graphite oxide frameworks for aiding superior thermal/anti-corrosion performance: integrated DFT-D & experimental evaluations. Chem Eng J 2022;437. https://doi.org/10.1016/j.cej.2022.135241.
[90] Ramezanzadeh B, Bahlakeh G, Ramezanzadeh M. Polyaniline-cerium oxide (PAni-CeO2) coated graphene oxide for enhancement of epoxy coating corrosion protection performance on mild steel. Corros Sci 2018;137:111–26. https://doi.org/10.1016/j.corsci.2018.03.038.
[91] Zhu Q, Li E, Liu X, Song W, Zhao M, Zi L, et al. Synergistic effect of polypyrrole functionalized graphene oxide and zinc phosphate for enhanced anticorrosion performance of epoxy coatings. Compos Part A Appl Sci Manuf 2020;130. https://doi.org/10.1016/j.compositesa.2019.105752.
[92] Chen Z, Gong B, Li X, Zhao D, Ying H, Yang W. Intelligent self-healing anti-corrosive coatings with crosslinked conducting polypyrrole hydrogel network. Colloids Surf A Physicochem Eng Asp 2023;675. https://doi.org/10.1016/j.colsurfa.2023.132078.
[93] Zhao Y, Yan S, He Y, Li Z, Li C, Li H. Synthesis of ultrathin α-zirconium phosphate functionalized with polypyrrole for reinforcing the anticorrosive property of waterborne epoxy coating. Colloids Surf A Physicochem Eng Asp 2022;635. https://doi.org/10.1016/j.colsurfa.2021.128052.
[94] He Z, Lin H, Zhang X, Chen Y, Bai W, Lin Y, et al. Self-healing epoxy composite coating based on polypyrrole@MOF nanoparticles for the long-efficiency corrosion protection on steels. Colloids Surf A Physicochem Eng Asp 2023;657. https://doi.org/10.1016/j.colsurfa.2022.130601.
[95] Samiee R, Ramezanzadeh B, Mahdavian M, Alibakhshi E, Bahlakeh G. Designing a non-hazardous nano-carrier based on graphene oxide@polyaniline-praseodymium (III) for fabrication of the active/passive anti-corrosion coating. J Hazard Mater 2020;398. https://doi.org/10.1016/j.jhazmat.2020.123136.
[96] Taheri NN, Ramezanzadeh B, Mahdavian M. Application of layer-by-layer assembled graphene oxide nanosheets/polyaniline/zinc cations for construction of an effective epoxy coating anti-corrosion system. J Alloys Compd 2019;800:532–49. https://doi.org/10.1016/j.jallcom.2019.06.103.
[97] Shahryari Z, Gheisari K, Yeganeh M, Ramezanzadeh B. Corrosion mitigation ability of differently synthesized polypyrrole (PPy-FeCl3 & PPy-APS) conductive polymers modified with Na2MoO4 on mild steel in 3.5% NaCl solution: comparative study and optimization. Corros Sci 2021;193. https://doi.org/10.1016/j.corsci.2021.109894.
[98] Zhang M, Zhang Y, Chen Y, Tian X, Liu L, Wang Y, et al. Dual-inhibitor composite BTA/PPy/MIL-88(Fe) for active anticorrosion of epoxy resin coatings. J Industr Eng Chem 2023;119:660–73. https://doi.org/10.1016/j.jiec.2022.12.012.
[99] Zhu Q, Li E, Liu X, Song W, Li Y, Wang X, et al. Epoxy coating with in-situ synthesis of polypyrrole functionalized graphene oxide for enhanced anticorrosive performance. Prog Org Coat 2020;140. https://doi.org/10.1016/j.porgcoat.2019.105488.
[100] Lu F, Liu C, Chen Z, Veerabagu U, Chen Z, Liu M, et al. Polypyrrole-functionalized boron nitride nanosheets for high-performance anti-corrosion composite coating. Surf Coat Technol 2021;420. https://doi.org/10.1016/j.surfcoat.2021.127273.
[101] Shahryari Z, Gheisari K, Yeganeh M, Ramezanzadeh B. MoO42−-doped oxidative polymerized pyrrole-graphene oxide core-shell structure synthesis and application for dual-barrier & active functional epoxy-coating construction. Prog Org Coat 2022;167. https://doi.org/10.1016/j.porgcoat.2022.106845.
[102] Hayatgheib Y, Ramezanzadeh B, Kardar P, Mahdavian M. A comparative study on fabrication of a highly effective corrosion protective system based on graphene oxide-polyaniline nanofibers/epoxy composite. Corros Sci 2018;133:358–73. https://doi.org/10.1016/j.corsci.2018.01.046.
[103] Mohammadkhani R, Ramezanzadeh M, Saadatmandi S, Ramezanzadeh B. Designing a dual-functional epoxy composite system with self-healing/barrier anti-corrosion performance using graphene oxide nano-scale platforms decorated with zinc doped-conductive polypyrrole nanoparticles with great environmental stability and non-toxicity. Chem Eng J 2020;382. https://doi.org/10.1016/j.cej.2019.122819.
[104] Najmi P, Keshmiri N, Ramezanzadeh M, Ramezanzadeh B. Synthesis and application of Zn-doped polyaniline modified multi-walled carbon nanotubes as stimuli-responsive nanocarrier in the epoxy matrix for achieving excellent barrier-self-healing corrosion protection potency. Chem Eng J 2021;412. https://doi.org/10.1016/j.cej.2021.128637.
[105] Haddadi SA, Ramezanzadeh M, Tehrani ME Haji Naghi, Ramezanzadeh B. Sodium lignosulfonate-loaded ZnAl-layered double hydroxide decorated graphene oxide nanolayers; toward fabrication of sustainable nanocomposite for smart corrosion prevention. J Clean Prod 2022;374. https://doi.org/10.1016/j.jclepro.2022.133980.
[106] Ramezanzadeh M, Ramezanzadeh B, Mahdavian M, Bahlakeh G. Development of metal-organic framework (MOF) decorated graphene oxide nanoplatforms for anti-corrosion epoxy coatings. Carbon N Y 2020;161:231–51. https://doi.org/10.1016/j.carbon.2020.01.082.
[107] Haeri Z, Ramezanzadeh B, Ramezanzadeh M. Recent progress on the metal-organic frameworks decorated graphene oxide (MOFs-GO) nano-building application for epoxy coating mechanical-thermal/flame-retardant and anti-corrosion features improvement. Prog Org Coat 2022;163:106645. https://doi.org/10.1016/J.PORGCOAT.2021.106645.
[108] Shahini MH, Mousavi M, Masoud Arabi A, Mahdavian M, Ramezanzadeh B. Ce-oxide quantum dots decorated graphene oxide (CeO-QDs-GO) nano-platforms synthesis and application in epoxy matrix for efficient anti-corrosion ability. J Industr Eng Chem 2021;101:51–65. https://doi.org/10.1016/j.jiec.2021.06.024.
[109] Qureshi T, Wang G, Mukherjee S, Akibul Islam M, Filleter T, Singh CV, et al. Graphene-based anti-corrosive coating on steel for reinforced concrete

infrastructure applications: challenges and potential. Construct Build Mater 2022; 351:128947. https://doi.org/10.1016/j.conbuildmat.2022.128947.
[110] Jena G, Philip J. A review on recent advances in graphene oxide-based composite coatings for anticorrosion applications. Prog Org Coat 2022;173:107208. https://doi.org/10.1016/j.porgcoat.2022.107208.
[111] Li J, Zheng H, Liu L, Meng F, Cui Y, Wang F. Modification of graphene and graphene oxide and their applications in anticorrosive coatings. J Coat Technol Res 2021;18:311–31. https://doi.org/10.1007/s11998-020-00435-z.
[112] Huang S, Kong G, Yang B, Zhang S, Che C. Effects of graphene on the corrosion evolution of zinc particles in waterborne epoxy zinc-containing coatings. Prog Org Coat 2020;140:105531. https://doi.org/10.1016/J.PORGCOAT.2019.105531.
[113] Pourhashem S, Duan J, Guan F, Wang N, Gao Y, Hou B. New effects of TiO2 nanotube/g-C3N4 hybrids on the corrosion protection performance of epoxy coatings. J Mol Liq 2020;317:114214. https://doi.org/10.1016/j.molliq.2020.114214.
[114] Liu J, Wang H, Antonietti M. Graphitic carbon nitride "reloaded": emerging applications beyond (photo)catalysis. Chem Soc Rev 2016;45:2308–26. https://doi.org/10.1039/c5cs00767d.
[115] Li C, Zhang C, He Y, Li H, Zhao Y, Li Z, et al. Benzotriazole corrosion inhibitor loaded nanocontainer based on g-C3N4 and hollow polyaniline spheres towards enhancing anticorrosion performance of waterborne epoxy coatings. Prog Org Coat 2023;174:107276. https://doi.org/10.1016/J.PORGCOAT.2022.107276.
[116] Anadebe VC, Chukwuike VI, Selvaraj V, Pandikumar A, Barik RC. Sulfur-doped graphitic carbon nitride (S-g-C3N4) as an efficient corrosion inhibitor for X65 pipeline steel in CO2- saturated 3.5% NaCl solution: electrochemical, XPS and Nanoindentation studies. Process Safety Environ Protect 2022;164:715–28. https://doi.org/10.1016/j.psep.2022.06.055.
[117] Zhang M, Zhang J, Feng Y, Zhang X, Guo R, Yan H. Flatness and corrosion protection of polypyrrole film enhanced by two-dimensional g-C3N4 nanosheets. Mater Today Commun 2021;29:102934. https://doi.org/10.1016/J.MTCOMM.2021.102934.
[118] Yan H, Li J, Zhang M, Zhao Y, Feng Y, Zhang Y. Enhanced corrosion resistance and adhesion of epoxy coating by two-dimensional graphite-like g-C3N4 nanosheets. J Colloid Interface Sci 2020;579:152–61. https://doi.org/10.1016/J.JCIS.2020.06.027.
[119] Chen C, He Y, Xiao G, Zhong F, Xia Y, Wu Y. Graphic C3N4-assisted dispersion of graphene to improve the corrosion resistance of waterborne epoxy coating. Prog Org Coat 2020;139:105448. https://doi.org/10.1016/J.PORGCOAT.2019.105448.
[120] Ma Y, Chen R, Fei G, Guo M, Li Y, Duan Y, et al. Enhanced anti-aging and anti-corrosion performance of waterborne epoxy coating layers over the dual effects of g-C3N4 photocatalysis. J Appl Polym Sci 2022;139. https://doi.org/10.1002/app.52356.
[121] Yan H, Li J, Zhang M, Zhao Y, Feng Y, Zhang Y. Enhanced corrosion resistance and adhesion of epoxy coating by two-dimensional graphite-like g-C3N4 nanosheets. J Colloid Interface Sci 2020;579:152–61. https://doi.org/10.1016/J.JCIS.2020.06.027.
[122] Liu Z, Zhu R, Zhang X, Zhu H. Improving anticorrosion performance of epoxy coating by hybrids of rGO and g-C3N4 nanosheets. J Coat Technol Res 2022;19:1219–32. https://doi.org/10.1007/s11998-021-00603-9.
[123] Zhou Z, Ji X, Pourhashem S, Duan J, Hou B. Investigating the effects of g-C3N4/graphene oxide nanohybrids on corrosion resistance of waterborne epoxy coatings. Compos Part A Appl Sci Manuf 2021;149:106568. https://doi.org/10.1016/J.COMPOSITESA.2021.106568.
[124] Xia Y, Zhang N, Zhou Z, Chen C, Wu Y, Zhong F, et al. Incorporating SiO2 functionalized g-C3N4 sheets to enhance anticorrosion performance of waterborne epoxy. Prog Org Coat 2020;147:105768. https://doi.org/10.1016/J.PORGCOAT.2020.105768.
[125] Xia Y, He Y, Chen C, Wu Y, Zhong F, Chen J. Co-modification of polydopamine and KH560 on g-C3N4 nanosheets for enhancing the corrosion protection property of waterborne epoxy coating. React Funct Polym 2020;146:104405. https://doi.org/10.1016/J.REACTFUNCTPOLYM.2019.104405.
[126] Pourhashem S, Rashidi A, Alaei M, Moradi MA, Maklavany DM. Developing a new method for synthesizing amine functionalized g-C3N4 nanosheets for application as anti-corrosion nanofiller in epoxy coatings. SN Appl Sci 2019;1. https://doi.org/10.1007/s42452-018-0123-7.
[127] Ma Y, Wang H, Sun L, Liu E, Fei G, Fan J, et al. Unidirectional electron transport from graphitic-C3N4 for novel remote and long-term photocatalytic anti-corrosion on Q235 carbon steel. Chem Eng J 2022;429:132520. https://doi.org/10.1016/J.CEJ.2021.132520.
[128] Huang Y, Liu J, Zhao C, Jia X, Ma M, Qian Y, et al. Facile synthesis of defect-modified thin-layered and porous g-C3N4 with synergetic improvement for photocatalytic H2 production. ACS Appl Mater Interfaces 2020;12:52603–14. https://doi.org/10.1021/acsami.0c14262.
[129] Zhang Y, Thomas A, Antonietti M, Wang X. Activation of carbon nitride solids by protonation: morphology changes, enhanced ionic conductivity, and photoconduction experiments. J Am Chem Soc 2009;131:50–1. https://doi.org/10.1021/ja808329f.
[130] Li L, Shi Y, Xu Z, Sun H, Amin MDS, Yang X, et al. Environmentally friendly synthesis of oxygen-doped g-C3N4 nanosheets for enhancing photocatalytic corrosion resistance of carbon steel. Prog Org Coat 2022;163:106628. https://doi.org/10.1016/J.PORGCOAT.2021.106628.
[131] Bu Y, Chen Z. Highly efficient photoelectrochemical anticorrosion performance of C3N4ZnO composite with quasi-shell-core structure on 304 stainless steel. RSC Adv 2014;4:45397–406. https://doi.org/10.1039/c4ra06641c.
[132] Ma X, Ma Z, Zhang H, Lu D, Duan J, Hou B. Interfacial Schottky junction of Ti3C2Tx MXene/g-C3N4 for promoting spatial charge separation in photoelectrochemical cathodic protection of steel. J Photochem Photobiol A Chem 2022;426:113772. https://doi.org/10.1016/J.JPHOTOCHEM.2022.113772.
[133] Lv Y, Zheng Y, Zhu H, Wu Y. Designing a dual-functional material with barrier anti-corrosion and photocatalytic antifouling properties using g-C3N4 nanosheet with ZnO nanoring. J Mater Sci Technol 2022;106:56–69. https://doi.org/10.1016/J.JMST.2021.07.029.
[134] Ge Y, Guo X, Zhou D, Liu J. Construction and excellent photoelectric synergistic anticorrosion performance of Z-scheme carbon nitride/tungsten oxide heterojunctions. Nanoscale. 2022;14:12358–76. https://doi.org/10.1039/d2nr03246e.
[135] Chafiq M, Chaouiki A, Suhartono T, Hazmatulhaq F, Ko YG. Interface engineering of LDH-based material as efficient anti-corrosive system via synergetic performance of host, interlayers, and morphological features of nature-mimic architectures. Chem Eng J 2023;462:142239. https://doi.org/10.1016/j.cej.2023.142239.
[136] Zhang J, Zhao J, Wang J, Tabish M, Zhang J. Enhancing the corrosion resistance of waterborne epoxy coating by fumarate intercalated LDHs prepared by high gravity technology. Prog Org Coat 2023;174:107271. https://doi.org/10.1016/j.porgcoat.2022.107271.
[137] Hang TTX, Truc TA, Duong NT, Pébère N, Olivier M-G. Layered double hydroxides as containers of inhibitors in organic coatings for corrosion protection of carbon steel. Prog Org Coat 2012;74:343–8. https://doi.org/10.1016/j.porgcoat.2011.10.020.
[138] Tabish M, Yasin G, Anjum MJ, Malik MU, Zhao J, Yang Q, et al. Reviewing the current status of layered double hydroxide-based smart nanocontainers for corrosion inhibiting applications. J Mater Res Technol 2021;10:390–421. https://doi.org/10.1016/J.JMRT.2020.12.025.
[139] Tabish M, Zhao J, Kumar A, Yan J, Wang J, Shi F, et al. Developing epoxy-based anti-corrosion functional nanocomposite coating with CaFe-Tolyl-triazole layered double hydroxide@g-C3N4 as nanofillers on Q235 steel substrate against NaCl corrosive environment. Chem Eng J 2022;450:137624. https://doi.org/10.1016/J.CEJ.2022.137624.
[140] Sanaei Z, Shamsipur A, Ramezanzadeh B. Manipulating a smart multi-functional nano-carrier based on l-cysteine-GO-ZIF67@ZIF8 core@shell MOFs-LDH for designing an excellent self-healing coating. Appl Mater Today 2023;30:101718. https://doi.org/10.1016/J.APMT.2022.101718.
[141] Tabish M, Yasin G, Anjum MJ, Malik MU, Zhao J, Yang Q, et al. Reviewing the current status of layered double hydroxide-based smart nanocontainers for corrosion inhibiting applications. J Mater Res Technol 2021;10:390–421. https://doi.org/10.1016/J.JMRT.2020.12.025.
[142] Lu C, Kim TH, Bendix J, Abdelmoula M, Ruby C, Nielsen UG, et al. Stability of magnetic LDH composites used for phosphate recovery. J Colloid Interface Sci 2020;580:660–8. https://doi.org/10.1016/J.JCIS.2020.07.020.
[143] Xing X, Sui Y, Zhao H, Yuan M, Chu X, Liu S, et al. Boosting the corrosion inhibition of Q235 steel by incorporating multi-responsive montmorillonite-based composite inhibitor into epoxy coating. Chem Lett 2022;51:940–4. https://doi.org/10.1246/cl.220287.
[144] Sun Y, Yuan S, Fan W, Lin D, Zhang K, Bai Z, et al. A smart composite coating with photothermal response, anti-UV and anti-corrosion properties. Chem Eng J 2023;452:138983. https://doi.org/10.1016/J.CEJ.2022.138983.
[145] Yotsuji K, Tachi Y, Sakuma H, Kawamura K. Effect of interlayer cations on montmorillonite swelling: comparison between molecular dynamic simulations and experiments. Appl Clay Sci 2021;204:106034. https://doi.org/10.1016/J.CLAY.2021.106034.
[146] Li G, Chen L, An Y, Gao M, Zhou H, Chen J. Investigating the effect of polytetrafluoroethylene on the tribological properties and corrosion resistance of epoxy/hydroxylated hexagonal boron nitride composite coatings. Corros Sci 2023;210:110820. https://doi.org/10.1016/j.corsci.2022.110820.
[147] Bao Q, He R, Liu Y, Wang Q. Multifunctional boron nitride nanosheets cured epoxy resins with highly thermal conductivity and enhanced flame retardancy for thermal management applications. Compos Part A Appl Sci Manuf 2023;164:107309. https://doi.org/10.1016/j.compositesa.2022.107309.
[148] Peng X, Su Z, Li C, Tang C. High mechanical and thermal performance of insulating paper cellulose modified with appropriate h-BN doping amount: a molecular simulation study. Adv Eng Mater 2023;25:2200949. https://doi.org/10.1002/adem.202200949.
[149] Moon S, Kim J, Park J, Im S, Kim J, Hwang I, et al. Hexagonal boron nitride for next-generation photonics and electronics. Adv Mater 2023;35:2204161. https://doi.org/10.1002/adma.202204161.
[150] Naclerio AE, Kidambi PR. A review of scalable hexagonal boron nitride (h-BN) synthesis for present and future applications. Adv Mater 2023;35:2207374. https://doi.org/10.1002/adma.202207374.
[151] Li T, Zhao S-R, Sheng X-X, Jiang Y-T, Ji L-Y, Wang F-R, et al. In-situ growth and excellent corrosion protection properties of molybdenum dioxide/boron nitride heterojunction composites. Prog Org Coat 2023;174:107289. https://doi.org/10.1016/j.porgcoat.2022.107289.
[152] Guimarey MJG, Ratwani CR, Xie K, Koohgilani M, Hadfield M, Kamali AR, et al. Multifunctional steel surface through the treatment with graphene and h-BN. Tribol Int 2023;180:108264. https://doi.org/10.1016/j.triboint.2023.108264.
[153] Zhou M, Zhao C, Liu P, Yu H. Adsorption behavior of Ti3C2Tx with h-BN nanosheet and their application in waterborne epoxy anti-corrosion coating. Appl Surf Sci 2022;586:152778. https://doi.org/10.1016/j.apsusc.2022.152778.

[154] Wu Y, He Y, Zhou T, Chen C, Zhong F, Xia Y, et al. Synergistic functionalization of h-BN by mechanical exfoliation and PEI chemical modification for enhancing the corrosion resistance of waterborne epoxy coating. Prog Org Coat 2020;142:105541. https://doi.org/10.1016/j.porgcoat.2020.105541.
[155] Dadvand M, Savadogo O. Effect of hBN on corrosion and wear performances of DC electrodeposited NiW and NiW–SiC on brass substrates. Coatings. 2022;12. https://doi.org/10.3390/coatings12071011.
[156] Jing Y, Wang P, Yang Q, He Y, Bai Y. Molybdenum disulfide with poly(dopamine) and epoxy groups as an efficiently anticorrosive reinforcers in epoxy coating. Synth Met 2020;259:116249. https://doi.org/10.1016/J.SYNTHMET.2019.116249.
[157] Cheng Y, Chuah GK. The synthesis and applications of α-zirconium phosphate. Chin Chem Lett 2020;31:307–10. https://doi.org/10.1016/j.cclet.2019.04.063.
[158] Zou B, Chang X, Yang J, Wang S, Xu J, Wang S, et al. Plasma treated h-BN nanoflakes as barriers to enhance anticorrosion of acrylic coating on steel. Prog Org Coat 2019;133:139–44. https://doi.org/10.1016/J.PORGCOAT.2019.04.040.
[159] Manzeli S, Ovchinnikov D, Pasquier D, Yazyev OV, Kis A. 2D transition metal dichalcogenides. Nat Rev Mater 2017;2:17033. https://doi.org/10.1038/natrevmats.2017.33.
[160] Tajik S, Dourandish Z, Garkani Nejad F, Beitollahi H, Jahani PM, Di Bartolomeo A. Transition metal dichalcogenides: synthesis and use in the development of electrochemical sensors and biosensors. Biosens Bioelectron 2022;216:114674. https://doi.org/10.1016/j.bios.2022.114674.
[161] Xia H, Shi Z, Gong C, He Y. Recent strategies for activating the basal planes of transition metal dichalcogenides towards hydrogen production. J Mater Chem A Mater 2022;10:19067–89. https://doi.org/10.1039/d2ta02458f.
[162] Yang R, Fan Y, Zhang Y, Mei L, Zhu R, Qin J, et al. 2D transition metal Dichalcogenides for Photocatalysis. Angew Chem Int Ed 2023;62:e202218016. https://doi.org/10.1002/anie.202218016.
[163] Joseph A, Vijayan AS, Shebeeb CM, Akshay KS, John Mathew KP, Sajith V. A review on tailoring the corrosion and oxidation properties of MoS2-based coatings. J Mater Chem A Mater 2023;11:3172–209. https://doi.org/10.1039/d2ta07821j.
[164] Tibbetts GG, Lake ML, Strong KL, Rice BP. A review of the fabrication and properties of vapor-grown carbon nanofiber/polymer composites. Compos Sci Technol 2007;67:1709–18. https://doi.org/10.1016/j.compscitech.2006.06.015.
[165] Ahn S, Kim G, Nayak PK, Yoon SI, Lim H, Shin H-J, et al. Prevention of transition metal dichalcogenide photodegradation by encapsulation with h-BN layers. ACS Nano 2016;10:8973–9. https://doi.org/10.1021/acsnano.6b05042.
[166] Ding H, Ahmed A, Shen K, Sun L. Assembly of exfoliated α-zirconium phosphate nanosheets: mechanisms and versatile applications. Aggregate. 2022;3:e174. https://doi.org/10.1002/agt2.174.
[167] Ra HN, Kim HG, Kim H, Peak SH, Kim YC, Kim SS. Effects of size and aspect ratio of zirconium phosphate (ZrP) on barrier properties of epoxy-ZrP nanocomposites. Prog Org Coat 2019;133:1–7. https://doi.org/10.1016/j.porgcoat.2019.02.032.
[168] Bouali I, Rocca E, Veys-Renaux D, Rhouta B, Khalil A, Aït Aghzzaf A. Ca2+-exchange in layered zirconium orthophosphate, α-ZrP: chemical study and potential application for zinc corrosion inhibition. Appl Surf Sci 2017;422:778–86. https://doi.org/10.1016/j.apsusc.2017.06.083.
[169] Zhao Y, He Y, Yan S, Li C, Li H, Chen W, et al. Eco-friendly design of α-zirconium phosphate modified by phytic acid for reinforcing the corrosion resistance of waterborne epoxy coating. Colloids Surf A Physicochem Eng Asp 2023;656:130472. https://doi.org/10.1016/J.COLSURFA.2022.130472.
[170] Naguib M, Kurtoglu M, Presser V, Lu J, Niu J, Heon M, et al. Two-dimensional nanocrystals produced by exfoliation of Ti3AlC2. Adv Mater 2011;23:4248–53. https://doi.org/10.1002/adma.201102306.
[171] Anasori B, Lukatskaya MR, Gogotsi Y. 2D metal carbides and nitrides (MXenes) for energy storage. Nat Rev Mater 2017;2:16098. https://doi.org/10.1038/natrevmats.2016.98.
[172] Sheng X, Zhao Y, Zhang L, Lu X. Properties of two-dimensional Ti3C2 MXene/thermoplastic polyurethane nanocomposites with effective reinforcement via melt blending. Compos Sci Technol 2019;181:107710. https://doi.org/10.1016/J.COMPSCITECH.2019.107710.
[173] Iqbal A, Kim H, Oh J-M, Chae J, Kim J, Kim M, et al. Effect of substitutional oxygen on properties of Ti3C2Tx MXene produced using recycled TiO2 source. Small Methods 2023:2201715. https://doi.org/10.1002/smtd.202201715. n/a.
[174] Yan H, Li W, Li H, Fan X, Zhu M. Ti3C2 MXene nanosheets toward high-performance corrosion inhibitor for epoxy coating. Prog Org Coat 2019;135:156–67. https://doi.org/10.1016/j.porgcoat.2019.06.013.
[175] Jia W, Cao H, Wang T, Min Y, Xu Q. Electrochemical behavior and anti-corrosion property of Ti3C2Tx MXene/LDH heterostructured coating on aluminum alloy. Surf Coat Technol 2023;463:129551. https://doi.org/10.1016/j.surfcoat.2023.129551.
[176] Cai M, Fan X, Yan H, Li Y, Song S, Li W, et al. In situ assemble Ti3C2Tx MXene@MgAl-LDH heterostructure towards anticorrosion and antiwear application. Chem Eng J 2021;419:130050. https://doi.org/10.1016/j.cej.2021.130050.
[177] Yan H, Cai M, Li W, Fan X, Zhu M. Amino-functionalized Ti3C2Tx with anti-corrosive/wear function for waterborne epoxy coating. J Mater Sci Technol 2020;54:144–59. https://doi.org/10.1016/j.jmst.2020.05.002.
[178] Haddadi SA, Hu S, Ghaderi S, Ghanbari A, Ahmadipour M, Pung S-Y, et al. Amino-functionalized MXene nanosheets doped with Ce(III) as potent nanocontainers toward self-healing epoxy nanocomposite coating for corrosion protection of mild steel. ACS Appl Mater Interfaces 2021;13:42074–93. https://doi.org/10.1021/acsami.1c13055.
[179] Zhao H, Ding J, Zhou M, Yu H. Air-stable titanium carbide MXene nanosheets for corrosion protection. ACS Appl Nano Mater 2021;4:3075–86. https://doi.org/10.1021/acsanm.1c00219.
[180] Cai M, Fan X, Yan H, Li Y, Song S, Li W, et al. In situ assemble Ti3C2Tx MXene@MgAl-LDH heterostructure towards anticorrosion and antiwear application. Chem Eng J 2021;419:130050. https://doi.org/10.1016/j.cej.2021.130050.
[181] Ding J, Zhao H, Yu H. Structure and performance insights in carbon dots-functionalized MXene-epoxy ultrathin anticorrosion coatings. Chem Eng J 2022;430:132838. https://doi.org/10.1016/J.CEJ.2021.132838.
[182] Qiang Y, Ran B, Li M, Xu Q, Peng J. GO-functionalized MXene towards superior anti-corrosion coating. J Colloid Interface Sci 2023;642:595–603. https://doi.org/10.1016/j.jcis.2023.03.167.
[183] Ning Y, Jian D, Liu S, Chen F, Song Y, Li S, et al. Designing a Ti3C2Tx MXene with long-term antioxidant stability for high-performance anti-corrosion coatings. Carbon N Y 2023;202:20–30. https://doi.org/10.1016/j.carbon.2022.10.042.
[184] Ding J, Zhao H, Yu H. Structure and performance insights in carbon dots-functionalized MXene-epoxy ultrathin anticorrosion coatings. Chem Eng J 2022;430:132838. https://doi.org/10.1016/j.cej.2021.132838.
[185] Ning Y, Jian D, Liu S, Song Y, Wang Q, Liu B. Fabrication of a SAPNI/I-Ti3C2Tx 3D structure hybrid for the enhancement of higher barrier and self-passivation coatings. J Alloys Compd 2023;946:169371. https://doi.org/10.1016/J.JALLCOM.2023.169371.
[186] Ding J, Wang H, Zhao H, Miah MR, Wang J, Zhu J. High-compact MXene-based coatings by controllable interfacial structures. Nanoscale. 2023. https://doi.org/10.1039/d3nr00490b.
[187] Li C, Xu J, Xu Q, Xue G, Yu H, Wang X, et al. Synthesis of Ti3C2 MXene@PANI composites for excellent anticorrosion performance of waterborne epoxy coating. Prog Org Coat 2022;165:106673. https://doi.org/10.1016/j.porgcoat.2021.106673.
[188] Shen L, Zhao W, Wang K, Xu J. GO-Ti3C2 two-dimensional heterojunction nanomaterial for anticorrosion enhancement of epoxy zinc-rich coatings. J Hazard Mater 2021;417:126048. https://doi.org/10.1016/j.jhazmat.2021.126048.
[189] Shahryari Z, Gheisari K, Yeganeh M, Ramezanzadeh B. MoO42−-doped oxidative polymerized pyrrole-graphene oxide core-shell structure synthesis and application for dual-barrier & active functional epoxy-coating construction. Prog Org Coat 2022;167:106845. https://doi.org/10.1016/J.PORGCOAT.2022.106845.
[190] Dehghani A, Bahlakeh G, Ramezanzadeh B, Mofidabadi A Hossein Jafari. Electronic DFT-D modeling of L-citrulline molecules interactions with Beta-CD aligned rGO-APTES multi-functional nano-capsule for anti-corrosion application. J Mol Liq 2022;354:118814. https://doi.org/10.1016/J.MOLLIQ.2022.118814.
[191] Dehghani A, Bahlakeh G, Ramezanzadeh B. Designing a novel targeted-release nano-container based on the silanized graphene oxide decorated with cerium acetylacetonate loaded beta-cyclodextrin (β-CD-CeA-MGO) for epoxy anti-corrosion coating. Chem Eng J 2020;400:125860. https://doi.org/10.1016/J.CEJ.2020.125860.
[192] Daradmare S, Pradhan M, Raja VS, Parida S. Encapsulating 8-hydroxyquinoline in graphene oxide-stabilized polystyrene containers and its anticorrosion performance. J Mater Sci 2016;51:10262–77. https://doi.org/10.1007/s10853-016-0254-4.
[193] Sun X, Ma C, Ma F, Wang T, Feng C, Wang W. A novel coating with SiO2 anchored on MXene loading tannic acid for self-healing anticorrosive performance. J Alloys Compd 2022;928:167202. https://doi.org/10.1016/J.JALLCOM.2022.167202.
[194] Xing X, Sui Y, Li Q, Yuan M, Zhao H, Zhou D, et al. Multifunctional ZnAl-MoO4 LDH assembled Ti3C2Tx MXene composite for active/passive corrosion protection behavior of epoxy coatings. Appl Surf Sci 2023;623:157092. https://doi.org/10.1016/J.APSUSC.2023.157092.
[195] Ning Y, Jian D, Liu S, Chen F, Song Y, Li S, et al. Designing a Ti3C2Tx MXene with long-term antioxidant stability for high-performance anti-corrosion coatings. Carbon N Y 2023;202:20–30. https://doi.org/10.1016/J.CARBON.2022.10.042.
[196] He X, Li S, Wu J, Chen Y, Zhang L, Sheng X. One-pot fabrication of an MXene-ZrP@PDA heterojunction for enhanced corrosion/wear resistance of waterborne epoxy coatings. Ind Eng Chem Res 2022;61:12576–89. https://doi.org/10.1021/acs.iecr.2c01885.
[197] Li L, Zhang Y, Shi Y, Guo F, Yang X, Shi W. A hydrophobic high-crystalline g-C3N4/epoxy resin composite coating with excellent durability and stability for long-term corrosion resistance. Mater Today Commun 2023;35:105692. https://doi.org/10.1016/J.MTCOMM.2023.105692.
[198] Barrejón M, Prato M. Carbon nanotube membranes in water treatment applications. Adv Mater Interfaces 2022;9:2101260. https://doi.org/10.1002/admi.202101260.
[199] Montazeri A, Javadpour J, Khavandi A, Tcharkhtchi A, Mohajeri A. Mechanical properties of multi-walled carbon nanotube/epoxy composites. Mater Des 2010;31:4202–8. https://doi.org/10.1016/j.matdes.2010.04.018.
[200] Papageorgiou DG, Li Z, Liu M, Kinloch IA, Young RJ. Mechanisms of mechanical reinforcement by graphene and carbon nanotubes in polymer nanocomposites. Nanoscale. 2020;12:2228–67. https://doi.org/10.1039/c9nr06952f.
[201] Shirkavand Hadavand B, Mahdavi Javid K, Gharagozlou M. Mechanical properties of multi-walled carbon nanotube/epoxy polysulfide nanocomposite. Mater Des 2013;50:62–7. https://doi.org/10.1016/j.matdes.2013.02.039.
[202] Li Y, Shang Y, He J, Li M, Yang M. Low-loading oxidized multi-walled carbon nanotube grafted waterborne polyurethane composites with ultrahigh mechanical properties improvement. Diamond Relat Mater 2022;130:109427. https://doi.org/10.1016/j.diamond.2022.109427.

[203] Montazeri A, Chitsazzadeh M. Effect of sonication parameters on the mechanical properties of multi-walled carbon nanotube/epoxy composites. Mater Design 1980-2015;56(2014):500–8. https://doi.org/10.1016/j.matdes.2013.11.013.
[204] Garg P, Singh BP, Kumar G, Gupta T, Pandey I, Seth RK, et al. Effect of dispersion conditions on the mechanical properties of multi-walled carbon nanotubes based epoxy resin composites. J Polym Res 2011;18:1397–407. https://doi.org/10.1007/s10965-010-9544-8.
[205] Ghahremani P, Mostafatabar AH, Bahlakeh G, Ramezanzadeh B. Rational design of a novel multi-functional carbon-based nano-carrier based on multi-walled-CNT-oxide/polydopamine/chitosan for epoxy composite with robust pH-sensitive active anti-corrosion properties. Carbon N Y 2022;189:113–41. https://doi.org/10.1016/J.CARBON.2021.11.067.
[206] Ding S, Wang X, Qiu L, Ni Y-Q, Dong X, Cui Y, et al. Self-sensing cementitious composites with hierarchical carbon fiber-carbon nanotube composite fillers for crack development monitoring of a maglev girder. Small. 2023;19:2206258. https://doi.org/10.1002/smll.202206258.
[207] Ge T, Zhao W, Wu X, Lan X, Zhang Y, Qiang Y, et al. Incorporation of electroconductive carbon fibers to achieve enhanced anti-corrosion performance of zinc rich coatings. J Colloid Interface Sci 2020;567:113–25. https://doi.org/10.1016/j.jcis.2020.02.002.
[208] Liao P-Q, Shen J-Q, Zhang J-P. Metal–organic frameworks for electrocatalysis. Coord Chem Rev 2018;373:22–48. https://doi.org/10.1016/j.ccr.2017.09.001.
[209] Sun Q, Qin L, Lai C, Liu S, Chen W, Xu F, et al. Constructing functional metal-organic frameworks by ligand design for environmental applications. J Hazard Mater 2023;447. https://doi.org/10.1016/j.jhazmat.2023.130848.
[210] Alipanah N, Yari H, Mahdavian M, Ramezanzadeh B, Bahlakeh G. MIL-88A (Fe) filler with duplicate corrosion inhibitive/barrier effect for epoxy coatings: electrochemical, molecular simulation, and cathodic delamination studies. J Industr Eng Chem 2021;97:200–15. https://doi.org/10.1016/J.JIEC.2021.01.035.
[211] Shahini MH, Mohammadloo HE, Ramezanzadeh M, Ramezanzadeh B. Recent innovations in synthesis/characterization of advanced nano-porous metal-organic frameworks (MOFs); current/future trends with a focus on the smart anti-corrosion features. Mater Chem Phys 2022;276:125420. https://doi.org/10.1016/J.MATCHEMPHYS.2021.125420.
[212] Yao J, Wang H. Zeolitic imidazolate framework composite membranes and thin films: synthesis and applications. Chem Soc Rev 2014;43:4470–93. https://doi.org/10.1039/c3cs60480b.
[213] Huang XC, Lin YY, Zhang JP, Chen XM. Ligand-directed strategy for zeolite-type metal-organic frameworks: zinc(II) imidazolates with unusual zeolitic topologies. Angew Chem Int Ed 2006;45:1557–9. https://doi.org/10.1002/anie.200503778.
[214] Park KS, Ni Z, Cô AP, Choi JY, Huang R, Uribe-Romo FJ, et al. Exceptional chemical and thermal stability of zeolitic imidazolate frameworks. https://www.pnas.org; 2006.
[215] Venna SR, Jasinski JB, Carreon MA. Structural evolution of zeolitic imidazolate framework-8. J Am Chem Soc 2010;132:18030–3. https://doi.org/10.1021/ja109268m.
[216] Dai H, Yuan X, Jiang L, Wang H, Zhang J, Zhang J, et al. Recent advances on ZIF-8 composites for adsorption and photocatalytic wastewater pollutant removal: fabrication, applications and perspective. Coord Chem Rev 2021;441:213985. https://doi.org/10.1016/j.ccr.2021.213985.
[217] Schelling M, Kim M, Otal E, Aguirre M, Hinestroza JP. Synthesis of a zinc–imidazole metal–organic framework (ZIF-8) using ZnO rods grown on cotton fabrics as precursors: arsenate absorption studies. Cellulose. 2020;27:6399–410. https://doi.org/10.1007/s10570-020-03216-4.
[218] Jung S, Chang S, Kim N-E, Choi S-O, Song Y-J, Yuan Y, et al. Curcumin/Zeolitic Imidazolate Framework-8 nanoparticle-integrated microneedles for pH-responsive treatment of skin disorders. ACS Appl Nano Mater 2022;5:13671–9. https://doi.org/10.1021/acsanm.2c03884.
[219] Zhong G, Liu D, Zhang J. The application of ZIF-67 and its derivatives: adsorption, separation, electrochemistry and catalysts. J Mater Chem A Mater 2018;6:1887–99. https://doi.org/10.1039/c7ta08268a.
[220] Yilmaz G, Peh SB, Zhao D, Ho GW. Atomic- and molecular-level design of functional metal–organic frameworks (MOFs) and derivatives for energy and environmental applications. Adv Sci 2019;6:1901129. https://doi.org/10.1002/advs.201901129.
[221] Lashgari SM, Yari H, Mahdavian M, Ramezanzadeh B, Bahlakeh G, Ramezanzadeh M. Application of nanoporous cobalt-based ZIF-67 metal-organic framework (MOF) for construction of an epoxy-composite coating with superior anti-corrosion properties. Corros Sci 2021;178:109099. https://doi.org/10.1016/J.CORSCI.2020.109099.
[222] Kadhom M, Al-Furaiji M, Salih S, Al-Obaidi MA, Abdullah GH, Albayati N. A review on UiO-66 applications in membrane-based water treatment processes. J Water Process Eng 2023;51:103402. https://doi.org/10.1016/j.jwpe.2022.103402.
[223] Ramezanzadeh M, Ramezanzadeh B, Bahlakeh G, Tati A, Mahdavian M. Development of an active/barrier bi-functional anti-corrosion system based on the epoxy nanocomposite loaded with highly-coordinated functionalized zirconium-based nanoporous metal-organic framework (Zr-MOF). Chem Eng J 2021;408:127361. https://doi.org/10.1016/J.CEJ.2020.127361.
[224] Dabaleh A, Shojaei A, Nematollahzadeh A, Molavi H. Development of pH-sensitive UiO-66/polyaniline nanohybrids with self-healing anticorrosive performance in epoxy coatings. Ind Eng Chem Res 2023;62:7447–63. https://doi.org/10.1021/acs.iecr.3c00056.
[225] Jouyandeh M, Tikhani F, Shabanian M, Movahedi F, Moghari S, Akbari V, et al. Synthesis, characterization, and high potential of 3D metal–organic framework (MOF) nanoparticles for curing with epoxy. J Alloys Compd 2020;829:154547. https://doi.org/10.1016/j.jallcom.2020.154547.
[226] Duan S, Dou B, Lin X, Zhao S, Emori W, Pan J, et al. Influence of active nanofiller ZIF-8 metal-organic framework (MOF) by microemulsion method on anticorrosion of epoxy coatings. Colloids Surf A Physicochem Eng Asp 2021;624:126836. https://doi.org/10.1016/j.colsurfa.2021.126836.
[227] Seidi F, Jouyandeh M, Taghizadeh M, Taghizadeh A, Vahabi H, Habibzadeh S, et al. Metal-organic framework (MOF)/epoxy coatings: a review. Materials. 2020;13. https://doi.org/10.3390/ma13122881.
[228] Zhou C, Pan M, Li S, Sun Y, Zhang H, Luo X, et al. Metal organic frameworks (MOFs) as multifunctional nanoplatform for anticorrosion surfaces and coatings. Adv Colloid Interface Sci 2022;305. https://doi.org/10.1016/j.cis.2022.102707.
[229] Cui G, Bi Z, Zhang R, Liu J, Yu X, Li Z. A comprehensive review on graphene-based anti-corrosive coatings. Chem Eng J 2019;373:104–21. https://doi.org/10.1016/j.cej.2019.05.034.
[230] Schriver M, Regan W, Gannett WJ, Zaniewski AM, Crommie MF, Zettl A. Graphene as a long-term metal oxidation barrier: worse than nothing. ACS Nano 2013;7:5763–8. https://doi.org/10.1021/nn4014356.
[231] Xiong L, Liu J, Yu M, Li S. Improving the corrosion protection properties of PVB coating by using salicylaldehyde@ZIF-8/graphene oxide two-dimensional nanocomposites. Corros Sci 2019;146:70–9. https://doi.org/10.1016/J.CORSCI.2018.10.016.
[232] Luo X, Zhou C, Chen B, Wu D, Li J, Kong J, et al. A superior corrosion-protective coating based on an insulated poly-2-amiothiazole noncovalently functionalized graphene. Corros Sci 2021;178:109044. https://doi.org/10.1016/J.CORSCI.2020.109044.
[233] Keshmiri N, Najmi P, Ramezanzadeh M, Ramezanzadeh B. Designing an eco-friendly lanthanide-based metal organic framework (MOF) assembled graphene-oxide with superior active anti-corrosion performance in epoxy composite. J Clean Prod 2021;319:128732. https://doi.org/10.1016/J.JCLEPRO.2021.128732.
[234] Majidi R, Ramezanzadeh M, Ramezanzadeh B. Developing a dual-functional self-healing nanocomposite utilizing oxidized-multiwall carbon nanotube/highly-porous metal-organic framework (OCNT/ZIF-8) nano-hybrid. Appl Mater Today 2023;32:101830. https://doi.org/10.1016/J.APMT.2023.101830.
[235] Dehghani A, Lashgari M, Bahlakeh G, Ramezanzadeh B. Chitosan biomolecules-modified graphene oxide nano-layers decorated by mesoporous ZIF-9 nanocrystals for the construction of a smart/pH-triggered anti-corrosion coating system. J Industr Eng Chem 2023;121:45–62. https://doi.org/10.1016/J.JIEC.2022.05.048.
[236] Mohammadkhah S, Ramezanzadeh M, Eivaz Mohammadloo H, Ramezanzadeh B, Ghamsarizade R. Construction of a nano-micro nacre-inspired 2D-MoS2-MOF-glutamate carrier toward designing a high-performance smart epoxy composite. J Industr Eng Chem 2023;121:358–77. https://doi.org/10.1016/J.JIEC.2023.01.039.
[237] Dehghani A, Sanaei Z, Fedel M, Ramezanzadeh M, Mahdavian M, Ramezanzade B. Fabrication of an intelligent anti-corrosion silane film using a MoO42− loaded Micro/mesoporous ZIF67-MOF/multi-walled-CNT/APTES core-shell nano-container. Colloids Surf A Physicochem Eng Asp 2023;656:130511. https://doi.org/10.1016/J.COLSURFA.2022.130511.
[238] Ren B, Chen Y, Li Y, Li W, Gao S, Li H, et al. Rational design of metallic anti-corrosion coatings based on zinc gluconate@ZIF-8. Chem Eng J 2020;384:123389. https://doi.org/10.1016/J.CEJ.2019.123389.
[239] Ramezanzadeh M, Ramezanzadeh B, Mahdavian M. Graphene skeletal nanotemplate coordinated with pH-responsive porous double-ligand metal-organic frameworks (DL-MOFs) through ligand exchange theory for high-performance smart coatings. Chem Eng J 2023;461:141869. https://doi.org/10.1016/j.cej.2023.141869.
[240] Ren B, Li Y, Meng D, Li J, Gao S, Cao R. Encapsulating polyaniline within porous MIL-101 for high-performance corrosion protection. J Colloid Interface Sci 2020;579:842–52. https://doi.org/10.1016/J.JCIS.2020.06.127.
[241] Jiang X, He S, Han G, Long J, Li S, Lau CH, et al. Aqueous one-step modulation for synthesizing monodispersed ZIF-8 nanocrystals for mixed-matrix membrane. ACS Appl Mater Interfaces 2021;13:11296–305. https://doi.org/10.1021/acsami.0c22910.
[242] Yang C, Xu W, Meng X, Shi X, Shao L, Zeng X, et al. A pH-responsive hydrophilic controlled release system based on ZIF-8 for self-healing anticorrosion application. Chem Eng J 2021;415. https://doi.org/10.1016/j.cej.2021.128985.
[243] Zhang Y, Wang J, Zhao S, Serdechnova M, Blawert C, Wang H, et al. Double-ligand strategy to construct an inhibitor-loaded Zn-MOF and its corrosion protection ability for aluminum alloy 2A12. ACS Appl Mater Interfaces 2021;13:51685–94. https://doi.org/10.1021/acsami.1c13738.
[244] Armelin E, Pla R, Liesa F, Ramis X, Iribarren JI, Alemán C. Corrosion protection with polyaniline and polypyrrole as anticorrosive additives for epoxy paint. Corros Sci 2008;50:721–8. https://doi.org/10.1016/j.corsci.2007.10.006.
[245] Deshpande PP, Jadhav NG, Gelling VJ, Sazou D. Conducting polymers for corrosion protection: a review. J Coat Technol Res 2014;11:473–94. https://doi.org/10.1007/s11998-014-9586-7.
[246] Chen Z, Li X, Gong B, Scharnagl N, Zheludkevich ML, Ying H, et al. Double stimuli-responsive conducting polypyrrole nanocapsules for corrosion-resistant epoxy coatings. ACS Appl Mater Interfaces 2023;15:2067–76. https://doi.org/10.1021/acsami.2c17466.
[247] Han R, He H, Liu X, Zhao L, Yang Y, Liu C, et al. Anti–corrosion and self-healing coatings with polyaniline/epoxy copolymer–urea–formaldehyde microcapsules for rusty steel sheets. J Colloid Interface Sci 2022;616:605–17. https://doi.org/10.1016/j.jcis.2022.02.088.

[248] Zhao Y, Huang M, Gao Z, He H, Chen Y, He F, et al. Preparation of polyaniline/cellulose nanofiber composites with enhanced anticorrosion performance for waterborne epoxy resin coatings. Polym Eng Sci 2023;63:1613–22. https://doi.org/10.1002/pen.26310.
[249] Li X, Li L, Zhang W, Li Y, Ma D, Lei Q, et al. Grafting of polyaniline onto polydopamine-wrapped carbon nanotubes to enhance corrosion protection properties of epoxy coating. Colloids Surf A Physicochem Eng Asp 2023;670:131548. https://doi.org/10.1016/J.COLSURFA.2023.131548.
[250] Alipanah N, Dehghani A, Abdolmaleki M, Bahlakeh G, Ramezanzadeh B. Designing environmentally-friendly pH-responsive self-redox polyaniline grafted graphene oxide nano-platform decorated by zeolite imidazole ZIF-9 MOF for achieving smart functional epoxy-based anti-corrosion coating. J Environ Chem Eng 2023;11:109048. https://doi.org/10.1016/J.JECE.2022.109048.
[251] Howarth AJ, Liu Y, Li P, Li Z, Wang TC, Hupp JT, et al. Chemical, thermal and mechanical stabilities of metal-organic frameworks. Nat Rev Mater 2016;1. https://doi.org/10.1038/natrevmats.2015.18.
[252] Liu T, Zhang D, Zhang R, Wang J, Ma L, Keil P, et al. Self-healing and corrosion-sensing coatings based on pH-sensitive MOF-capped microcontainers for intelligent corrosion control. Chem Eng J 2023;454:140335. https://doi.org/10.1016/J.CEJ.2022.140335.
[253] Liu D, Gu W, Zhou L, Wang L, Zhang J, Liu Y, et al. Recent advances in MOF-derived carbon-based nanomaterials for environmental applications in adsorption and catalytic degradation. Chem Eng J 2022;427. https://doi.org/10.1016/j.cej.2021.131503.
[254] Xiao W, Cheng M, Liu Y, Wang J, Zhang G, Wei Z, et al. Functional metal/carbon composites derived from metal-organic frameworks: insight into structures, properties, performances, and mechanisms. ACS Catal 2023;13:1759–90. https://doi.org/10.1021/acscatal.2c04807.
[255] Ramezanzadeh M, Ramezanzadeh B, Mahdavian M. Graphene skeletal nanotemplate coordinated with pH-responsive porous double-ligand metal-organic frameworks (DL-MOFs) through ligand exchange theory for high-performance smart coatings. Chem Eng J 2023;461:141869. https://doi.org/10.1016/J.CEJ.2023.141869.
[256] Côté AP, Benin AI, Ockwig NW, O'Keeffe M, Matzger AJ, Yaghi OM. Porous, crystalline, covalent organic frameworks. Science 1979;310(2005):1166–70. https://doi.org/10.1126/science.1120411.
[257] Gu C-C, Xu F-H, Zhu W-K, Wu R-J, Deng L, Zou J, et al. Recent advances on covalent organic frameworks (COFs) as photocatalysts: different strategies for enhancing hydrogen generation. Chem Commun 2023. https://doi.org/10.1039/D3CC01970E.
[258] Li X, Cai S, Sun B, Yang C, Zhang J, Liu Y. Chemically robust covalent organic frameworks: progress and perspective. Matter. 2020;3:1507–40. https://doi.org/10.1016/j.matt.2020.09.007.
[259] Zhao Z, Feng H, Qin D, Li W, Wang W, Chen S. pH-responsive intelligent antibacterial coatings based on 2D-COF for controlled release of capsaicin. ACS Appl Polym Mater 2023;5:2124–35. https://doi.org/10.1021/acsapm.2c02138.
[260] Geng K, Arumugam V, Xu H, Gao Y, Jiang D. Covalent organic frameworks: polymer chemistry and functional design. Prog Polym Sci 2020;108:101288. https://doi.org/10.1016/j.progpolymsci.2020.101288.
[261] Gong Y-N, Guan X, Jiang H-L. Covalent organic frameworks for photocatalysis: synthesis, structural features, fundamentals and performance. Coord Chem Rev 2023;475:214889. https://doi.org/10.1016/j.ccr.2022.214889.
[262] Shi Y, Yang J, Gao F, Zhang Q. Covalent organic frameworks: recent progress in biomedical applications. ACS Nano 2023;17:1879–905. https://doi.org/10.1021/acsnano.2c11346.
[263] Mohajer F, Mohammadi Ziarani G, Badiei A, Iravani S, Varma RS. Recent advances in covalent organic frameworks (COFs) for wound healing and antimicrobial applications. RSC Adv 2023;13:8136–52. https://doi.org/10.1039/d2ra07194k.
[264] Wu C, Xia L, Xia S, Van der Bruggen B, Zhao Y. Advanced covalent organic framework-based membranes for recovery of ionic resources. Small. 2023;19:2206041. https://doi.org/10.1002/smll.202206041.
[265] Aslam AA, Irshad A, Nazir MS, Atif M. A review on covalent organic frameworks as adsorbents for organic pollutants. J Clean Prod 2023;400:136737. https://doi.org/10.1016/j.jclepro.2023.136737.
[266] Wang Z, Zhang S, Chen Y, Zhang Z, Ma S. Covalent organic frameworks for separation applications. Chem Soc Rev 2020;49:708–35. https://doi.org/10.1039/c9cs00827f.
[267] Liu X, Huang D, Lai C, Zeng G, Qin L, Wang H, et al. Recent advances in covalent organic frameworks (COFs) as a smart sensing material. Chem Soc Rev 2019;48:5266–302. https://doi.org/10.1039/C9CS00299E.
[268] Zhang M, Yu X, Lin Y, Liu J, Wang J. Anti-corrosion coatings with active and passive protective performances based on v-COF/GO nanocontainers. Prog Org Coat 2021;159:106415. https://doi.org/10.1016/j.porgcoat.2021.106415.
[269] Zhang C, Li W, Guo Z, Sun T, Wang W, Chen S. Controllable construction of mesoporous silica/2D-COF nanocomposites reinforced epoxy coatings with excellent self-repairing and long-lasting anticorrosion performances. Prog Org Coat 2023;177:107441. https://doi.org/10.1016/j.porgcoat.2023.107441.
[270] Liu T, Li W, Zhang C, Wang W, Dou W, Chen S. Preparation of highly efficient self-healing anticorrosion epoxy coating by integration of benzotriazole corrosion inhibitor loaded 2D-COF. J Industr Eng Chem 2021;97:560–73. https://doi.org/10.1016/j.jiec.2021.03.012.
[271] Li W, Zhang X, Zhang C, Yu M, Ren J, Wang W, et al. Exploring the corrosion resistance of epoxy coated steel by integrating mechanochemical synthesized 2D covalent organic framework. Prog Org Coat 2021;157:106299. https://doi.org/10.1016/j.porgcoat.2021.106299.
[272] Chen J, Liu T, Zhang X, Jiang Y, Xiao F, Li W, et al. Polyhedral oligomeric silsesquioxane grafted covalent organic frameworks for simultaneously improved tribological and corrosion resistance of epoxy coatings. Prog Org Coat 2022;172:107164. https://doi.org/10.1016/j.porgcoat.2022.107164.
[273] Najmi P, Keshmiri N, Ramezanzadeh M, Ramezanzadeh B, Arjmand M. Design of nacre-inspired 2D-MoS2Nanosheets assembled with mesoporous covalent organic frameworks (COFs) for smart coatings. ACS Appl Mater Interfaces 2022;14:54141–56. https://doi.org/10.1021/acsami.2c14542.
[274] Keshmiri N, Najmi P, Ramezanzadeh M, Ramezanzadeh B, Bahlakeh G. Ultrastable porous covalent organic framework assembled carbon nanotube as a novel nanocontainer for anti-corrosion coatings: experimental and computational studies. ACS Appl Mater Interfaces 2022;14:19958–74. https://doi.org/10.1021/acsami.1c24185.
[275] Najmi P, Keshmiri N, Ramezanzadeh M, Ramezanzadeh B, Arjmand M. Porous 2D Ti3C2 MXene nanosheets sandwiched between imine-based covalent organic frameworks (COFs) for excellent corrosion protective coatings. Chem Eng J 2023;456:141001. https://doi.org/10.1016/J.CEJ.2022.141001.
[276] Alipanah N, Dehghani A, Abdolmaleki M, Bahlakeh G, Ramezanzadeh B. Designing environmentally-friendly pH-responsive self-redox polyaniline grafted graphene oxide nano-platform decorated by zeolite imidazole ZIF-9 MOF for achieving smart functional epoxy-based anti-corrosion coating. J Environ Chem Eng 2023;11:109048. https://doi.org/10.1016/J.JECE.2022.109048.
[277] Feng J, Chen J, Wang S, Jia M, Zhang Z, Yu T, et al. Rational design of inhibitor-encapsulated bio-MOF-1 for dual corrosion protection. Inorg Chem 2022;61:18285–92. https://doi.org/10.1021/acs.inorgchem.2c03151.
[278] Keramatinia M, Majidi R, Ramezanzadeh B. La-MOF coordination polymer: An effective environmentally friendly pH-sensitive corrosion inhibitive-barrier nanofiller for the epoxy polyamide coating reinforcement. J Environ Chem Eng 2022;10:108246. https://doi.org/10.1016/J.JECE.2022.108246.
[279] Chen H, Yu Z, Yang G, Liao K, Peng B, Pang Y, et al. A novel pH-responsive smart anticorrosion coating based on sepiolite and MOF for high-performance corrosion protection. Surf Coat Technol 2022;446:128768. https://doi.org/10.1016/J.SURFCOAT.2022.128768.
[280] Chen L, Yu Z, Yin D, Cao K, Xie C, Zhu L, et al. Preparation and anticorrosion properties of GO-Ce-MOF nanocomposite coatings. J Appl Polym Sci 2022;139:51571. https://doi.org/10.1002/app.51571.
[281] Alipanah N, Yari H, Mahdavian M, Ramezanzadeh B, Bahlakeh G. Fabrication of MIL-88A sandwiched in graphene oxide nanocomposites using a green approach to induce active/barrier protective functioning in epoxy coatings. J Clean Prod 2021;321:128928. https://doi.org/10.1016/J.JCLEPRO.2021.128928.
[282] Zhang M, Zhang Y, Chen Y, Tian X, Liu L, Wang Y, et al. Dual-inhibitor composite BTA/PPy/MIL-88(Fe) for active anticorrosion of epoxy resin coatings. J Industr Eng Chem 2023;119:660–73. https://doi.org/10.1016/J.JIEC.2022.12.012.
[283] Majidi R, Ramezanzadeh M, Ramezanzadeh B. Developing a dual-functional self-healing nanocomposite utilizing oxidized-multiwall carbon nanotube/highly-porous metal-organic framework (OCNT/ZIF-8) nano-hybrid. Appl Mater Today 2023;32:101830. https://doi.org/10.1016/J.APMT.2023.101830.
[284] Mohammadkhah S, Ramezanzadeh M, Eivaz Mohammadloo H, Ramezanzadeh B, Ghamsarizade R. Construction of a nano-micro nacre-inspired 2D-MoS2-MOF-glutamate carrier toward designing a high-performance smart epoxy composite. J Industr Eng Chem 2023;121:358–77. https://doi.org/10.1016/j.jiec.2023.01.039.
[285] Gu S, Shi H, Zhang C, Wang W, Liu F, Han EH. Mesoporous CeO2 containers in water-borne epoxy coatings for dual active corrosion protection of mild steel. Prog Org Coat 2021;158:106376. https://doi.org/10.1016/J.PORGCOAT.2021.106376.
[286] Kamburova K, Boshkova N, Boshkov N, Radeva T. Composite coatings with polymeric modified ZnO nanoparticles and nanocontainers with inhibitor for corrosion protection of low carbon steel. Colloids Surf A Physicochem Eng Asp 2021;609:125741. https://doi.org/10.1016/J.COLSURFA.2020.125741.
[287] Chenan A, Ramya S, George RP, Kamachi Mudali U. Hollow mesoporous zirconia nanocontainers for storing and controlled releasing of corrosion inhibitors. Ceram Int 2014;40:10457–63. https://doi.org/10.1016/J.CERAMINT.2014.03.016.
[288] Lamprakou Z, Bi H, Weinell CE, Tortajada S, Dam-Johansen K. Smart epoxy coating with mesoporous silica nanoparticles loaded with calcium phosphate for corrosion protection. Prog Org Coat 2022;165:106740. https://doi.org/10.1016/J.PORGCOAT.2022.106740.
[289] Honarvar Nazari M, Zhang Y, Mahmoodi A, Xu G, Yu J, Wu J, et al. Nanocomposite organic coatings for corrosion protection of metals: a review of recent advances. Prog Org Coat 2022;162:106573. https://doi.org/10.1016/J.PORGCOAT.2021.106573.
[290] Jiang BK, Chen AY, Gu JF, Fan JT, Liu Y, Wang P, et al. Corrosion resistance enhancement of magnesium alloy by N-doped graphene quantum dots and polymethyltrimethoxysilane composite coating. Carbon N Y 2020;157:537–48. https://doi.org/10.1016/j.carbon.2019.09.013.
[291] Liu Z, Zhu R, Zhang X, Zhu H. Improving anticorrosion performance of epoxy coating by hybrids of rGO and g-C3N4 nanosheets. J Coat Technol Res 2022;19:1219–32. https://doi.org/10.1007/s11998-021-00603-9.
[292] Xia Y, He Y, Chen C, Wu Y, Zhong F, Chen J. Co-modification of polydopamine and KH560 on g-C3N4 nanosheets for enhancing the corrosion protection property of waterborne epoxy coating. React Funct Polym 2020;146:104405. https://doi.org/10.1016/J.REACTFUNCTPOLYM.2019.104405.
[293] Sanaei Z, Shamsipur A, Ramezanzadeh B. Trisodium phosphate-loaded hierarchically ordered meso-nanoporous ZIF-67/ZIF-8 metal-organic frameworks assembled rGO-Zn-Al-LDH: a multi-level pH-triggered nano-vehicle for epoxy

coating long-lasting self-repairing/barrier properties improvement. Chem Eng J 2023;451:138872. https://doi.org/10.1016/J.CEJ.2022.138872.
[294] Ahmadinia A, Farshi Azhar F. Fabrication of bi-functionalized nanocomposite coating for simultaneous improved thermal stability and corrosion protection performance based on polyaniline-reduced graphene oxide/organo-modified montmorillonite. Compos Interfaces 2022;29:1161–85. https://doi.org/10.1080/09276440.2021.2007719.
[295] Huang H, Li M, Tian Y, Xie Y, Sheng X, Jiang X, et al. Exfoliation and functionalization of α-zirconium phosphate in one pot for waterborne epoxy coatings with enhanced anticorrosion performance. Prog Org Coat 2020;138. https://doi.org/10.1016/j.porgcoat.2019.105390.
[296] AhadiParsa M, Dehghani A, Ramezanzadeh M, Ramezanzadeh B. Rising of MXenes: novel 2D-functionalized nanomaterials as a new milestone in corrosion science - a critical review. Adv Colloid Interface Sci 2022;307:102730. https://doi.org/10.1016/J.CIS.2022.102730.
[297] Gojny FH, Wichmann MHG, Fiedler B, Kinloch IA, Bauhofer W, Windle AH, et al. Evaluation and identification of electrical and thermal conduction mechanisms in carbon nanotube/epoxy composites. Polymer (Guildf) 2006;47:2036–45. https://doi.org/10.1016/j.polymer.2006.01.029.

Mohammad Ghaderi received his BSc (2019) and MSc (2022) degrees in chemical engineering from Sharif University of Technology. Currently, he is a PhD student at the Technical University of Denmark under the supervision of Dr. Huichao Bi and Prof. Kim Dam-Johansen. His current research focuses on developing novel inhibitive pigments for anti-corrosive coatings.

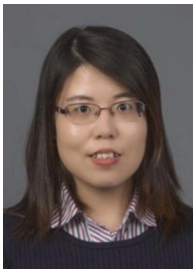

Dr. Huichao Bi holds a BSc from Tianjin University and a PhD from the University of Oxford. She began her academic career as a Lecturer at Tianjin University and later became a Research Associate at the University of Cambridge. Subsequently, she worked as a Postdoctoral Fellow at the University of Toronto. Since 2018, Dr. Bi has been working as an Assistant Professor at the Technical University of Denmark. Her expertise lies in corrosion and corrosion protection by coatings, encompassing the development of innovative functional coatings, advanced anti-corrosive materials, non-destructive evaluation of coating performance and coating integrity management.

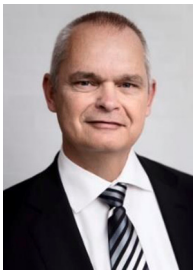

Prof. Kim Dam-Johansen holds an MSc and a PhD from the Technical University of Denmark (DTU). He began his academic career as an assistant teacher at the Engineering Academy of Denmark/DTU in 1986, followed by becoming an Associate Professor in 1990 and a full professor in 1993. He has established the Combustion and Harmful Emission Control Centre (CHEC) and the Hempel Foundation Coatings Science and Technology Centre (CoaST). In 1998, he became the Group Vice President of Hempel A/S and, from 2000, he served as the Head of the Chemical and Biochemical Engineering Department at DTU.